

## REVIEW



Cite this: *Polym. Chem.*, 2025, **16**, 4479

Received 25th July 2025,  
Accepted 12th September 2025  
DOI: 10.1039/d5py00741k  
[rsc.li/polymers](http://rsc.li/polymers)

## Smart polymers for 3D printing applications: current status and future outlook

Nishikanta Singh, Priyank Sinha, Durgesh Kumar Sinha and Sanjib Banerjee  \*

Stimuli-responsive smart polymers have attracted substantial attention for their ability to undergo reversible physicochemical changes in response to external stimuli such as temperature, pH, light, magnetic fields, and biochemical cues. When integrated with 3D printing techniques, such as stereolithography, fused deposition modelling, direct ink writing, and selective laser sintering, these polymers enable the fabrication of architecturally complex, functional, and adaptive systems. This review outlines the molecular design strategies, printing compatibilities, and post-processing approaches essential for achieving dynamic performance in 3D-printed structures. Emphasis is placed on applications in biomedical devices, soft robotics, and sensing platforms. The synergy between smart polymer chemistry and AM technologies presents a promising pathway toward programmable materials and next-generation responsive systems with customized structural and functional properties.

### 1. Introduction

In reaction to slight changes in their surroundings, smart or stimuli-responsive polymers show notable, reversible physical or chemical changes. Based on the molecular arrangement and state, these materials can respond to a range of stimuli, including pH, temperature, light, magnetic or electric fields, or biological molecules, causing visible changes like swelling, collapsing, or transitions from solution to gel.<sup>1</sup> Soluble linear smart polymers transition from a single-phase to a two-phase system near specific conditions, leading to reversible sol-gel

behavior. In contrast, cross-linked smart networks reorganize their polymer chains under these conditions, shifting between collapsed and expanded states. Additionally, smart surfaces can alter their hydrophilicity in response to external stimuli, enabling adaptive and responsive interfaces. These responsive transformations can be harnessed in the development of advanced smart devices for various applications, such as minimally invasive injectable systems,<sup>2</sup> pulsatile drug delivery platforms,<sup>3</sup> and innovative scaffolds for cell culture and tissue engineering.<sup>4</sup> Additionally, many polymers can be readily modified either before or after polymerization to introduce functionalities into the backbone/side chain end/end chain of these polymers,<sup>5,6</sup> such as biological receptors, into their structure through prepolymerization or post polymerization tech-

Department of Chemistry, Indian Institute of Technology Bhilai, Durg 491001, Chhattisgarh, India. E-mail: [sanjib.banerjee@iitbhilai.ac.in](mailto:sanjib.banerjee@iitbhilai.ac.in)



Nishikanta Singh

*Nishikanta Singh obtained his B.Sc. degree from Sambalpur University, followed by an M.Sc. from Guru Ghasidas Vishwavidyalaya, Bilaspur. He is presently undertaking his Ph.D. research in the Department of Chemistry at IIT Bhilai, guided by Dr. Sanjib Banerjee. His work focuses on designing and developing functional polymeric materials that exhibit stimuli-responsive behavior.*



Priyank Sinha

*Priyank Sinha obtained an Int. M.Sc. degree from the Center for Basic Sciences, Pt. Ravishankar Shukla University Raipur. He is currently pursuing his Ph.D. at the Department of Chemistry, Indian Institute of Technology Bhilai under the supervision of Dr. Sanjib Banerjee. His current research focuses on development of stimuli-responsive functional polymeric materials for 3D printing.*

niques.<sup>7</sup> Researchers have demonstrated extensive flexibility in designing chemical structures, architectures, and modifications, enabling the development of countless applications using these smart materials.<sup>8</sup>

The introduction of a single-laser curing system by Kodama at the Nagoya Municipal Industrial Research Institute in the 1980s opened a new path for fabricating three-dimensional objects.<sup>9</sup> Hull and coworkers later enhanced the technology and brought it to the commercial market in 1984.<sup>10</sup> In 1989, S. Crump developed an extrusion-based technique for producing 3D polymer structures, which later became known as fused deposition modeling (FDM).<sup>11</sup> This technique launched a new age of manufacturing and processing technologies and laid the foundation for layer-by-layer production.<sup>12</sup> An alternative to traditional manufacturing techniques, additive manufacturing (AM), often known as 3D printing (3DP), is a layer-by-layer production technology that creates complex, nearly net-shaped structures. AM ushered in a new era of production thanks to its advantages like customization, speed, material versatility, reduced or no assembly requirements, and minimal geometric constraints. Over time, AM has progressed from being primarily a prototyping tool to a scalable, practical manufacturing method. This technology is broadly classified into several key types, including fused deposition modelling, direct ink writing, 3D inkjet printing, stereolithography, selective laser sintering, binder jetting, and others.<sup>13</sup> However, all these methods are variations of controllable bottom-up techniques designed to produce diverse structures and shapes, which have been significantly advanced.<sup>14</sup> Because of practical constraints, engineers and scientists often have to adjust product designs

to meet requirements at various stages using traditional design approaches. This focus on conventional manufacturing limits the ability to fully optimize efficiency. Combined additive manufacturing technologies have advanced industries like aerospace,<sup>15,16</sup> healthcare,<sup>17,18</sup> sensing,<sup>19,20</sup> robotics,<sup>21,22</sup> and consumer products,<sup>23,24</sup> offering greater design flexibility and enabling products to be tailored more precisely to individual needs (Fig. 1).

The evolution of three-dimensional (3D) printing has fundamentally reshaped modern manufacturing by offering unprecedented freedom in design, customization, and material utilization.<sup>25</sup> Unlike traditional subtractive methods, 3D printing builds objects layer by layer, enabling the fabrication of intricate geometries with minimal material waste. This additive approach has proven especially valuable in applications where tailored solutions and rapid prototyping are crucial.<sup>26</sup> In recent years, 3D printing has moved beyond its role in conceptual modelling to become a practical tool for producing functional components across industries,<sup>27</sup> including aerospace,<sup>28</sup> biomedical engineering, and wearable electronics.<sup>29</sup> When combined with smart polymers-materials that can respond dynamically to external stimuli-3D printing offers the capability to produce intelligent systems that are both structurally complex and functionally adaptive.<sup>30</sup> The compatibility of smart polymers with a variety of 3D printing techniques further amplifies their potential, enabling the development of next-generation devices capable of dynamically responding to environmental stimuli instantaneously.<sup>31</sup>

The goal of this review is to present a thorough analysis of smart polymers' present state and potential future developments



**Durgesh Kumar Sinha**

*Durgesh Kumar Sinha completed his B.Sc. and M.Sc. degrees in Chemistry at the Government Digvijay Autonomous Postgraduate College, Rajnandgaon, Chhattisgarh. He is presently pursuing his Ph.D. in the Department of Chemistry at IIT Bhilai, Chhattisgarh, under the guidance of Dr. Sanjib Banerjee. His research is centered on the development of innovative polymerization strategies for creating stimuli-responsive hydrogel-based polymeric materials.*



**Sanjib Banerjee**

*Dr. Sanjib Banerjee is an Associate Professor of Chemistry at the Indian Institute of Technology (IIT) Bhilai. He obtained his M.Sc. in Chemistry from the University of Calcutta, followed by a Ph.D. in Polymer and Materials Chemistry from the Indian Association for the Cultivation of Science. He then pursued postdoctoral research at the University of Massachusetts Lowell and at ENSCM, France.*

*Dr. Banerjee began his academic career at IIT Bhilai in 2017 as an Assistant Professor and was promoted to Associate Professor in 2021. His research contributions have earned recognition from several esteemed organizations, including the SERB Ramanujan Fellowship (2016), the SERB Early Career Research Award (2019), the Royal Society of Chemistry's Polymer Chemistry Emerging Investigator distinction (2020), Wiley's Next Generation of Polymer Researchers award (2022), and the Bronze Medal from the Chemical Research Society of India (CRSI) for 2024.*

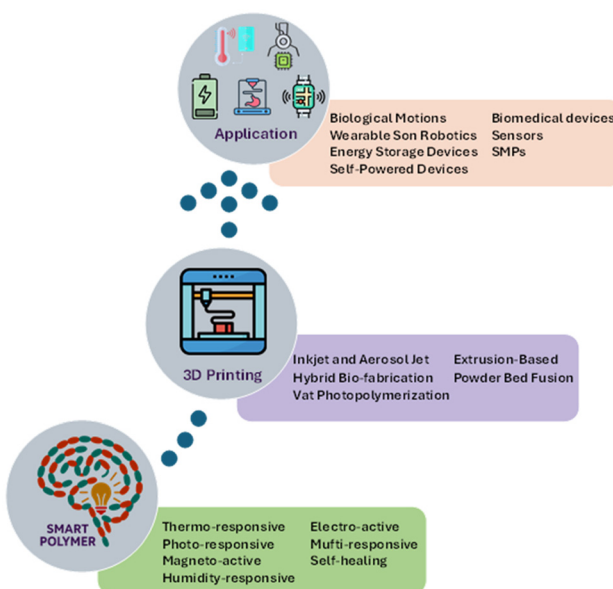


Fig. 1 Brief overview of 3D printing applications of smart polymers.

in relation to 3D printing technology. It begins with a foundational introduction to stimuli-responsive polymers, discussing their classifications based on the type of external stimuli they respond to such as temperature,<sup>32</sup> pH,<sup>33</sup> light,<sup>34</sup> redox potential,<sup>35</sup> and magnetic fields,<sup>36</sup> explaining the mechanisms that govern their behavior. The subsequent sections delve into the major 3D printing methodologies that are compatible with these materials,<sup>37,38</sup> including stereolithography,<sup>39</sup> selective laser sintering,<sup>40</sup> inkjet printing,<sup>41</sup> and extrusion-based<sup>42</sup> techniques. Material design strategies, including polymer functionalization and composite development, are also explored in detail.<sup>43</sup> Finally, the review presents a broad spectrum of applications where 3D-printed smart polymers are making an impact, mainly in biomedical engineering, sensing, and soft robotics.<sup>44</sup>

## 2. Fundamentals of smart polymers

Stimuli-responsive polymers, often referred to as smart polymers, are advanced materials capable of undergoing controlled and reversible alterations in their chemical or physical properties when exposed to specific external triggers. These polymers emulate biological adaptability, allowing them to alter their conformation, solubility, permeability, or other functional characteristics in a controlled manner.<sup>45–47</sup> Smart polymers are broadly classified based on the nature of the external stimulus they respond to. This classification highlights the diversity of stimuli that can be harnessed to manipulate polymer behaviour and allows for the rational design of systems tailored to specific applications.

### 2.1. Single stimuli-responsive polymers

#### 2.1.1. Thermo-responsive polymers.

Thermo-responsive polymers constitute an important class of smart materials,

characterized by their capacity to exhibit notable physico-chemical transformations when subjected to temperature changes. A key feature extensively investigated within this group is the reversible phase transition associated with the lower critical solution temperature (LCST). When such polymers are dissolved in aqueous environments and heated beyond their LCST, they shift from a hydrated, extended chain conformation to a collapsed, globular structure.<sup>32,48</sup> This transformation results in a macroscopic phase separation, typically observed as a sudden cloudiness in solution, attributed to changes in the polymer's solubility. This process is fully reversible; upon cooling below the LCST, the polymer reverts to its original hydrated state.<sup>49</sup> The temperature at which this transition occurs is highly tunable and depends on multiple factors, such as the polymer's chain length, stereoregularity, end-group composition, and the nature and proportion of comonomers incorporated during synthesis.<sup>50</sup> The presence of polar solvents like water and alcohols enhances this thermal response due to their capacity to engage in hydrogen bonding with the polymer chains.<sup>49,51</sup> PNIPAM-based copolymers and composites enhanced with additives like glucose and sucrose to improve responsiveness and porosity. As illustrated in Fig. 2a, PNIPAM networks crosslinked with aggregation-induced emission (AIE)-active azonaphthol exhibit a temperature-dependent fluorescence behavior. Below the LCST, the polymer chains are hydrated and extended, resulting in weak fluorescence. Upon heating above the LCST, the chains collapse and aggregate due to hydrophobic interactions, leading to strong fluorescence emission. In addition, 3D-printed

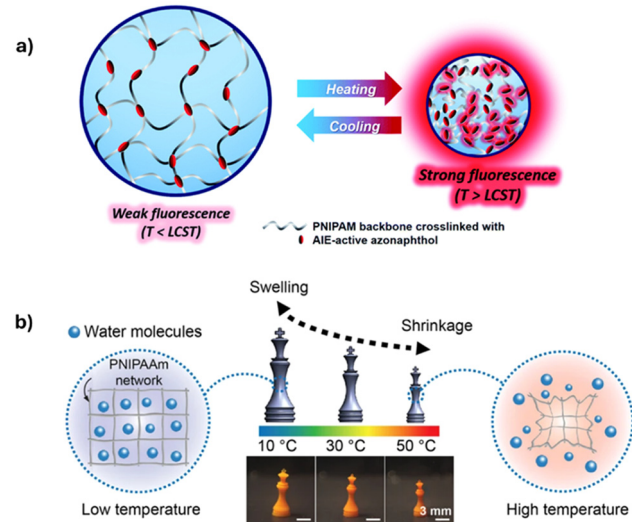


Fig. 2 (a) Temperature-responsive behaviour of Azo-PNIPAM hydrogel. Reproduced with permission from ref. 55. Copyright 2020, Royal Society of Chemistry. (b) Schematic representation of the temperature-responsive behavior of the 3D printed hydrogel, showing phase transitions characterized by swelling at lower temperatures and shrinkage at higher temperatures. The central images display the corresponding shape changes of the printed structure at different temperatures. Reproduced with permission from ref. 32. Copyright 2018, Nature.

PNIPAM hydrogel structures demonstrate pronounced swelling at 10 °C and shrinkage at 50 °C, as shown by the reversible deformation of a chess piece model (Fig. 2b). This dual property of thermo-responsive volume change and optical functionality highlights the potential of PNIPAM-based hydrogels for applications in soft actuators, sensors, and stimuli-responsive optical devices. Apart from PNIPAM, several other polymer families exhibit similar behavior, including certain PDMAEMA,<sup>52</sup> PTEGMA,<sup>53</sup> and PIPOZ.<sup>54</sup> Polymers responsive to temperature stimuli are suitable for several additive manufacturing techniques, especially direct ink writing (DIW). This extrusion-based process supports the use of shear-thinning inks like PNIPAM formulations. Additionally, techniques such as projection micro-stereolithography and other light-assisted methods have been successfully used to fabricate high-resolution structures incorporating these hydrogels. 3D-printed thermo-responsive hydrogels have enabled the fabrication of functional devices such as actuators, valves, and biomimetic systems that deform in response to heat. The use of sugar additives to induce porosity in the polymer matrix has led to faster actuation speeds, improving their performance in soft robotics and bioinspired devices. These materials are also being explored in therapeutic delivery and tissue engineering, where temperature-regulated material behaviour is advantageous for controlled release and dynamic scaffold design.

**2.1.2. pH-responsive polymers.** pH-sensitive polymers are a subclass of smart materials that exhibit reversible alterations in properties such as volume, conformation, or solubility in response to changes in environmental pH. These responses are primarily driven by the protonation or deprotonation of ionizable functional groups along the polymer backbone, which modulate electrostatic interactions and influence the polymer's ability to absorb water. Typical examples include polymers containing acidic groups (poly(acrylic acid), alginate<sup>56</sup>) or basic groups (Chitosan<sup>57</sup>). Poly(acrylic acid) swells in basic environments due to ionization of carboxyl groups, whereas chitosan swells under acidic conditions as its amine groups become protonated. On the other hand, polymers with basic functionalities, tertiary amines present in poly(*N*,*N*-dimethylaminoethyl methacrylate) become protonated in acidic media,<sup>58</sup> increasing hydrophilicity and chain expansion. These polymers are often used independently or in blends to fine-tune responsiveness and mechanical properties. pH-sensitive polymers are compatible with extrusion-based methods, such as DIW,<sup>59</sup> where their shear-thinning behavior makes them suitable for smooth deposition. Furthermore, ionic crosslinking, especially for materials like alginate, allows for rapid gelation post-printing using calcium chloride or other multivalent ions.<sup>60</sup> This has enabled the creation of complex 3D structures with high fidelity and stability under physiological conditions. Liu *et al.*<sup>61</sup> developed pH-responsive polymeric hydrogel microstructures using femtosecond direct laser writing, enabling dynamic color and shape modulation at the microscale. Their 4D printed woodpile structures exhibited vivid structural colors in acidic environments (pH < 7), which faded or shifted under basic conditions (pH > 7) due to swell-

ing induced by ionized carboxylate groups. This swelling altered the lattice periodicity, affecting light diffraction. Notably, the color and shape changes were fully reversible upon returning to acidic pH, highlighting the potential of such microstructures for tunable photonic devices and sensors (Fig. 3). These materials are widely employed in targeted drug delivery, where they release therapeutic agents in response to the pH of specific body regions—such as the acidic stomach or neutral intestines. Additionally, they are being investigated for biosensors that respond to biochemical changes and injectable scaffolds for wound healing or tissue regeneration, where environmental pH shifts signal healing stages. The reversible swelling–deswelling behavior also makes them excellent candidates for actuators and adaptive membranes.

**2.1.3. Photo-responsive polymers.** Photo-responsive polymers are smart polymeric systems that respond to light, typically ultraviolet (UV), visible, or near-infrared radiation, by altering their structural, mechanical, or chemical properties.<sup>62</sup> Light triggers can induce changes such as swelling/deswelling, crosslinking, degradation, or conformational shifts through photo-induced chemical reactions or molecular rearrangements.<sup>63</sup> These transformations are precise, tunable, and can be spatially localized, making them ideal for complex functional materials. Commonly used photo-sensitive systems include azobenzene-functionalized polymers,<sup>64</sup> which undergo reversible *trans*–*cis* isomerization under UV and visible light. Other examples include polymers with spirobifluorene<sup>65</sup> and spirooxazine<sup>66</sup> which can experience reversible photo-dissociation or polarity changes. These light-sensitive moieties are often integrated into polymer networks such as poly(ethylene glycol) (PEG), gelatin methacrylate (GelMA), or poly(*N*-isopropylacrylamide) to impart photo-responsiveness without compromising biocompatibility. Photo-responsive polymers are particularly suited to light-assisted 3D printing methods such as

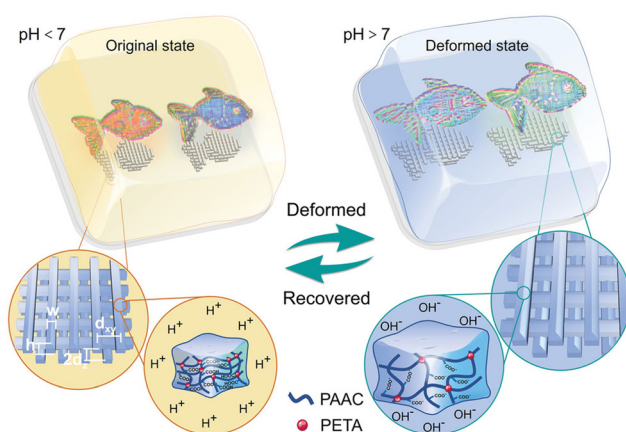


**Fig. 3** Schematic of pH-responsive color and shape changes in 4D printed woodpile microstructures. Vivid structural colors appear at pH < 7, while swelling at pH > 7 due to electrostatic repulsion between ionized carboxylate groups alters the lattice and fades the color. This transition is fully reversible upon pH restoration. Reproduced with permission from ref. 61. Copyright 2023, Wiley.

digital light processing (DLP)<sup>67</sup> and stereolithography.<sup>68</sup> These techniques allow for spatial and temporal control over polymerization, enabling high-resolution fabrication of intricate geometries. Yang *et al.*<sup>69</sup> integrated carbon black, for its superior photothermal conversion efficiency, into a shape-memory polyurethane designed for Fused Deposition Modeling (FDM) 3D printing (Fig. 4a and b). In their study, the printed structure demonstrated the ability to recover its original cubic form from a compressed state when exposed to a light source of  $87 \text{ mW cm}^{-2}$  or natural sunlight at  $76 \text{ mW cm}^{-2}$  (Fig. 4c). Building on this material, the researchers also created a “sunflower” model to showcase a “bud-to-bloom” transformation (Fig. 4d). This experiment captured the progressive deformation of the sunflower structure at 40-second intervals under illumination at  $87 \text{ mW cm}^{-2}$ . As the exposure duration increased, the petals gradually unfolded, mimicking the natural blooming process of a sunflower. Complete opening of the petals was achieved after 280 seconds of illumination. Applications of photo-responsive hydrogels include soft actuators, shape-shifting devices, and biomimetic systems that change conformation when exposed to light. Polymer-based microrobots can fold, bend, or rotate in response to directional UV exposure, mimicking plant tropisms. In biomedical engineering, these materials are explored for controlled drug delivery, where light can trigger site-specific release, and cell culture platforms, where surface properties can be dynamically modified with light to direct cell behavior. Additionally, they are being considered for optically tunable

biosensors and reconfigurable optical elements in flexible electronics.

**2.1.4. Magnetic-responsive polymers.** Magnetic-responsive polymers are composite materials that respond to external magnetic fields by changing their shape, position, or internal structure.<sup>70,71</sup> This dynamic behaviour is achieved by incorporating magnetic nanoparticles (MNPs) into the polymer network, allowing the material to undergo non-contact, remotely controlled actuation. These polymers are typically fabricated from biocompatible polymers such as sodium alginate,<sup>72</sup> methylcellulose,<sup>73</sup> and poly(acrylic acid),<sup>74</sup> which are embedded with iron oxide nanoparticles ( $\text{Fe}_3\text{O}_4$ ), superparamagnetic iron oxide nanoparticles (SPIONs), or ferrite particles. Tang *et al.*<sup>75</sup> illustrates the fabrication and actuation process of integrated magneto-thermo-sensitive hydrogel, elastomer structures using extrusion printing. In the first step, Fig. 5a, extrusion printing enables the precise deposition of a thermosensitive PNIPAM polymer matrix embedded with  $\text{Fe}_3\text{O}_4$  magnetic nanoparticles and LAPONITE® rheological modifier, alongside a silicone elastomer (Ecoflex) ink containing nanosilica to improve viscosity and a photo initiator for enhanced interfacial adhesion. The viscoelastic properties of these inks, including shear-thinning behaviour and yield stress, ensure printability by allowing smooth extrusion while maintaining structural integrity post-printing. In the second step, Fig. 5b, the elastomer is thermally cured on a heated platform ( $110^\circ\text{C}$ ) followed by UV curing of the magnetic hydrogel in a nitrogen atmosphere to promote covalent interlinking between the hydrogel and elastomer networks. Finally, in Fig. 5c, actuation is achieved under an alternating magnetic field, which induces magnetothermal heating *via* Néel and Brownian relaxation of  $\text{Fe}_3\text{O}_4$  nanoparticles. When the hydrogel temperature surpasses its LCST, it undergoes volume

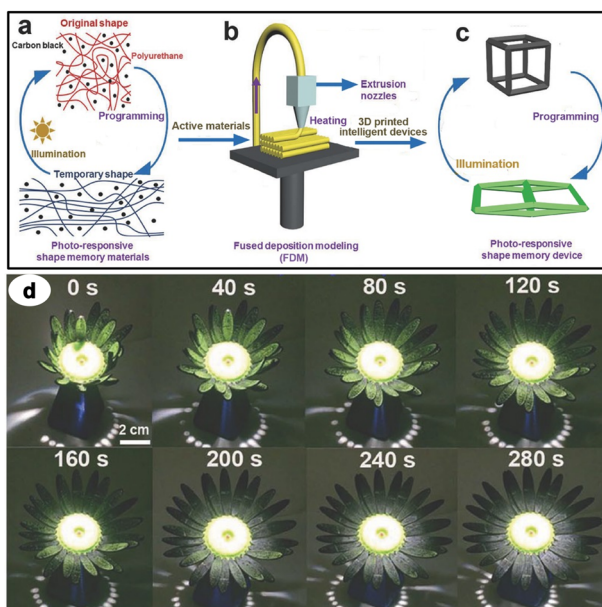


**Fig. 4** (a) Photoresponsive shape-memory behavior of carbon black-PU composite. (b) Fabrication of 3D-printed structures *via* FDM, where controlled layer-by-layer deposition occurs on a glass substrate. (c) Light-triggered shape recovery of the 3D-printed device. (d) Displaying the deformation of photosensitive printed sunflowers transitioning from bud to bloom under light exposure. Scale bar represents 2 centimeters. Reproduced with permission from ref. 69. Copyright 2017, Wiley.

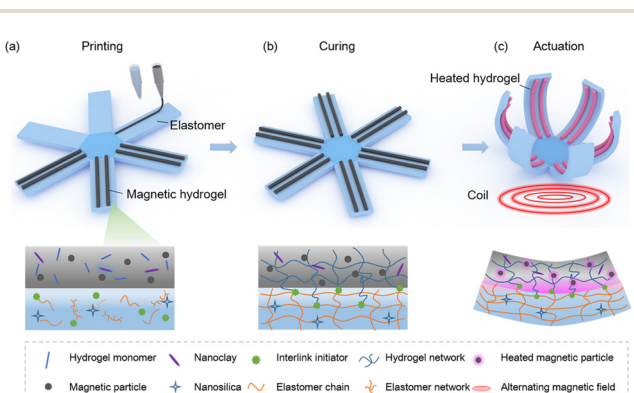


**Fig. 5** 3D printing and deformation behaviour of a composite system composed of magnetic hydrogel and elastomer for magnetic hyperthermia applications. (a) Extrusion-based printing and (b) subsequent curing of magnetic hydrogel inks (represented as black strips) along with elastomeric layers (shown as blue sheets). (c) Shape change of the printed composite structure under exposure to an alternating magnetic field, where the magnetic hydrogel (depicted as pink strips) is locally heated using a coil that generates the field. Reproduced with permission from ref. 75. Copyright 2021, Elsevier.

shrinkage, driving deformation of the entire bilayer structure. This design enables the magnetic hydrogel to function as the active layer and the elastomer as the passive layer, creating a programmable and responsive soft actuator. Magnetic-responsive hydrogels are highly promising for soft robotics, bio-actuators, and remotely controlled biomedical devices. These systems can perform functions such as bending, folding, rolling, jumping, or crawling when exposed to magnetic stimuli.

**2.1.5. Enzyme-responsive polymers.** Enzyme-responsive polymers are specifically engineered to degrade or change shape in response to enzymatic activity, particularly proteases.<sup>76</sup> Upon exposure to the corresponding enzyme, these bonds are cleaved, triggering a cascade of physicochemical changes such as polymer degradation, solubility shift, or structural reorganization.<sup>77</sup> Enzymes offer a localized and disease-specific trigger since they are found naturally in a variety of tissues and pathological states.<sup>78</sup> Certain hydrolases,<sup>79</sup> proteases,<sup>80</sup> or glycosidases<sup>77</sup> are overexpressed in cancerous tissues or inflamed environments. This responsiveness leverages the biological function of enzymes to trigger structural changes, making these materials highly attractive for biomedical applications where biocompatibility and biodegradability are essential.<sup>81</sup> Polymers composed of multiple materials that can undergo autonomous transformations in shape and dimensions present distinct benefits for applications such as targeted cargo delivery and controlled substance release. Narupai *et al.*<sup>82</sup> shown in Fig. 6a, a cylindrical hydrogel was designed using a bilayer base of Temp-Ink and pH-Ink combined with an enzymatically degradable Enz-Ink, forming the cylinder body. When placed in a container with a narrow channel, the cylinder initially remained trapped due to

its large size. Upon exposure to proteinase K, enzymatic degradation reduced the hydrogel's dimensions, enabling the residual disk to pass through the gap. This concept was extended to demonstrate cargo delivery (Fig. 6b), where an enclosed Enz-Ink cylinder loaded with F127 (triblock copolymer) and fluorescent latex beads was placed in a multi-chamber system featuring size-selective barriers. The construct rolled into a designated chamber and, following enzymatic treatment, degraded to release its encapsulated cargo. This work highlights the versatility of multi-material hydrogels in developing smart systems that respond to environmental cues for targeted transport and release. These hydrogels are especially well-suited for DIW 3D printing. Methacrylated bovine serum albumin (MA-BSA)-based emulsions exhibit shear-thinning behaviour and structural integrity post-printing, which enables precise layer-by-layer deposition. The use of UV photopolymerization after printing allows the transformation of the gel into a solid, yet enzymatically degradable, hydrogel network. This technique facilitates the creation of complex, multi-layered geometries responsive to enzymatic degradation. Enzyme-responsive hydrogels hold great potential for smart drug delivery by enabling targeted release through controlled degradation in specific biological environments. They can serve as biodegradable scaffolds that respond to biological cues, supporting tissue regeneration and healing processes. These hydrogels are also useful for cargo transport systems where encapsulated payloads, such as fluorescent beads, are released only upon enzymatic action. In soft robotics and actuators, enzyme-responsive components can dynamically adapt their shape or function in enzyme-rich environments, offering precise and bioinspired responsiveness.

## 2.2. Dual-responsive polymer

**2.2.1. Thermal and pH-responsive polymer.** Polymers responsive to both temperature and pH represent an advanced class of dual-stimuli smart materials. These polymers can change volume, structure, and mechanical properties when exposed to physiological temperature variations or shifts in environmental pH.<sup>83</sup> Temperature responsiveness typically stems from LCST behaviour, while pH sensitivity arises from ionizable groups in the polymer matrix that swell or shrink depending on protonation states. Odent *et al.*<sup>84</sup> demonstrated the fabrication of hydrogel actuators *via* stereolithography 3D printing, as shown in Fig. 7a, where photopolymerization of NIPAM and CEA (2-carboxyethylacrylate) with controlled cross-linking and composition produced multilayered structures with anisotropic swelling properties. This design enabled programmable actuation in response to environmental stimuli. Fig. 7b demonstrated a dual-responsive actuator combining thermo-sensitive PNIPAM and pH-responsive poly(2-carboxyethylacrylate) layers, which exhibited reversible bidirectional bending driven by differential swelling under temperature and pH changes, showcasing their potential in soft robotics and smart material applications. NIPAM provides thermo-responsiveness with its LCST around 32 °C, while CEA introduces carboxyl groups that ionize under alkaline conditions, making

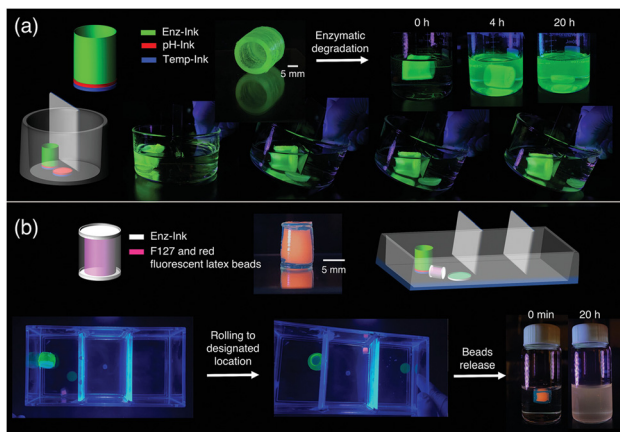


**Fig. 6** (a) A 3D-printed cylinder composed of Temp-Ink, pH-Ink, and Enz-Ink is shown in two states—before and after enzymatic degradation by proteinase K, where the enzyme-enabled breakdown allows the cylinder to pass through a narrow gap beneath a barrier. (b) A similar enzyme-responsive cylinder embedded with red fluorescent latex beads is capable of rolling to a target location and releasing the encapsulated beads upon exposure to proteinase K. Reproduced with permission from ref. 82. Copyright 2021, Wiley.

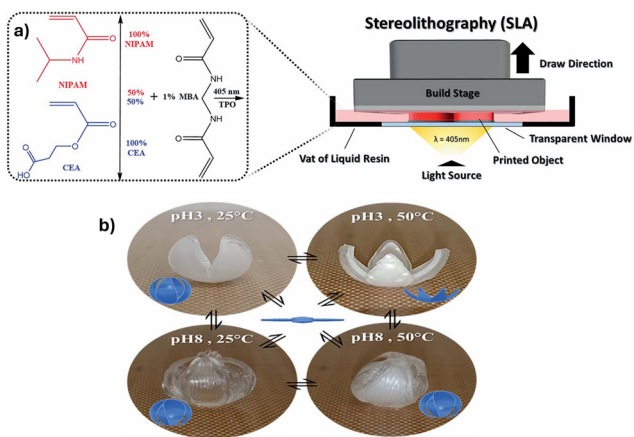


**Fig. 7** (a) Schematic representation of the chemical components and rapid bottom-up fabrication of gradient-like structures through photopolymerization of NIPAM and CEA using TPO as the photoinitiator and MBA as the crosslinker. (b) Demonstration of dual-responsive actuation to temperature and pH in 3D-printed gradient-like hydrogels with compositionally varied layers across the structure. Reproduced with permission from ref. 84. Copyright 2019, Royal Society of Chemistry.

the hydrogel pH responsive. The resulting PNIPAM–PCEA copolymer network exhibits sharp and reversible changes under both stimuli. The hydrogel system was successfully printed using extrusion-based 3D printing. The ink formulation exhibited excellent shear-thinning behaviour and self-supporting characteristics, allowing it to form stable, multi-layered constructs. Post-printing, chemical crosslinking was used to stabilize the architecture and lock in dual-responsive behaviour. The dual-responsive printed hydrogels demonstrated reversible bending and swelling behaviour, making them suitable for 4D printing applications. Specifically, the hydrogel was utilized to fabricate bilayer actuators that bent and curled reversibly in response to temperature and pH shifts. Soft robotic fingers and gripping devices that responded dynamically in a controlled environment. Programmable shape-transforming structures mimicking natural movements like blooming or wrapping.

**2.2.2. Light and thermo-responsive polymer.** Polymers that respond to both temperature and light represent a multifunctional class of smart materials with dynamic responsiveness. These systems undergo reversible physical changes, such as swelling, contraction, or optical transparency shifts, when exposed to either heat or specific wavelengths of light.<sup>85</sup> Dual responsiveness enhances their versatility for controlled actuation and stimulus-triggered behaviour in real-time environments. In the referenced study, the hydrogel system was constructed from PNIPAM, a thermo-responsive polymer, combined with a photochromic monomer such as spirobifluorene methacrylate.<sup>86</sup> PNIPAM imparts LCST behaviour, while SPMA introduces photo-switching functionality, shifting between spirobifluorene (hydrophobic) and merocyanine (hydrophilic) forms under light. This dual mechanism enables the hydrogel to adjust both its hydrophilicity and optical properties under

independent or combined stimuli. Although not directly printed in this study, the material characteristics, such as reversible volume change, mechanical robustness, and rheological tunability make the hydrogel highly suitable for extrusion-based 3D printing and light-assisted printing methods like DLP. These printing platforms can leverage the light-responsiveness for spatial control of swelling patterns or actuation, making the hydrogels ideal candidates for 4D printing architectures.<sup>87</sup> Park *et al.*<sup>88</sup> illustrates the design and actuation behaviour of a mechanically reinforced PNIPAM/BC\_AuNP hydrogel system. The composite hydrogel was prepared by radical polymerization of NIPAM in the presence of bacterial cellulose (BC) and gold nanoparticles (AuNPs), resulting in a network with enhanced mechanical strength and dual responsiveness to temperature and visible light. The AuNPs enable efficient photothermal conversion, leading to localized heating upon 532 nm light irradiation Fig. 8a. This localized heating causes PNIPAM chains in the irradiated region to shrink, inducing site-specific bending of the hydrogel actuator Fig. 8b. Utilizing this property, PNIPAM/BC\_AuNP-PAM bilayer structures were molded into various shapes, including a rabbit ear and hand-shaped actuator Fig. 8c and d. These constructs exhibited programmable, remote-controllable deformations such as partial ear folding and sequential finger bending, mimicking complex motions like counting. Dual-responsive hydrogels show strong potential for applications in soft robotics, where they bend, twist, or curl in response to light and temperature inputs, enabling programmable actuation. They are promising for optical switches and smart displays, as light-induced color changes allow variable opacity for adaptive

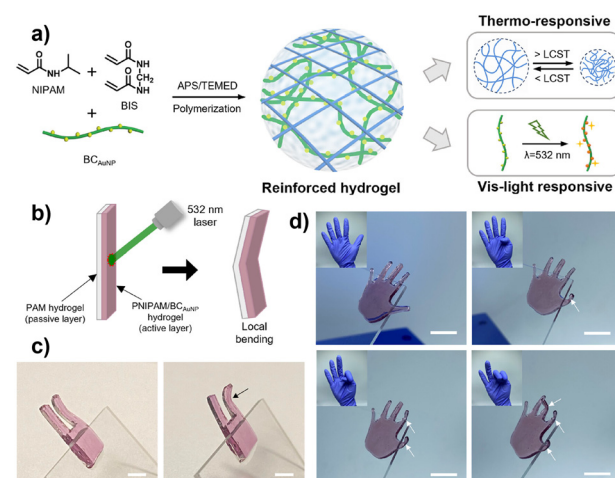


**Fig. 8** (a) Schematic illustration of the preparation of light and temperature-responsive PNIPAM/BC u-NP hydrogel. Demonstration of light-responsive motion of hydrogel actuators. (b) Schematic illustration of local bending motion of a light-responsive actuator. (c) Rabbit-mimicking actuator exhibiting ear-folding motion-like localized bending upon irradiation. (d) Light-induced finger bending motion of a hand-shaped actuator. For all samples, the active layer consisted of PNIPAM/BCAuNP. All scale bars are 10 mm. Reproduced with permission from ref. 88. Copyright 2024, American Chemical Society.

windows. In controlled drug delivery, localized light and thermal exposure regulate swelling to trigger precise release. These hydrogels are also suited for biomedical devices and diagnostics as smart sensors that detect or respond to physiological heat and illumination. The combined responsiveness to both stimuli offers enhanced spatiotemporal control, supporting complex shape-changing systems, smart actuators, and biomimetic designs.

### 2.3. Multi-stimuli responsive polymers

Multi-stimuli responsive polymers are a class of intelligent soft materials engineered to exhibit functional transformations when exposed to two or more external triggers, such as thermal variation, ionic concentration, pH gradients, or optical stimulation.<sup>89</sup> These polymers integrate multiple responsive moieties into a single matrix, allowing complex and programmable actuation behaviours that are highly desirable for 4D printing applications.<sup>87</sup> Gladman *et al.*<sup>90</sup> developed a multi-material DIW method to 3D print functionally graded hydrogels capable of responding to multiple stimuli, including temperature, ionic strength, and light. By combining thermo-responsive PNIPAM with anisotropic fillers like cellulose nanofibers and spatially varying the ink composition, they fabricated programmable structures that undergo complex, reversible shape changes. Lee *et al.*<sup>91</sup> developed a multifunctional hydrogel system responsive to magnetic fields, temperature, pH, and  $\text{Ca}^{2+}$  ions, enabling the 3D printing of micromachines like microrollers and microscrews with both reversible and irreversible shape transformations. Using a PNIPAM-AAc copolymer for dual thermal and pH sensitivity, and incorporating magnetic nanoparticles *via* two-photon polymerization, they created microscale, magnetically actuated structures capable of environmental navigation, microchannel blockage, and targeted cargo delivery, offering significant potential for minimally invasive therapies and organ-on-chip applications. Downs *et al.*<sup>90</sup> demonstrates a droplet-network-based strategy for fabricating patterned, multi-material hydrogels with stimuli-responsive properties. Initially, nanoliter-sized pre-gel droplets are dispensed into a lipid-containing oil, where lipid monolayers form around each droplet (Fig. 9a). When adjacent droplets come into contact, lipid bilayers are established at their interfaces (Fig. 9b). Subsequent UV-induced photopolymerization disrupts these bilayers, yielding continuous PNIPAM-based hydrogel structures (Fig. 9c) that can be phase-transferred into aqueous environments for further use (Fig. 9d). By introducing functional additives such as gold nanoparticles, magnetic particles, or PEGDAAm into selected droplets, multi-material hydrogel constructs are created with responsiveness to temperature, light, and magnetic fields (Fig. 9e and f). Moreover, manual assembly of droplets allows for the formation of complex networks where different pre-gel compositions are spatially organized, enabling programmable shape changes and movements under external stimuli (Fig. 9g). This approach highlights the versatility of droplet networks for designing soft materials with tailored, multi-stimuli responsiveness. These bioinspired actuators demon-

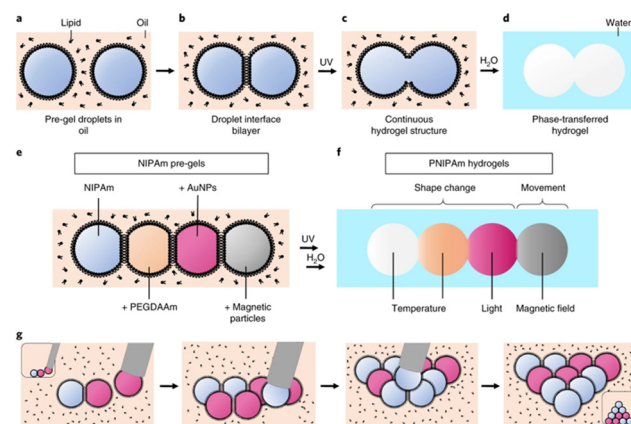


Fig. 9 (a–d) Illustration of hydrogel structure formation using a droplet pair: pre-gel droplets are immersed in oil containing lipids, forming monolayer coatings (a); when two droplets contact, a lipid bilayer forms at their junction (b); exposure to light triggers polymerization, breaking the bilayer and producing a single hydrogel structure (c); the resulting hydrogel can then be moved into an aqueous solution (d). (e) Different pre-gel mixtures—such as those with PEGDAAm, gold nanoparticles, or magnetic nickel particles—can be encapsulated in separate droplet compartments. (f) Post-polymerization, the structure contains multiple integrated, stimulus-responsive hydrogel types. (g) Diagram showing the manual assembly of a 10-droplet network from two pre-gel types using a syringe, with top-down views included as insets. Reproduced with permission from ref. 90. Copyright 2020, Nature.

strate precise, stimulus-specific deformations, highlighting their potential for applications in 4D printing, soft robotics, and adaptive biomedical devices.

## 3. 3D printing techniques for smart polymers

3D printing has emerged as a transformative fabrication technique that constructs intricate structures layer by layer, allowing for the creation of complex geometries and tailored functionalities. Compared to conventional manufacturing processes, 3D printing provides significant benefits, including accelerated prototyping and the ability to produce highly customized components that are challenging or unfeasible to manufacture using traditional methods. The ability to swiftly produce on-demand 3D structures has significantly advanced both scientific research and industrial applications. Presently, additive manufacturing encompasses seven major categories and more than 50 distinct techniques, each tailored to meet specific demands regarding biomaterial compatibility, fabrication speed, and structural precision.<sup>92–95</sup> Due to their versatility, rapid prototyping technologies have evolved into a flexible and powerful platform for next-generation advanced manufacturing.<sup>96,97</sup> With the continued development of 3D printing technique, the implementation of smart polymers has undergone significant transformation. An increasing number of researchers across diverse scientific disciplines are now employing rapid prototyping techniques to design and fabri-

cate multifunctional soft devices with intricate architectures that are unachievable through conventional manufacturing methods. These advancements hold immense promises for revolutionizing various aspects of human life soon. The functional integration of smart polymers into 3D printing has led to novel capabilities in bioengineering, soft robotics, sensors, and actuators. Understanding the classifications and mechanisms of 3D printing techniques is essential for the rational design and fabrication of smart polymer-based structures. The application of 3D printing technique to fabricate smart polymers follows similar commercial 3D printing strategies to create intelligent structures for a variety of engineering purposes.<sup>98</sup> However, successful integration of smart polymers in 3D printing technique requires that the printing systems be compatible with these functional materials or support multi-material printing, particularly in scenarios where internal deformation mismatches within the printed structure lead to actuation or programmed shape changes.<sup>99–101</sup> Various 3D printing technique have been tailored to specific types of feedstock and operational mechanisms, each offering distinct advantages and limitations. These techniques can be categorized based on the physical state of the feedstock and the mechanism of solidification into five major classes, discussed below in detail.

### 3.1. Vat photopolymerization

Vat photopolymerization is a light-induced printing process in which a liquid resin is selectively cured layer-by-layer to form a solid object.<sup>102</sup> This technique is particularly well-suited for low-viscosity, UV-curable smart polymer systems, including shape-memory acrylate formulations, light-responsive hydrogels, and drug-encapsulating polymer networks. It encompasses several subcategories such as stereolithography, digital light processing, and continuous liquid interface production.<sup>103–107</sup> In vat photopolymerization, a transparent vat is filled with a liquid resin containing monomers or oligomers, photoinitiators, and functional additives. A UV or visible light source is used to selectively expose the resin, initiating crosslinking in predefined regions that correspond to the cross-sectional slices of a computer-aided design (CAD) model. Following the curing of each layer, the build platform shifts vertically—either upward or downward, depending on the system configuration—to enable the application of a new resin layer. This cycle continues iteratively until the complete three-dimensional structure is fabricated.<sup>108</sup>

**3.1.1. Stereolithography (SLA).** SLA is the first and one of the most commonly employed vat photopolymerization techniques. It utilizes a focused UV laser to selectively cure a photosensitive resin typically composed of acrylate or methacrylamide monomers at the surface of the liquid, resulting in the layer-by-layer formation of a solid 3D structure (see Fig. 10a and b).<sup>10</sup> Following the curing of each layer, the build platform moves incrementally to allow subsequent layers to be polymerized atop the previous ones. SLA systems come in various configurations, differing in laser orientation (top-down or bottom-up) and movement direction of the build platform.

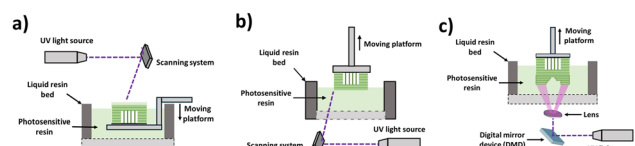


**Fig. 10** Schematics of 3D printing techniques (a) SLA (top-down), (b) SLA (bottom-up) and (c) DLP. Reproduced with permission from ref. 108. Copyright 2022, Elsevier.

Its high resolution has made it a valuable tool for fabricating microscale and even submicron polymer structures. The resolution is typically in the range of 25–100  $\mu\text{m}$ , enabling high-precision microstructures suitable for biomedical scaffolds and optical components. SLA supports the fabrication of smart polymers that respond to light, temperature, or humidity, although it is limited by oxygen inhibition and shrinkage-induced deformation.

A major benefit of SLA is its nozzle-free operation, which avoids issues such as nozzle clogging<sup>109</sup> and allows for the processing of highly viscous resins that are unsuitable for extrusion-based methods. However, SLA also presents several limitations, including expensive equipment, generation of chemical waste, and the necessity for post-processing to ensure full curing and interlayer adhesion. Dimensional instability due to resin shrinkage and a trade-off between resolution and print speed are additional concerns. Moreover, the exclusive use of photocurable resins necessitates the incorporation of photoinitiators, which, if not fully reacted, may leave residual monomers and initiator fragments posing potential cytotoxicity risks in biomedical applications.<sup>109</sup> To optimize SLA for polymer-based applications, it is critical to understand and control key resin properties such as curing kinetics, light absorption characteristics, sensitivity, and penetration depth. These parameters directly influence printing fidelity, mechanical integrity, and the overall performance of the printed components.<sup>110</sup>

**3.1.2. Digital light processing (DLP).** DLP utilizes a digital micromirror device to project an entire layer of patterned light, curing each cross-section simultaneously (Fig. 10c). Unlike SLA, which employs a focused UV laser, DLP uses a broad-spectrum light source to polymerize entire layers simultaneously.<sup>38</sup> The printing process closely resembles that of SLA, wherein the build platform either moves upward lifting the printed object from a vat of photopolymer to allow resin replenishment for the next layer or downward, submerging it to form a new layer on the exposed surface.<sup>111</sup> This approach significantly improves printing speed while maintaining high resolution. DLP enables spatial control over crosslinking density, which is essential for producing functionally graded smart devices. Its compatibility with multi-material and photo-reactive smart polymers makes it ideal for 3D printing applications.

The DLP technique offers a distinct advantage over SLA by enabling the simultaneous curing of an entire layer in a single

light exposure, thereby enhancing overall printing efficiency. It is also capable of achieving high-resolution fabrication at both micro and nanoscale levels.<sup>112</sup> The printed objects produced *via* DLP exhibit similar mechanical and surface characteristics to those fabricated by SLA, particularly in terms of smooth surface finish, which is superior to that achieved by extrusion-based techniques such as fused filament fabrication (FFF).<sup>113</sup> Compared to SLA, DLP is generally faster and more cost-effective, as it eliminates the need for laser scanning across the horizontal plane. Instead, layer formation is controlled solely by the vertical movement of the build platform, streamlining the printing process.<sup>114</sup>

**3.1.3. Continuous liquid interface production (CLIP).** CLIP is an advanced photopolymerization-based additive manufacturing technique that utilizes a continuous, bottom-up approach to fabricate high-resolution 3D objects. Unlike traditional layer-by-layer SLA, CLIP employs a UV light source projected through an oxygen-permeable, UV-transparent window located at the base of a resin vat. A key feature of this system is the formation of a persistent “dead zone” which is a thin liquid interface maintained by oxygen inhibition that prevents the polymerized resin from adhering to the window surface. This enables a non-stop curing process, allowing for significantly faster build rates and the production of parts with smoother surfaces and superior mechanical properties.<sup>115</sup>

CLIP is compatible with a variety of photopolymer resins, including acrylate- and methacrylate-based systems, elastomeric materials, and polyurethane-based smart polymers, which can be engineered for specific responsiveness. This makes it suitable for fabricating complex 3D and 4D structures such as flexible lattices, biomedical scaffolds, soft robotic components, and shape-changing devices. Its high throughput, fine surface finish, and capability to produce functionally graded materials position CLIP as a transformative technology in the additive manufacturing landscape, particularly in fields like biomedical engineering, soft electronics, and custom prosthetics.

### 3.2. Powder bed fusion

Powder bed fusion involves the selective fusion of polymer powders using thermal or photonic energy to create the 3D printed object.<sup>116</sup> It is advantageous for its ability to build complex, support-free geometries with high strength and low weight.<sup>117</sup> It is also compatible with thermoplastic smart polymers and composites.<sup>118</sup>

**3.2.1. Selective laser sintering (SLS).** SLS is an additive manufacturing method that constructs three-dimensional objects in a layer-wise manner by employing a laser to selectively sinter or fuse powdered materials at designated regions (see Fig. 11a).<sup>119</sup> This fusion can occur through various mechanisms, including solid-state sintering, partial or complete melting, or chemically induced bonding. In SLS, a thin layer of powder such as a polymer, composite, ceramic, or metal is uniformly spread over a build platform using a roller or blade. A laser is used to selectively scan the powder bed, generating localized heat that fuses the particles in specific areas. After

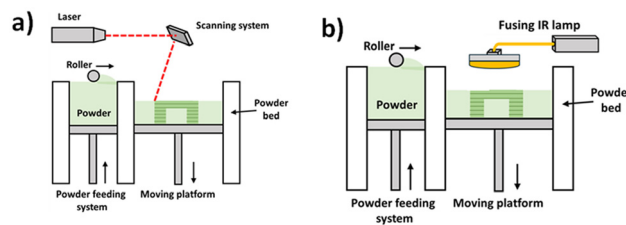


Fig. 11 Schematics of 3D printing techniques (a) SLS, and (b) MJF. Reproduced with permission from ref. 108. Copyright 2022, Elsevier.

each layer is consolidated, a fresh layer of powder is spread over the surface, and the cycle continues iteratively until the complete three-dimensional object is produced.<sup>119</sup>

For polymer-based SLS, common materials include thermoplastics like polyamide (PA), thermoplastic polyurethane (TPU), and polyether ether ketone (PEEK), which offer good mechanical properties and thermal resistance. In some SLS systems, liquid binders may be used in conjunction with powders to promote particle bonding.<sup>119</sup> SLS provides a respectable resolution range (typically 20–150 µm), supports complex geometries without the need for support structures, and allows for the reuse of unfused powder, enhancing material efficiency.<sup>119</sup>

Despite its advantages, SLS is not without challenges. One of the main drawbacks is the thermal stress introduced by rapid heating and cooling cycles, which can lead to warping, shrinkage, and dimensional inaccuracies.<sup>119</sup> These thermal effects are particularly pronounced in polymer powders with high shrinkage coefficients, and they necessitate careful control of printing parameters and thermal management. A comprehensive understanding of the thermal characteristics, rheological behavior, and particle size distribution of polymer powders is crucial for optimizing the quality and functional performance of components fabricated *via* SLS.

**3.2.2. Multi jet fusion (MJF).** MJF is a proprietary advancement over SLS, where a fusing agent is selectively deposited onto the powder bed, followed by infrared heating to induce fusion (Fig. 11b). MJF allows for higher resolution and better mechanical homogeneity. It is gaining popularity for printing magneto-responsive or conductive polymer powders with enhanced surface finish and fidelity. MJF is developed by Hewlett-Packard Inc. (HP), patented in 2014 and introduced to the market in 2016.<sup>120</sup> Like SLS, polymer particles are deposited layer by layer in MJF. However, it employs a distinct energy source and consolidation mechanism. Instead of a laser, MJF uses infrared (IR) lamps in combination with inkjet-deposited functional agents to selectively melt regions of the powder bed.<sup>120</sup> During printing, fusing agents containing carbon black and other additives are deposited onto the powder surface at voxel resolution, corresponding to the part geometry. These agents absorb IR radiation, converting it into heat to induce local melting. Simultaneously, a detailing agent is printed along the perimeter to suppress fusion through localized cooling, enhancing edge definition and print accuracy.<sup>121</sup>

MJF delivers a planar energy input across the entire powder layer, enabling fast and uniform melting compared to the point-by-point scanning mechanism of SLS.<sup>122</sup> As a result, MJF achieves a geometry-independent layer processing time of approximately 10 seconds, with build rates reaching up to  $5058\text{ cm}^3\text{ h}^{-1}$  substantially higher than the  $\sim 1200\text{ cm}^3\text{ h}^{-1}$  rate of SLS.<sup>122</sup> This reduction in processing time makes MJF particularly suitable for high-volume and time-efficient production.<sup>123</sup>

Material options for MJF are currently limited, with polyamide 12 (PA12) being the most widely used polymer due to its low melt viscosity, high coalescence rate, and good mechanical performance.<sup>124,125</sup> Recent studies have also explored PA12 reinforced with glass beads to improve mechanical strength and microstructural uniformity.<sup>126</sup> Compared to SLS, MJF-printed parts have shown improved elongation at break<sup>127</sup> and reduced anisotropy, particularly in the Z-direction, where tensile strength can be 25% higher.<sup>128</sup> This enhancement is largely attributed to the uniform heat distribution and the action of the fusing agent, which leads to denser, less porous structures.<sup>129</sup>

### 3.3. Material extrusion

Extrusion-based additive manufacturing is a versatile fabrication technique that constructs smart and customized structures by continuously depositing material layer by layer.<sup>130</sup> This method is particularly well-suited for producing a broad spectrum of objects, ranging from microscale prototypes to large-scale architectural or functional components.<sup>131</sup> Material extrusion refers to the deposition of molten or viscoelastic material through a nozzle, followed by solidification through cooling or crosslinking. It is one of the most flexible and accessible printing methods. In extrusion-based printing, the sequentially deposited layers are bonded together through one of two primary mechanisms.

**3.3.1. Fused deposition modeling (FDM).** FDM, also known as Fused Filament Fabrication (FFF), is among the most extensively utilized additive manufacturing techniques owing to its adaptability, low cost, eco-friendliness, and ease of operation. A key advantage of this process is that it operates without the need for organic solvents.<sup>132</sup> In FDM, thermoplastic filaments are heated, melted, and extruded through a nozzle to layer-by-layer constructions in three dimensions (Fig. 12a). Owing to its adaptability, FDM has found extensive applications in various sectors including electronics, medi-

cine, automotive, and aerospace industries.<sup>133</sup> The incorporation of diverse smart polymers into the filament feedstock enables the fabrication of complex hierarchical mesostructures.<sup>134</sup> Advancements in FDM technology such as Arburg Plastic Free forming have significantly broadened the range of TRP-based inks compatible with FDM systems.<sup>135,136</sup> However, the use of TRP-based filaments presents challenges, including filament fragility leading to inconsistent extrusion and structural deformation post-printing, which results in low mechanical integrity and suboptimal print performance.<sup>137</sup> To address these limitations, functional fillers are often integrated into TRP-based inks to enhance rheological behavior, improve tensile strength, and optimize the overall printability of the fabricated components.<sup>138</sup>

**3.3.2. Direct ink writing (DIW).** DIW also referred to as robot-assisted shape deposition<sup>139</sup> or direct write fabrication/robocasting,<sup>140</sup> is an extrusion-based additive manufacturing technique wherein liquid-phase materials such as thermo-responsive polymers are precisely deposited layer-by-layer onto a substrate to fabricate three-dimensional structures (Fig. 12b). The rheological characteristics of TRP-based inks critically influence both the printing resolution and overall performance. A high consistency index generally enhances the geometrical fidelity of printed constructions, albeit with an increased likelihood of nozzle clogging. Thus, achieving a well-optimized ink formulation exhibiting high viscosity ( $10^3\text{--}10^6\text{ mPa s}$ ), pseudoplastic behavior, and a discernible yield stress is essential for effective DIW processing.<sup>141</sup> Compared to other 3D printing techniques, DIW offers a more cost-effective and time-efficient route to fabricate complex 3D and 4D hierarchical mesostructures.<sup>92</sup> The utilization of TRP-based inks with tailored viscoelastic properties ensures the structural integrity of printed architecture, enabling them to retain shape even under the weight of successive layers. These inks typically undergo a volume phase transition, providing a biomimetic platform to enhance the functional capabilities of the final constructs. This approach has enabled the design of intricate porous scaffolds,<sup>142</sup> applications in tissue engineering,<sup>143</sup> and the development of soft electronic devices.<sup>144</sup> For instance, the coil-to-globule transitions in TRP-based hydrogels result in rapid volume shrinkage, facilitating solvent and drug release through both burst and sustained diffusion mechanisms.<sup>145</sup> Additionally, TRP-based 3D printing has been employed for fabricating hierarchical mesostructures embedded with bioactive agents for controlled drug delivery applications.<sup>146</sup>

The inherent simplicity and versatility of DIW have allowed its adoption in producing smart structures for personalized biomedical devices, bioceramic implants, and lithium-ion batteries.<sup>147,148</sup> The incorporation of TRP-based inks further enhances the physicomechanical,<sup>149</sup> thermal,<sup>150</sup> and biological<sup>151</sup> properties of 3D-printed constructs, broadening their functional applicability. However, while these TRP-based architectures offer design flexibility, they often suffer from poor physical robustness and interfacial affinity, posing significant limitations for broader AM applications. Overcoming these challenges necessitates additional research into the modifi-

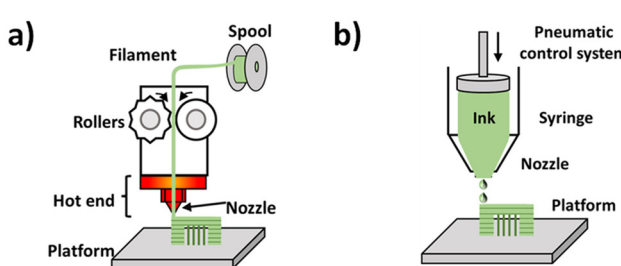


Fig. 12 Schematics of 3D printing techniques (a) FDM/FFF, and (b) DIW. Reproduced with permission from ref. 108. Copyright 2022, Elsevier.

cation and compatibility of TRP-based inks.<sup>96,152,153</sup> For example, the modification of gelatin has enabled DIW printing of customized 3D objects at physiological temperature (37 °C), achieving structurally stable geometries without requiring support materials.<sup>154–157</sup> Enhanced printing performance was observed with increasing concentrations of modified gelatin, and the resultant structures demonstrated promising potential in tissue scaffolding, drug delivery, and sustainable packaging due to their biodegradability and biocompatibility. Rastin *et al.*<sup>156</sup> developed a multifunctional bioink for 3D bioprinting by integrating thermoresponsive methylcellulose and kappa-carrageenan hydrogels with the conductive polymer PEDOT:PSS. This composite ink offered the added advantage of electrical conductivity, further advancing the utility of TRP-based systems in functional 3D printing platforms.

### 3.4. Material jetting

Material jetting involves the deposition of droplets of polymeric ink that solidify *via* thermal, photonic, or phase-change processes. It is ideal for patterning fine features and multi-material constructs.

**3.4.1. Inkjet printing.** Inkjet printing differs fundamentally from other 3D printing techniques by enabling drop-on-demand deposition using diverse feedstocks, including colloidal bioinks, hydrogels, and aqueous biopolymers (Fig. 13a). This process involves the precise deposition of microdroplets onto a substrate to construct 3D structures through layer-by-layer curing. Inkjet printing operates primarily *via* two modes namely continuous inkjet and drop-on-demand inkjet printing.<sup>158,159</sup> In continuous inkjet printing, inks exhibiting shear-thinning behavior are ejected through a nozzle and subsequently form droplets.<sup>160</sup> Conversely, drop-on-demand printing is a non-contact technique where droplets are generated either by thermal or piezoelectric actuation. The thermal variant utilizes localized heating to form vapor bubbles that expel TRP-based inks. In the piezoelectric mode, electrical stimulation induces acoustic pulses *via* piezoelectric materials, triggering droplet ejection.<sup>161,162</sup> Owing to its ability to precisely control droplet size, placement, and volume, inkjet printing has found broad utility in bioengineering, bioelectronics, and the automotive industry. It is valued for its high-resolution output, cost-efficiency, and non-invasive deposition capabilities.<sup>163</sup>

Recent advancements in the integration of TRP-based inks have significantly improved their bioavailability, solubility, and

thermal stability, enhancing their multifunctionality for various biomedical applications.<sup>164–166</sup> Inkjet printing of TRP-based inks requires finely tuned formulations to avoid nozzle clogging, particularly through the use of particles with diameters less than 5 µm. To achieve this, nanosuspensions have been developed *via* high-pressure homogenization, enabling the stable inkjet printing of drug-loaded TRP systems. For instance, folic acid nanosuspensions with particle sizes well below 5 µm and 10% (w/w) drug loading have been formulated for this purpose.<sup>167</sup> This approach, which enhances the solubility of poorly water-soluble drugs, facilitates patient-specific drug delivery through precise, inkjet-based fabrication.

**3.4.2. PolyJet printing.** PolyJet is an additive manufacturing technique that utilizes photopolymer jetting, wherein liquid photopolymer droplets are selectively deposited and cured using UV light in a layer-by-layer fashion to fabricate 3D structures (Fig. 13b). The printhead incorporates a roller to evenly spread each layer and UV lamps to ensure rapid and complete photopolymerization of the deposited droplets. A distinct support material is co-printed, specifically designed for easy removal either by mechanical separation or dissolution in water.<sup>168–170</sup> Similar to thermal-based 3D printing methods, the mechanical properties of PolyJet-printed parts—such as elastic modulus and fracture stress—are influenced by the build orientation, although tensile strength remains relatively unaffected by the printing direction.<sup>171</sup>

PolyJet is an advanced inkjet-based 3D printing technique that significantly enhances dimensional control by enabling the *in situ* photopolymerization of materials.<sup>172</sup> Unlike conventional inkjet printing, which is generally limited to 2D or 2.5D structures due to the fluidic behavior of low-viscosity inks, PolyJet printing deposits droplets of photopolymer that are immediately cured by UV light, allowing the fabrication of fully 3D architectures. This layer-by-layer approach facilitates the creation of complex geometries with high resolution and smooth surface finishes.<sup>173</sup> A key advantage of PolyJet is its compatibility with multi-material printing. By utilizing multiple nozzles, different inks with varied functionalities can be printed simultaneously, enabling the development of heterogeneous structures with programmable properties. This capability makes PolyJet particularly suitable for 4D printing applications, where shape evolution or functional transformation over time is desired. Several notable examples demonstrate the potential of PolyJet in fabricating shape memory polymers (SMPs) and self-actuating structures. Raviv *et al.*<sup>174</sup> developed self-evolving 3D structures that deform in response to thermal stimuli, while Ding *et al.*<sup>175</sup> printed composite materials with pre-programmed shape transformation behavior upon heating. Wu *et al.*<sup>176</sup> fabricated SMP composites with active actuation, and Yap *et al.*<sup>177</sup> produced honeycomb-patterned SMPs using PolyJet technology. Wagner *et al.*<sup>178</sup> constructed shape-shifting auxetic structures, and Ge *et al.*<sup>179</sup> applied the technique for active origami fabrication. Additionally, Meisel *et al.*<sup>178</sup> demonstrated the integration of functional SMP elements to impart actuation capabilities within 3D printed components.

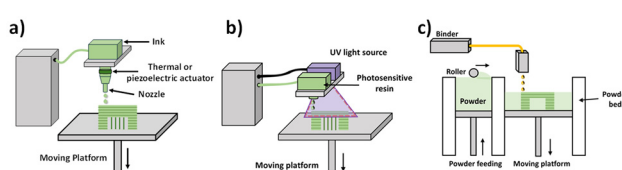


**Fig. 13** Schematics of 3D printing techniques (a) inkjet printing, (b) PolyJet printing, and (c) binder jetting. Reproduced with permission from ref. 108. Copyright 2022, Elsevier.

These developments under core PolyJet's unique potential in the domain of 4D printing, combining geometric freedom, high resolution, and temporal reconfigurability, thereby paving the way for advanced applications in biomedical devices, robotics, and smart materials systems.

### 3.5. Binder jetting

Binder jetting uses inkjet nozzles to deposit a liquid binder selectively onto a powder bed (Fig. 13c). The bonded powder forms a solid body, which can be post-processed by infiltration or sintering. Although not widely used for smart polymers, binder jetting has potential in producing porous scaffolds and gradient materials, where functionality can be introduced post-printing *via* infusion with smart gels or elastomers. Its advantages include the ability to print large and complex geometries without support structures, though printed parts typically require densification and functionalization.

## 4. Material design and formulation strategies

Material design and formulation strategies form the backbone of developing smart polymers suitable for AM, particularly in the context of 4D printing where shape evolution, actuation, or functionality in response to external stimuli is critical.<sup>38</sup> The effectiveness of smart materials in AM systems relies on the precise engineering of their molecular structure, responsiveness, rheological behavior, and interfacial interactions during and after printing.<sup>180</sup> This section elaborates on two key pillars of smart material development *i.e.* the synthesis and functionalization of polymeric systems, and the formulation of composites and hybrid materials compatible with different AM platforms such as SLA, FDM, and DIW.

### 4.1 Polymer synthesis and functionalization

The synthesis of smart polymers for AM requires a meticulous approach to molecular design that enables the integration of responsive functionalities without compromising printability. Reineke *et al.*<sup>181</sup> demonstrated the thoughtful molecular design behind smart polymers tailored for additive manufacturing (Fig. 14a). A series of triallyl levoglucosan (TALG)-based networks were synthesized *via* UV-initiated thiol-ene chemistry using bio-based thiols, allowing control over thermomechanical and degradable properties. One formulation (TALG-poly3SH-1) was successfully 3D printed using UV-assisted DIW (Fig. 14b-d). Thermoresponsive polymers, shape-memory polymers (SMPs), photoresponsive materials, and hydrogels represent the most prominent classes of smart materials utilized in AM.<sup>38</sup>

In shape-memory systems, thermoplastic matrices like poly(lactic acid) (PLA) or polyurethanes are designed to exhibit a defined transition temperature, which allows the material to be temporarily deformed and subsequently recover its original shape upon heating.<sup>182,183</sup> When functionalized with magnetic fillers such as  $\text{Fe}_3\text{O}_4$  nanoparticles, these SMPs can be remo-

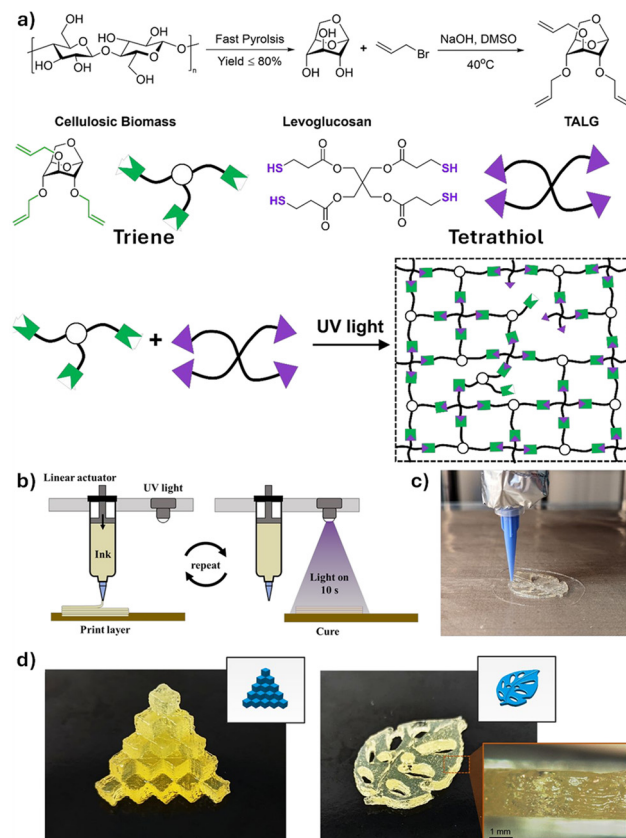


Fig. 14 (a) Schematic diagram of DIW 3D printing ink with triene and tetrathiol as the main components and its photopolymerization reaction. (b) A schematic illustration of the DIW process used for 3D printing. (c) Real-time image capturing the extrusion of TALG-poly3SH-1 resin during printing. (d) Representative 3D printed structures fabricated using the TALG-poly3SH-1 formulation. Reproduced with permission from ref. 181. Copyright 2023, Royal Society of Chemistry.

tely actuated using external magnetic fields.<sup>183</sup> For example, in one study, PLA-based SMPs combined with magnetically active fillers were used in DIW printing followed by UV-curing to generate programmed geometries capable of reversible magnetic shape transformations.<sup>183</sup> Such thermomagnetic actuation has expanded the functional scope of printed components in robotics and biomedical devices.<sup>108</sup>

Hydrogels used in 3D printing, particularly in DIW and SLA, are typically synthesized from hydrophilic monomers such as acrylamide, (PEG),<sup>184</sup> (PNIPAm)<sup>185</sup> or (HEMA).<sup>186</sup> These hydrogels can be prepared as homopolymers, copolymers, or semi-interpenetrating networks (semi-IPNs), and their mechanical properties are controlled by adjusting the degree and type of crosslinking.<sup>186,187</sup> Covalent crosslinking using bifunctional agents like *N,N'*-methylenebisacrylamide or ionic crosslinking using divalent cations are common strategies.<sup>188</sup> The selection of polymer and crosslinker strongly influences the network density, which in turn governs swelling behavior, print fidelity, and actuation responsiveness. For applications requiring shear-thinning behavior for extrusion-based printing, the self-assembly of physical gels through

hydrogen bonding or hydrophobic interactions is employed to achieve desired rheological characteristics.<sup>189</sup>

In the case of SLA and DLP printing, functionalization strategies aim to incorporate photo-crosslinkable groups such as acrylates or methacrylates onto the polymer backbone. These groups enable rapid curing under ultraviolet light, forming robust crosslinked networks. A critical aspect of resin formulation for SLA includes balancing viscosity and reactivity: low-molecular-weight reactive diluents are often added to reduce viscosity and enhance flow, though excessive dilution can lead to brittle networks.<sup>116</sup> Tailored resins incorporating dynamic covalent chemistries, such as Diels–Alder adducts or disulfide linkages, have also been developed to impart recyclability and healability to printed structures.<sup>116,190</sup>

Liquid crystal elastomers (LCEs), which display anisotropic contraction upon heating, have gained increasing attention in the field of smart 3D printing.<sup>191</sup> These materials require specialized synthesis involving mesogenic monomers and precise alignment techniques. In hot-DIW printing, for instance, shear forces in the nozzle orient the mesogens along the print path, which is then locked in place by thermal or photo-crosslinking.<sup>192</sup> This directional alignment imparts programmable deformation behavior upon activation, allowing for sophisticated shape morphing in soft actuators.

The scope of functionalization extends beyond stimuli responsiveness to include bioactivity, conductivity, and degradation. Polymers can be post-modified using click chemistry, esterification, or thiol–ene photopolymerization, charged groups, or nanoparticles, enabling applications in tissue engineering, bioelectronics, and environmental sensing.<sup>193–195</sup>

As such, polymer synthesis and functionalization provide a powerful toolkit for tuning material performance and compatibility with AM technologies.

## 4.2 Composites and hybrids

While synthetic strategies ensure that polymers are responsive and printable, they often require augmentation with additional components to meet the multifunctional demands of AM-based applications. Fig. 15 illustrates the functional integration of smart polymer composites in advanced 3D and 4D printed devices, emphasizing their role in sensing and actuation applications. In the context of intelligent sensors, Ren *et al.*<sup>196</sup> developed forked electrodes composed of 4D printed carbon black (CB)/polylactic acid (PLA) composites and shape-memory polyurethane (PU), demonstrating a coplanar design that enables highly sensitive detection of environmental stimuli (Fig. 15a). The thermal or mechanical deformation modulates inter-electrode spacing, inducing measurable capacitance variations, thus allowing dynamic signal responsiveness. Similarly, Wang *et al.*<sup>197</sup> utilized conductive graphene/PLA (GPLA) as an active thermoplastic layer and a paper-based passive constraint layer to fabricate reversible bilayer actuators with intrinsic strain-sensing capability (Fig. 15b). These actuators operate through thermally activated contraction and relaxation cycles enabled by stored pre-strain and shape-memory behavior during FDM printing. This material has been used as a click grab actuators based on the thermal actuation (Fig. 15b(a1)–(a5)). Composite and hybrid systems have therefore emerged as essential material platforms for smart 3D printing, offering synergistic enhancements in

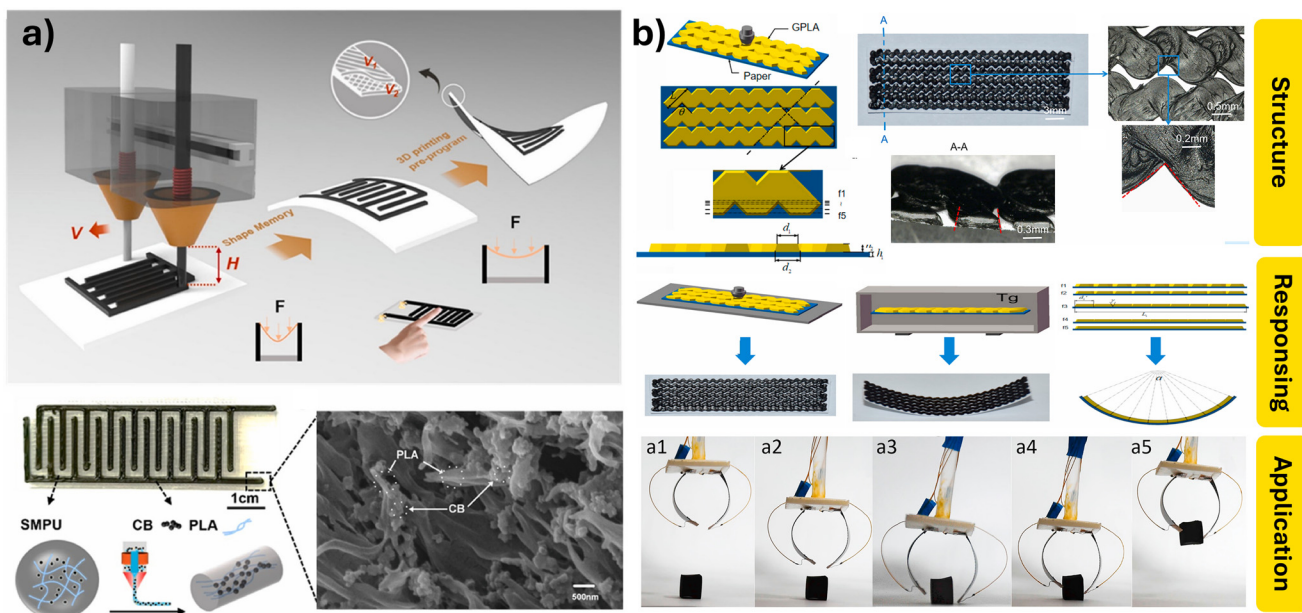


Fig. 15 (a) FDM 3D printing of CB/PLA composites and the response behavior. Reproduced with permission from ref. 196. Copyright 2023, Elsevier. (b) Structure, response behavior, and application of GPLA composites printed by FDM. Reproduced with permission from ref. 197. Copyright 2021, Elsevier.

mechanical robustness, responsiveness, and functional versatility.<sup>108</sup> These systems typically consist of a polymer matrix embedded with organic or inorganic fillers that serve as mechanical reinforcements, stimuli-sensitive actuators, or conductive networks.

In the case of FDM, where thermoplastics such as PLA or ABS are used as the base material, composite filaments are prepared by incorporating fibers or particulate fillers.<sup>198</sup> Carbon nanotubes (CNTs), graphene nanoplatelets, and carbon fibers are frequently used to enhance tensile strength, thermal conductivity, and electrical response.<sup>108</sup> For instance, CNT-modified filaments have been shown to facilitate inter-layer welding *via* microwave absorption, thereby improving the mechanical integrity of the printed parts.<sup>199</sup> The addition of such fillers not only tailors mechanical and thermal properties but also enables the creation of strain sensors and electrically responsive devices.

DIW formulations benefit greatly from composite approaches, particularly for applications requiring actuation or sensing. Hydrogels are often loaded with piezoelectric ceramics such as barium titanate or zinc oxide to create structures that respond to mechanical stress with electrical output. Similarly, incorporating  $\text{Fe}_3\text{O}_4$  or neodymium magnets enables remote actuation under magnetic fields.<sup>183</sup> Achieving uniform dispersion of these fillers is critical, as agglomeration can compromise both printability and performance. Surface functionalization of nanoparticles, as well as the use of surfactants or dispersants, helps maintain homogeneity and stability of the ink. These composite formulations must also exhibit shear-thinning behavior, which is essential for smooth extrusion and shape fidelity during DIW printing.

Photopolymer resins used in SLA and DLP can be enhanced with nano- or microscale fillers to improve structural performance.<sup>116</sup> For example, the addition of nanosilica or carbon black increases stiffness and thermal stability. Hybrid resin formulations can also include reactive ceramic precursors that convert to functional ceramics upon post-processing. Dual-cure strategies, involving both photo- and thermal-curing steps, are increasingly used to fabricate multi-functional parts with gradient properties.

A particularly promising approach involves multi-material printing, where multiple formulations are deposited simultaneously or sequentially to produce structures with spatially varying properties. This strategy is well suited for soft robotics and biomedical applications, where different regions of a single printed object may require distinct stiffness, bioactivity, or responsiveness. For instance, silicone elastomers with different crosslinking densities have been printed side by side to create pneumatic actuators capable of complex deformation.

The integration of functional fillers also opens the door to 4D printing, wherein the printed object changes shape or function over time. The dimensionality of fillers plays a crucial role in this context. Zero-dimensional fillers like metal nanoparticles provide isotropic conductivity, while one-dimensional fillers such as CNTs offer directional reinforcement. Two-

dimensional materials like graphene and MXenes impart a combination of mechanical strength, thermal conductivity, and electrochemical functionality. Moreover, the use of stimuli-responsive fillers, including thermochromic dyes, fluorescent particles, and liquid metal droplets, add further layers of complexity and utility to printed systems.

Ultimately, the design of composites and hybrid materials must balance printability, structural integrity, and functional output. Formulation strategies that optimize polymer-filler interactions, rheological behavior, and curing kinetics are indispensable for realizing the full potential of smart polymers in AM. As additive manufacturing continues to evolve, these hybrid materials will play an increasingly central role in bridging the gap between structural design and functional performance.

## 5. Applications of 3D-printed smart polymers

### 5.1. Conductive sensors

Sensors give continuous data, which is necessary for prompt and precise health assessments, in contrast to conventional intermittent analytical procedures.<sup>200</sup> In order to improve quality of life and maybe prolong life expectancy, this continuous monitoring capability is especially crucial for controlling changes.<sup>201</sup> The development of 3D printing technology has greatly improved sensor production and design. Unprecedented customizability made possible by 3D printing makes it possible to create sensors suited to demand.<sup>202</sup> With the use of this technology, sensors can become smaller, less intrusive, and more pleasant for extended usage. Furthermore, 3D printing makes it easier to combine multipurpose materials with intricate sensor structures, which results in the creation of increasingly sophisticated and effective biosensors. Since electrical conductivity gives materials the ability to function as actuators and sensors, the most common method for detecting electrical signals is to incorporate a conductive phase into polymer matrices.<sup>203–205</sup> For example, Song *et al.* developed a flexible pressure sensor with a layered sandwich-like architecture using a modified electrohydrodynamic (EHD) jetting process (Fig. 16a(i) and a(ii)). This sensor demonstrated the ability to respond to environmental stimuli (Fig. 16a(iii) and a(iv)) and detect multiple physiological signals (Fig. 16a(v) and a(vi)). The sensing mechanism was based on a mesh composed of polyethylene oxide (PEO) embedded with graphene and polyaniline (PANI), printed *via* EHD, which exhibited a fast and proportional resistance change under external pressure (Fig. 16a(iii) and a(iv)). Variations in resistance allowed real-time monitoring of physiological activities, such as pulse signals during different physical states *e.g.*, swallowing, coughing, or drinking; (Fig. 16a(v)) and subtle throat movements (Fig. 16a(vi)). This work highlights the potential of 3D printing in improving sensor performance for health monitoring applications. This sensor tracks a number of physiological factors and simulates environmental circumstances.<sup>208</sup>

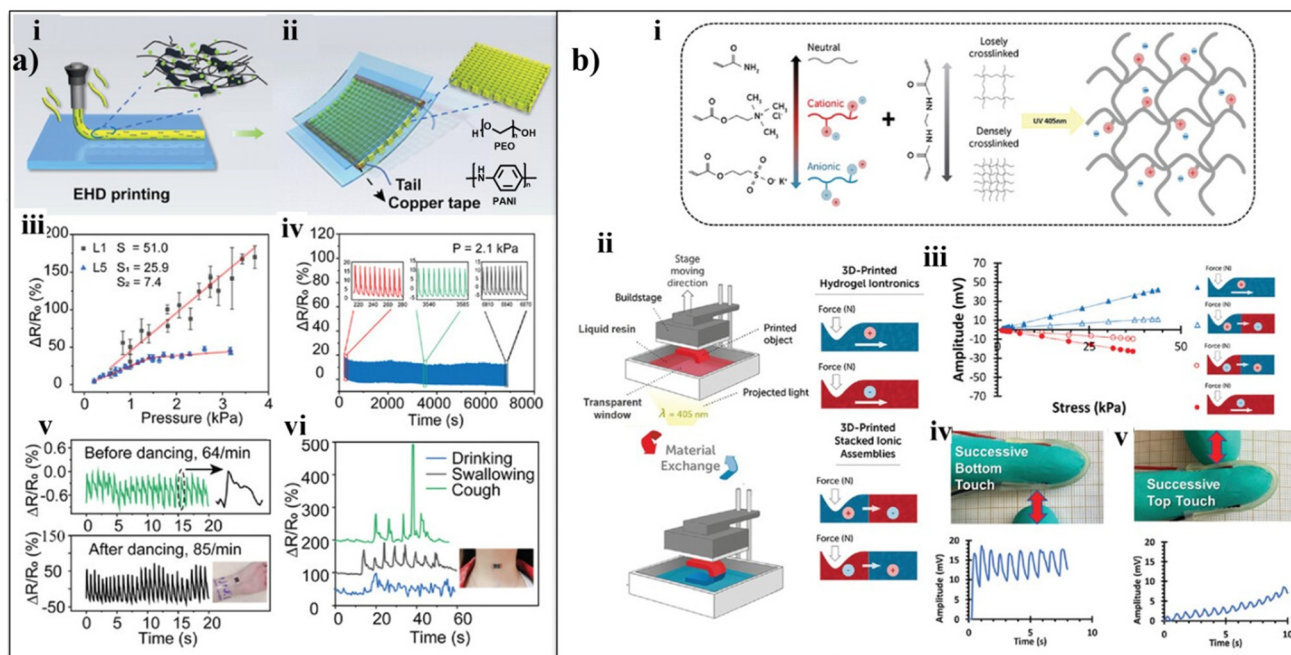


**Fig. 16** (a) (i) EHD jetting was used to deposit a sensing layer composed of PEO, PANI, and graphene. (ii) Illustration showing the cross-sectional structure of the completed layered pressure sensor. (iii) Sensor resistance variation under applied pressure for configurations with one and five jetted layers. (iv) Stability of the sensor's resistance over 1000 cycles of loading and unloading at a 0.15 Hz frequency. (v) Detection of pulse waveforms captured by the sensor both before and after physical exercise (dancing). (vi) Resistance signal profiles corresponding to human actions such as coughing, swallowing, and drinking. Reproduced with permission from ref. 206. Copyright 2022, ACS. (b) (i) Schematic of the copolymerization reaction involving AAm with either AETA or SPA, using MBA as the crosslinker, utilized in SLA printing. (ii) Demonstration of SLA-based fabrication of multilayered ionic structures through alternating resin vats, enabling control over ionic species, charge densities, and crosslinking levels within the ionictronic components. (iii) Voltage output response as a function of stress applied to compartments containing either SPA or AETA at 30 mol% concentration. (iv and v) A 3D-printed dual-compartment finger sleeve mimicking tactile responses at the fingertip and fingernail, exhibiting distinct sensitivity profiles. Reproduced with permission from ref. 207. Copyright 2023, Wiley.

This invention shows how 3D printing can improve sensor responsiveness and functioning, which is essential for applications involving health monitoring. Ionic conductors, in addition to electrical conductors, are able to detect mechanical forces and biological motions. Raguez's team explored ionictronic, as shown in Fig. 16b, hydrogels in pressure sensing, utilizing the piezooionic effect, where voltage is produced due to charge migration from compressed regions. The hydrogel system, based on PAAm, was compatible with stereolithography 3D printing (Fig. 16b(i)). Incorporating ionic co-monomers into the resin (Fig. 16b(ii)) introduced mobile counterions, granting the material ionic conductivity. Sensor performance could be tuned by altering ion concentration, crosslinking density, and charge distribution (Fig. 16b(iii)). A two-layer tactile sensor was printed to emulate fingertip sensation, showing distinct responses at the top and bottom contact zones (Fig. 16b(iv) and b(v)). This gradient sensitivity was controlled by sequentially switching resin compositions during the printing process using different reservoirs.<sup>209</sup>

Avoiding skin irritation or allergic reactions is frequently the main concern in these applications, and these can be easily controlled with the right material selections. However, the standards for biocompatibility become much stricter when

these sensors are meant to be used with interior tissues or organs. In such cases, the compatibility between sensor materials and internal body components like organs, tissues, or cells plays a critical role in ensuring biocompatibility. Zhu *et al.* conducted an *in vivo* experiment in which they relocated the sensor from the external skin surface to directly interface with the organ surface. The authors combined using the DIW method adapts to dynamic biological surfaces, enabling continuous spatial mapping of lung deformation through the use of an ionic hydrogel.<sup>210</sup> The ionic hydrogel was fabricated as a thin layer functioning as a sensing component after lithium chloride was dissolved in the PAAm matrix; it showed conductivity change with deformation. The surrounding electrodes extracted the sheet conductivity distribution, which was subsequently converted into lung deformation spatiotemporal mapping data.

## 5.2 Capacitive sensors

Sensors provide an additional means of detecting mechanical impulses from organs in addition to resistive sensors. The basic idea behind capacitive sensors is the detection of capacitance change, which can be impacted by pressure, deformations, or object proximity.<sup>211</sup> Because of this feature, they

are very useful for applications that call for accurate assessment of physical changes, like tracking physiological movements and identifying minute pressure changes. Their multi-layered constructions may be manufactured with greater flexibility thanks to 3D printing. Yi *et al.* explored the influence of flexible dielectric layer deformation on the variation in capacitance of capacitive sensors.<sup>212</sup> The team utilized DIW to fabricate hemicylindrical microstructures with Ecoflex, a stretchable aliphatic-aromatic copolyester, serving as the dielectric layer. Compared to conventional planar designs, this microstructured configuration enhanced material deformation under equivalent pressures, enabling the sensor to detect subtle stimuli such as water droplets. Research suggests that aliphatic-aromatic copolymers may degrade with low toxicity, despite the fact that this sensor's use is now restricted to *in vitro* settings.<sup>213</sup> This implies that by choosing other materials for the PDMS/CNT layer, there might be ways to make the capacitive sensor biodegradable. Because of the contentious nature of CNT toxicity in particular,<sup>214</sup> care should be taken while using them in *in vivo* research.

The capability of capacitive sensors to operate as passive wireless sensors based on inductor-capacitor (LC)—a concept that was first put forth in 1967—is one of its key advantages.<sup>217</sup> A resonant LC circuit is formed by linking the sensing capacitor with a spiral-shaped inductor. The LC tank is remotely connected to a readout coil, which measures its impedance. As a result, the LC tank's resonant frequency shifts in response to the capacitor change.<sup>218</sup> Because there is no need for physical connections or batteries,<sup>218</sup> the system is appropriate for medical sensing applications.<sup>219</sup> Capacitive sensors, for example, can be used to assess biomechanical impulses from soft tissues or monitor internal organ functioning without invasive wiring,<sup>219</sup> which lowers infection. Herbert *et al.* employed aerosol jet printing (AJP) to develop a stretchable and flexible capacitive sensor, using polyimide as the dielectric layer and a silver nanoparticle-based composite for the electrodes (Fig. 17(vi) and (vii)).<sup>215</sup> Changes in applied pressure and deflection lead to modifications in the thickness of the dielectric layer. Variations in the applied pressure and deflection would alter the dielectric layer's thickness, which would alter the capacitance accordingly. Although polyimide has demonstrated support for cell viability and growth across various common cell types, more thorough research is required to evaluate its potential for therapeutic application.<sup>220</sup>

In addition to the previously described inkjet or aerosol jet printing, the FD approach is a straightforward processing technique that can be used to adjust microstructures for sensing purposes. For instance, by designing an origami-inspired insole integrated with wireless pressure sensing capabilities, Kim *et al.* concentrated their efforts on *in vitro* mechanical data (Fig. 17(viii)).<sup>221</sup> By instantaneously adjusting geometric designs, 3D printing allows for the customization of mechanical properties. Conductive thin layers and a dielectric layer with complex microstructures typically make up the construction of sensitive capacitors, making them appropriate for 3D printing processes. Additionally, capacitive sensors are a vital

device aimed at enhancing medical diagnostics and tracking treatment progress, due to their wireless capabilities, accuracy, and adaptability, which greatly advance personalized medicine.

### 5.3. Fluidic wearable sensors

Because the fluidic sensors don't come into direct contact with human tissue, they depend on 3D-printed polymers that offer chemical stability and compatibility with biofluids. The development of sweat sensors represents a significant application of this technology, enabling non-invasive monitoring of biomarkers for the diagnosis and real-time tracking of human health conditions.<sup>222</sup> Because these sensors need to be minimally harmful to the skin, biocompatibility is essential. Furthermore, for the printed materials to be comfortable and useful when worn, their ductility is crucial. Advanced 3D printing techniques are used to achieve this level of precision. For example, the complex microstructures required for effective sweat collection and analysis are frequently fabricated using DLP and DIW.<sup>223</sup> These techniques need the careful selection of materials based on their mechanical characteristics and capacity to create uniformly fine channels. Furthermore, these sensors' usefulness in individualized healthcare is increased by the addition of new features like multi-analyte detection<sup>224</sup> and real-time data transmission.<sup>225</sup>

A bioelectronic patch, for instance, was created by Kim *et al.* to assess many electrolyte levels in perspiration (Fig. 18a (i)–(iii)).<sup>224</sup> This example showcased the core components typically present in wearable sweat sensors, such as a sensing reservoir, mechanically optimized packaging, and a narrow inlet channel that enables sweat to enter the device through a combination of capillary action and the intrinsic pressure of perspiration.<sup>226</sup> The electrode geometry could be precisely controlled thanks to the DIW printing method, which guaranteed good ion detection sensitivity and specificity. By combining these elements, the wearable sweat sensor was capable of effectively monitoring multiple electrolytes present in sweat, offering useful information for evaluations of fitness and health. Combining advanced materials with high-precision 3D printing underscores the promise of wearable technology for non-invasive health monitoring, enabling the assessment of electrolyte levels, hydration status, and overall physiological condition.

While Kim *et al.*<sup>227</sup> applied 3D printing indirectly to build the base structure of a wearable sensor, Wu *et al.*<sup>228</sup> used a direct method by implementing DLP to fabricate detailed elements like inlets, valves, and reservoirs (Fig. 18b(i)–(iii)).<sup>228</sup> Their 3D-printed, centrally symmetric device allowed for step-wise sweat collection through capillary burst valves (CBVs), which controlled flow based on burst pressure. Optimized resin printing allowed for clear, time-resolved colorimetric analysis of chloride levels in sweat.

Rogers' team also incorporated capillary burst valves into their sweat sensor design, while also taking into account the device's mechanical performance to account for potential deformations during practical use.<sup>229</sup> Using methacrylate-

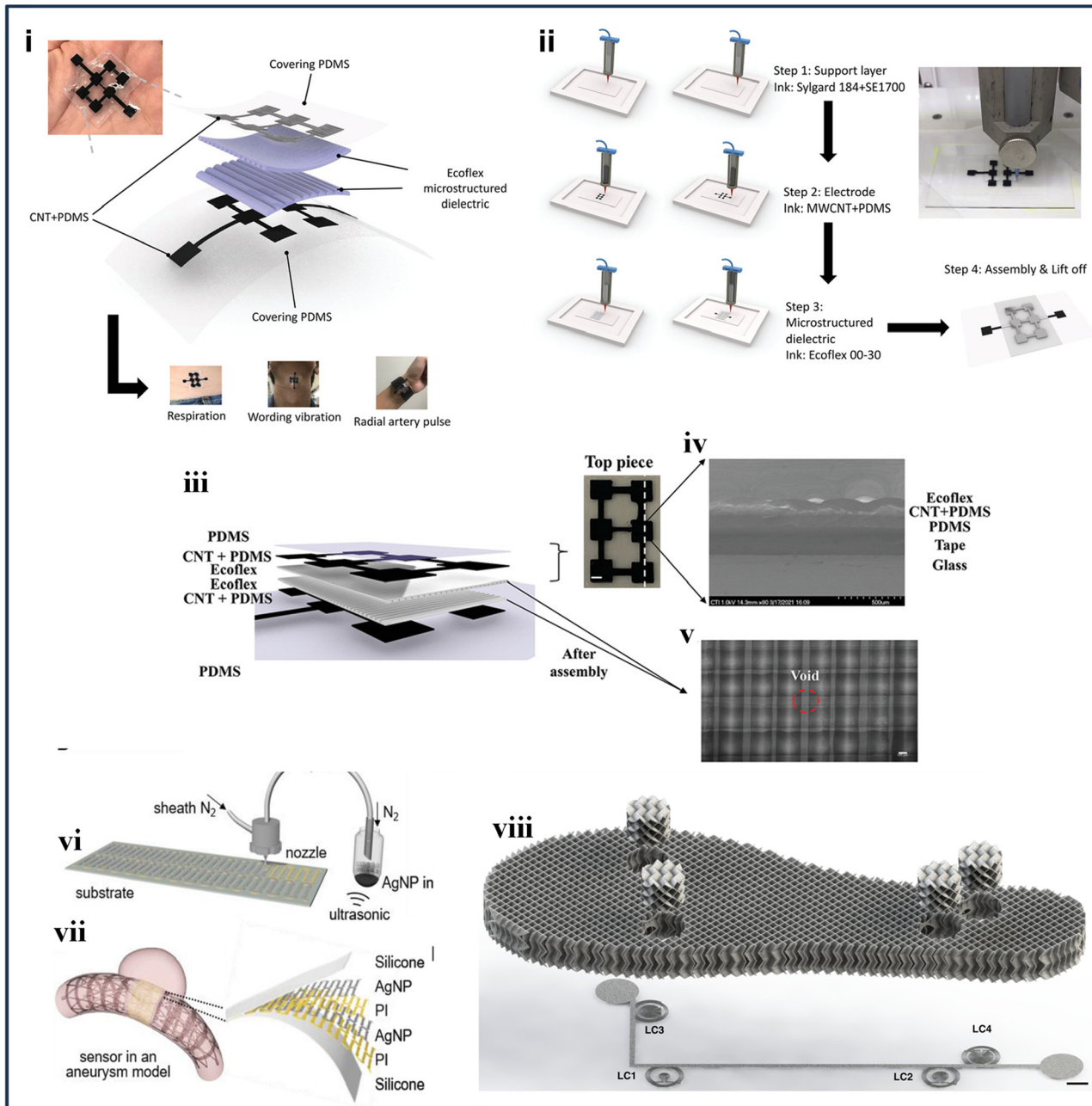


**Fig. 17** (i) A photograph and schematic illustration of a fully 3D-printed, multilayered nanocomposite capacitive pressure sensor designed for monitoring various physiological parameters. (ii) Step-by-step diagram showing the 3D printing process: fabrication of the PDMS support layer, deposition of a conductive layer composed of MWCNT and CNT, and printing of an Ecoflex-based dielectric layer with microstructures. (iii) Schematic breakdown of each layer within the M2A3DNC sensor assembly. (iv) Cross-sectional SEM image showing the stacked 3D-printed layers deposited on double-sided tape attached to a glass slide. (v) Microscopic view of the microstructured dielectric grid; scale bar: 100  $\mu$ m. Reproduced with permission from ref. 212. Copyright 2021, Wiley. (vi and vii) Diagram showing the aerosol jet printing setup used to fabricate silver electrodes using an ultrasonic atomizer, alongside a multilayer capacitive sensor embedded within an aneurysm simulation model. Reproduced with permission from ref. 215. Copyright 2019, Wiley. (viii) Illustration of a 3D-printed insole incorporating four LC sensors located beneath cylindrical origami components fabricated via FDM. Reproduced with permission from ref. 216. Copyright 2022, Springer Nature.

based resin in DLP printing, fluid microcuvettes exhibited minimal volume change (<0.5%) and low skin-interfacial stress (14 kPa at 30% strain). This research broadened the scope of colorimetric sweat analysis to encompass copper, pH levels, and glucose. It underscores the value of 3D printing in creating

flexible, complex, and thin wearable sensors, emphasizing the need for mechanically resilient polymers that can withstand continuous skin deformation.

Nevertheless, there are a number of difficulties in incorporating 3D printing into microfluidics. Reaching the high-resolu-

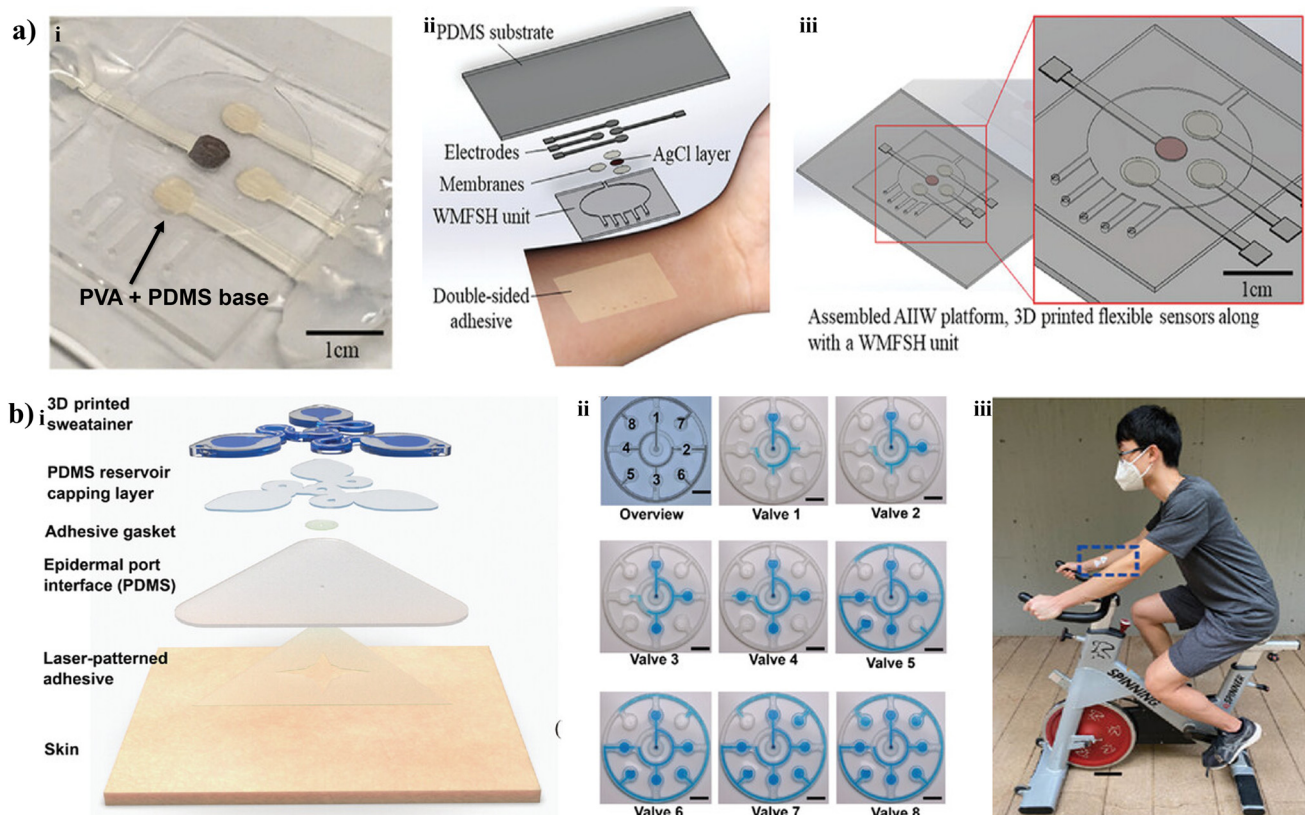


**Fig. 18** (a) (i) Image of the AllW patch integrating 3D-printed ion-sensing electrodes with a wearable microfluidic sample-handling module. (ii) Breakdown of the AllW patch showing individual elements. (iii) Diagram displaying the layout of AllW patch components both prior to and after final assembly. Reproduced with permission from ref. 224. Copyright 2021, Wiley. (b) (i) schematic illustrating the main parts of the sweatainer platform and its interface with skin, produced using DLP printing. (ii) time-lapse sequence showing fluid entry into various chamber-by-volume designs in a specific order. (iii) Image of the sweatainer device adhered to a user's skin during physical activity. Reproduced with permission from ref. 228. Copyright 2023, AAAS.

tion prints required to produce intricate microchannels and minute details crucial for efficient fluid management and sensing is a major challenge. Cutting-edge 3D printing methods such as DLP and DIW provide enhanced resolution, yet continued development is required to meet the precision standards of intricate biomedical applications.<sup>230</sup> Achieving high-resolution 3D printing for wearable electronics and biomedical devices remains challenging, particularly in materials that require both mechanical compliance and biocompatibility. Polymer design plays a critical role in overcoming these barriers. For example, tailoring the soft-to-hard segment ratio in polyurethane elastomers improves stretchability while maintaining load-bearing capacity. Block copolymers, such as PEG-*b*-PLA or PU-based systems, provide morphological control through phase-separated domains, enabling improved print fidelity and tunable elasticity. In hydrogel systems, cross-linking density can be adjusted to regulate stiffness and deformation recovery, crucial for skin-mounted or conformable devices. Furthermore, surface modification with biofunctional groups like RGD peptides or zwitterions enhances cytocompatibility and adhesion. These strategies emphasize the need for polymer-level innovation in tandem with advances in printing

resolution and device integration. Furthermore, it might be challenging to guarantee the reproducibility and dependability of printed microfluidic devices because changes in print quality can have an impact on the sensors' functionality.<sup>231</sup> Furthermore, complex design and fabrication procedures are needed to combine several functions. Within a unified device, functionalities like fluid management and electronic sensing are integrated. The complexity of the production process is increased by the frequent use of materials and exact control over the spatial distribution of several materials.<sup>232</sup>

#### 5.4. Actuators designed to replicate biological motions

The potential of actuators with form adaptation to ambient settings as manipulation grippers and robotic locomotors is attracting study interest.<sup>233,234</sup> Soft robotics is based on these flexible actuators, which can mimic some biological behaviors. Bioactuators are used in drug delivery vehicles,<sup>235</sup> artificial muscles,<sup>236</sup> and physiological monitoring<sup>237</sup> when the right size and degrees of freedom are available. In applications related to health, bioactuators' capacity to change shape in reaction to external stimuli is very advantageous. For example, bioactuators in artificial muscles can replicate the contractions

of natural muscles, making prosthetic limbs more pleasant and effective.<sup>238</sup> Bioactuators can adjust to the body's movements in physiological monitoring, guaranteeing precise and continuous data gathering without putting the patient through undue discomfort.<sup>233</sup> Shape-adaptive actuators in drug delivery can maneuver through the intricate ecosystems of the body to deliver medication exactly where it is needed, improving therapeutic effectiveness and minimizing side effects.<sup>239</sup> Furthermore, bioactuators can be used in minimally invasive surgical instruments, providing accurate control and manipulation inside the body, which lowers surgery risks and recuperation times for patients. Additionally, bioactuators can help with rehabilitation equipment<sup>240</sup> by providing programmable

and controlled movements to help patients regain their strength and mobility. This allows therapy to be tailored to each patient's needs and improves overall results.

Numerous design options provided by 3D printing make it possible to easily adjust the characteristics of bioactuators. In order to create actuators with specific mechanical properties and functionality, this technology makes it possible to precisely fabricate complex geometries and integrate several materials into a single device. Using 3D printing to create material actuators that blend rigid and flexible parts to produce desired actuation characteristics is an efficient approach. Song *et al.*, for instance, used SLA to create a multi-material actuator system (Fig. 19a).<sup>241</sup> The design incorporated

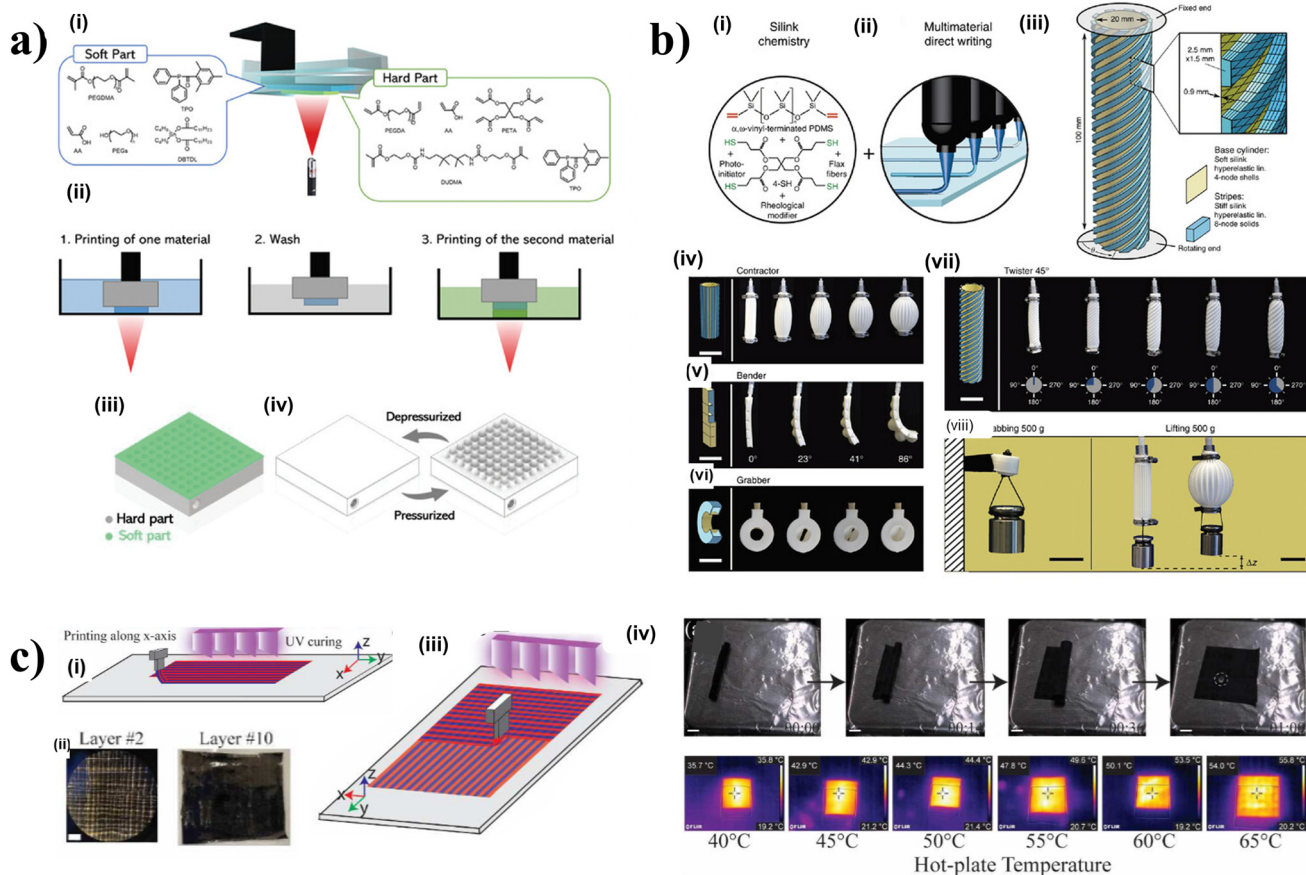


**Fig. 19** (a) (i) Composition details of the resin formulations used for both soft and rigid components in SLA. (ii) Workflow illustrating the multi-material SLA printing process. (iii) Schematic of a 3D-printed microactuator chip, featuring a side-positioned air inlet. The chip dimensions are 20 mm x 20 mm x 3 mm, with a soft membrane layer measuring 200  $\mu\text{m}$  in thickness. (iv) In its inactive form, the actuator chip maintains a flat profile, while inflation causes the soft membrane to bulge and expand outward. Reproduced with permission from ref. 241. Copyright 2023, MDPI. (b) (i) Chemical diagram showing vinyl-functionalized silicone formulations, which are mixed with a thiol-based crosslinker, fumed silica for viscosity control, flax fiber reinforcements, and a photoinitiator. (ii) Single step multimaterial fabrication of actuators using a DIW setup. (iii) Description and dimensional data of the actuator designed for torsional deformation. (iv) Contractile actuator layout with longitudinal stiffening elements embedded along the long axis of a flexible silicone tube (lead angle  $\alpha = 0^\circ$ ). (v) A bending-type actuator, achieved by printing air chambers onto a stiffer silicone film, capable of reaching  $90^\circ$  bending under 6 kPa of applied air pressure. (vi) Gripping actuator architecture comprising a large, stiff outer silicone cylinder and an inflatable soft tube at the center. (vii) Torsional motion achieved by helically printing stiff strips around the soft inner tube, with a lead angle of  $45^\circ$  as one example. The twist increased with internal air pressure. (viii) Demonstration of both the gripping and contracting actuators successfully lifting external loads. Reproduced with permission from ref. 242. Copyright 2018, Springer. (c) (i and iii) UV-assisted printing demonstrations along the x and y in-plane axes, respectively. (ii) Optical and photographic images of printed multilayer thin films, showing examples with 2 and 10 layers; (iv)  $90^\circ$ -rolled composite structures undergoing expansion over time when heated to 60 °C; infrared thermographic images visualizing temperature gradients during composite expansion. Reproduced with permission from ref. 243. Copyright 2022, Elsevier.

two distinct polymer phases: a soft, deformable region made from poly(ethylene glycol) dimethacrylate (PEGDMA) and poly(acrylic acid) (PAA), and a rigid region composed of tetraacrylate and diacrylate crosslinkers (Fig. 19a(i)). The switch between materials during printing was achieved *via* resin vat exchange (Fig. 19a(ii)). This strategy enabled the fabrication of a microactuator featuring a rigid air chamber and a flexible membrane. Upon applying pneumatic pressure, the membrane inflated through the cavity of the chamber, modifying the surface texture of the printed device (Fig. 19a(iii) and a(iv)). Thus, the authors created a microactuator in which the flexible part functions as an inflated membrane and the rigid part as an air chamber. When under pressure, the membrane deforms and protrudes from the chamber's hollow portion, changing the chip's surface roughness. Furthermore, actuators with incorporated sensors and electronics can be created *via* 3D printing, improving their usability and compatibility with medical equipment. Odent *et al.* showcased a line of multi-responsive actuators produced by SLA as one example.<sup>84</sup> The hydrogel's temperature and pH responsiveness arise from PNIPAM's LCST and PCEA's acidic dissolution. Controlled motion was achieved using gradients in surface area-to-volume ratio, crosslinking density, and chemical composition. This work highlights additive manufacturing's versatility in creating bioactuators from the same polymers responsive to multiple stimuli. Additionally, studies indicate PNIPAM and PCEA exhibit low cytotoxicity. And appropriate actuator integration into bio-related environments, despite the lack of biocompatibility experiments.

Schaffner *et al.* provided a clear demonstration of a flexible actuator design (Fig. 19b), especially in the methodical explanation of the twisting mode.<sup>244</sup> Their formulation included vinyl-terminated PDMS as the matrix, with flax fibers embedded to reinforce the stiff regions (Fig. 19b(i) and b(ii)). During actuation, the rigid strips maintained structural stiffness, while the soft elastomeric substrate allowed flexible deformation. By adjusting the lead angle of the printed fiber-reinforced elements, actuators could undergo contraction, elongation, and twisting motions as governed by classical lamination theory (Fig. 19b(iii)). The inclusion of a thiol-based crosslinker significantly improved bonding at the interfaces between materials of differing mechanical properties, as well as between printed layers, enhancing structural integrity. The versatility of this design was demonstrated through several configurations (Fig. 19b(iv)–b(viii)), and the use of biocompatible materials like PDMS and natural flax fibers further emphasized its suitability for biomedical applications.

To create a dual stimuli-responsive actuator, for example, Ravichandran *et al.* created a 3D printing method known as multiphase direct ink writing (MDIW) (Fig. 19c(i)–(iii)).<sup>245</sup> A special print head allowed the creation of multiphase materials in one step. Connected multipliers could split two feedstocks and produce  $2^{n+1}$  alternating layers at once (where  $n$  is the number of multipliers). The printed TPU-D/PCL layers could fix and recover shapes due to TPU-D's molecular relaxation at high temperatures and PCL's stiff crystal region that

holds temporary shapes (Fig. 19c(iv)). This layered composite can be heated to activate movement after being shaped and frozen. Both PCL and TPU are biocompatible, providing valuable ideas for improving 3D printing techniques to make bioactuators.<sup>246</sup>

Although bioactuators can bend, lift, and grip objects, adding sensors to actuating systems opens up new possibilities for haptic and smart wearable technology. Lewis's team described a soft somatosensitive actuator that, when used for its grasping function, has haptic, proprioceptive, and thermocceptive sensing capabilities.<sup>247</sup> Using multimaterial EMB3D printing, EMIM-ES and Pluronic F127 were used to create pneumatic channels and conductive sensors. Sensor resistance changes tracked actuator movements, measuring contact pressure, driving force, and bending angle. Furthermore, these chemical energy-harvesting natural actuators typically have better efficiency ( $\geq 50\%$ ) than artificial ones ( $< 30\%$ ).<sup>247</sup> This suggests that more biocompatible polymers and finer shapes are important components for 3D-printed bioactuators in the future.

## 5.5 Wearable soft robots mimicking muscle movements

In order to support the NASA Apollo mission, wearable robots were first created in the 1960s. The field of wearable robotics has expanded over time to encompass assistive and rehabilitation robotics, haptic devices, and first responder systems.<sup>248</sup> Since these systems need to be long-lasting, biodegradability is usually not an issue. Rather, it is important that it be compatible with human skin and other bodily parts. The development of wearable soft robotics has been completely transformed by 3D printing, which provides design flexibility and the capacity to construct intricate structures in a single step.<sup>249</sup> 3D printing enables the production of personalized assistive devices and prosthetics, enhancing user quality of life. It also simplifies and reduces the cost of fabricating advanced wearable robotics by allowing one-step creation of complex, functional structures. Although many smart polymer systems rely on tailored molecular design, device-level integration using commercially available polymers has also enabled impactful demonstrations in biomedical and robotic applications. For example, Mohammadi *et al.* reported an FDM-printed prosthetic hand fabricated from thermoplastic polyurethane (TPU), which provided the required flexibility and durability to perform tasks such as the tripod hold of a pencil and the pinch grasp of an egg (Fig. 20(i)).<sup>253</sup> The selection of TPU guarantees sufficient biocompatibility and offers appropriate gripping friction. Furthermore, elastomers like silicone are frequently employed because of their resilience, flexibility, and capacity to bear repeated compression and stretching without deteriorating.<sup>254,255</sup> These characteristics are essential for wearable soft robotics components that must remain functioning while adjusting to body movements. Because of their distinct electrical and mechanical characteristics, other cutting-edge materials including hydrogels and conductive polymers are used to create wearable robotic systems that are more responsive and intelligent, improving user comfort and performance.

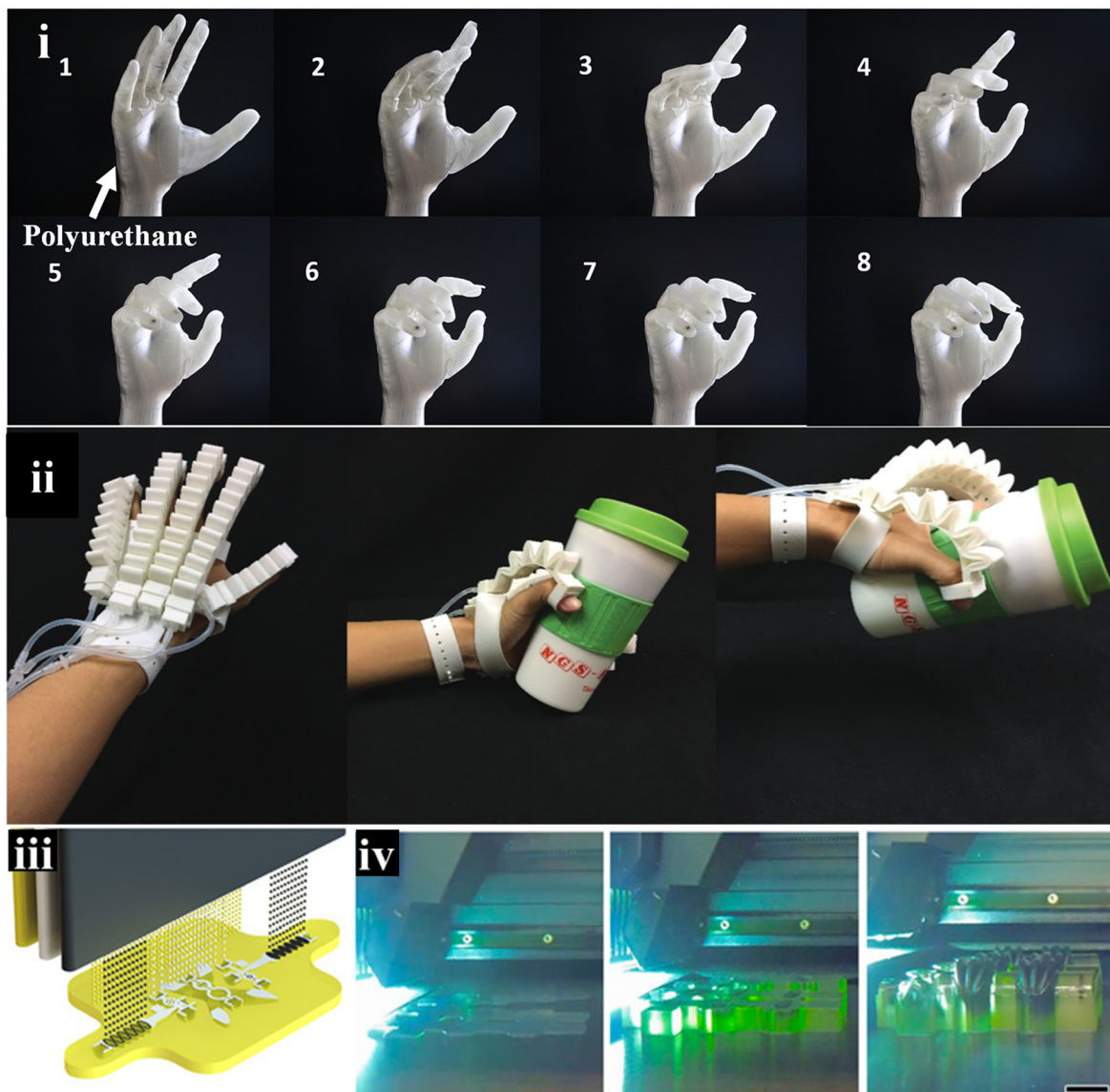


**Fig. 20** (i) Finger movement of printed material. Reproduced with permission from ref. 250. Copyright 2020, PLOS. (ii) The 3D-printed assistive glove. Reproduced with permission from ref. 251. Copyright 2018, Wiley. (iii) Schematic representation of multimaterial polyJet 3D printing used to fabricate soft robots with embedded fluidic channels, utilizing rigid (white), flexible (black), and dissolvable (yellow) printing materials. (iv) Sequential images showing different stages of the 3D printing process for the soft robotic structure. Scale bar: 2 cm. Reproduced with permission from ref. 252. Copyright 2021, AAAS.

Additionally, as previously shown, the adaptability of FDM materials and procedures allows for the creation of comfortable and functional rehabilitation devices in addition to manual human hands. Similarly, Keong and Hua developed rehabilitation gloves incorporating elastomeric polymer actuators (silicone-based materials and TPU) produced *via* FDM, enabling assisted gripping motions for rehabilitation (Fig. 20(ii)).<sup>251</sup> Fig. 10b shows that the built robotic gripper could grasp various objects from both inward and outward directions. A rehabilitative glove device was developed based on the gripper, which enhanced the finger movement of stroke patients by simulating human finger bending motion. Although the concept of an exoskeleton is appealing, more research is

necessary to include sensory systems that allow for precise control.<sup>251</sup>

The creation of wearable soft robotics using modern 3D printing technology is a major step forward for medical applications like assistive technology. More recently, Sochol's group demonstrated a fully 3D-printed soft robotic system using PolyJet multimaterial photopolymers, including compliant elastomers, rigid structural polymers, and a water-soluble sacrificial support material allowing the integration of fluidic circuitry for precise motion control (Fig. 20(iii) and (iv)).<sup>252</sup> Using multimaterial PolyJet 3D printing, flexible interconnects, structural components, and fluidic channels were fabricated simultaneously with MED610, Agilus30, and a water-soluble support (SUP706).

The printed fluidic elements functioned like electrical components, such as diodes and transistors, controlling flow direction and pressure response. These components enabled advanced applications in soft robotics, including adaptive hands and multifunctional soft robotic turtles. While the polymers in these examples are commercially available rather than newly synthesized, their translation into functional devices *via* additive manufacturing highlights how 3D printing bridges polymer materials and smart applications.

The applied gate pressure might be changed to vary the number of bent fingers in this system, which is made up of typically open fluidic transistors with distinct pressure-gain characteristics. In terms of both operating techniques and feasible functions, the scenario significantly influences 3D-printed wearable robotics. The three examples listed above illustrate various tendencies in soft robotics: independent systems that perform human jobs, extensions that complement the human body, and realistic printed parts used as prostheses. Every branch has enormous potential and might greatly raise people's standard of living. For instance, helping someone with a disability with everyday tasks. Furthermore, their uses include tissue-mimicking active simulators for research, artificial organs, and soft surgical instruments, all of which call for different levels of biocompatibility.<sup>256</sup> 3D printing is essential for accomplishing biomimicry, even though polymeric biomaterials solve biocompatibility issues. The prerequisites for developing biological soft robotics are perfectly satisfied by the combination of these two elements. Anthropomorphic prostheses have advanced greatly, according to several proof-of-concept investigations, thanks to the synergistic development of bidirectional cerebral interactions.<sup>257</sup> The circumstances suggest that the need for polymeric biomaterial engineering and 3D printing may grow in the near future. A thorough review of 3D-printed soft robotics including more successful examples was published by Yap *et al.*<sup>258</sup>

### 5.6. Passive energy storage devices: batteries, supercapacitors, and fuel cells

Implantable and external medical devices depend on sophisticated energy storage technologies, including batteries, supercapacitors, and fuel cells.<sup>259,260</sup> For example, small, dependable batteries are necessary for implanted devices like pacemakers and neurostimulators to function continuously.<sup>261</sup> In a similar vein, effective energy storage and management systems enable real-time data and quick response times for emergency medical equipment and wearable health monitors.<sup>262</sup> Additionally, treating diabetes and supporting heart functions in artificial hearts require effective energy storage technologies. Reliable batteries are essential for the smooth operation of insulin pumps and continuous glucose monitoring devices (CGMs), which dispense insulin and continuously check blood sugar levels.<sup>263</sup> Similar to this, sophisticated battery systems are necessary for the long-term operation of artificial hearts, also known as ventricular assist devices (VADs), which supplement or replace the heart's pumping function.<sup>264</sup> These uses demonstrate how important energy storage technologies

are to supplying long-term power sources for life-saving medical equipment.

Batteries have undergone significant advancements in terms of energy and power density, durability, and lifespan, making them a vital power solution for biosensors and smart wearable technologies.<sup>265</sup> Because 3D printing can create complex Three-dimensional architectures enhance the loading of active materials while maintaining efficient ion transport, thanks to their high surface-to-volume ratios, it is becoming more and more popular as a means of achieving better energy and power densities. As a result, the use of 3D printing in batteries has been thoroughly examined. Nevertheless, the printing of batteries based on polymeric biomaterials has not received much attention. The concept focuses on increasing graphite content in graphite/PLA composite filaments, enabling their use as printable negative electrodes in lithium-ion batteries, for instance, was investigated by Maurel *et al.*<sup>266</sup> Using FDM, Gao *et al.* fabricated negative electrode discs yielding  $200 \text{ mA h g}^{-1}$  at C/20 after six cycles. They also created a 3D carbon framework with PLA, which was later removed and coated with PANI and PAA to serve as cathodes for Zn-organic batteries.<sup>267</sup>

Making sure that all of the parts, such as electrodes, electrolytes, and casings, are composed of biodegradable materials is the difficult part of building a fully degradable battery.<sup>268</sup> The remaining non-biodegradable components continue to be a major problem, even though using one or two biodegradable materials can lessen the environmental impact. Materials science advancements are needed to create substitutes for traditional battery components in order to achieve complete biodegradability. Additionally, these materials need to retain the performance attributes needed for real-world uses, like To successfully integrate these novel materials, researchers must also take production techniques like 3D printing into account, which adds another level of complexity.<sup>269</sup> Although there are still many scientific and engineering obstacles to overcome, the successful creation of entirely biodegradable batteries would transform the industry and make implantable medical devices safer and more ecologically friendly. A fully biodegradable battery, for instance, was recently created by Huang *et al.* using alginate hydrogel as the electrolyte, magnesium as the anode, and molybdenum trioxide as the cathode.<sup>270</sup> Both *in vitro* and *in vivo* experiments demonstrated its biocompatibility and biodegradability despite being a primary battery system. Although it hasn't been investigated for 3D printing manufacture yet, the outcome opens up new possibilities for implantable devices.

### 5.7. Self-powered devices

The development of biomedical systems has advanced significantly with the introduction of self-powered devices.<sup>271</sup> By using the body's biomechanical movements to generate energy, these devices do away with the requirement for external power sources, increasing their potential for use in implantable and wearable electronics. Low-energy biomedical sensors can be continuously powered by thermoelectric devices, which transform body heat into electrical energy.<sup>272</sup> Piezoelectric

devices use mechanical stress to create electricity, which can be used to track physiological characteristics like muscle activity and heart rate.<sup>273</sup> Triboelectric devices can power motion sensors and other biomechanical processes by means of contact electrification and electrostatic induction.<sup>274</sup> In dynamic situations with frequent heat fluxes, pyroelectric devices employ temperature variations to generate energy.<sup>275</sup> Integrating self-powered technologies into biomedical systems enhances efficiency and adaptability, enabling devices like pacemakers, glucose monitors, and health sensors to operate without frequent battery replacements. 3D printing supports this by offering precise control over materials and design, improving device performance in healthcare applications.<sup>276</sup>

The advancement of devices based on thermoelectric, piezoelectric, triboelectric, and pyroelectric systems heavily relies on 3D printing improves the functionality and integration of these devices by making it possible to precisely fabricate complicated structures and sophisticated shapes. For example, the technology enables the development of micro-scale characteristics necessary for thermoelectric and piezoelectric devices to convert energy efficiently. For instance, wearable thermoelectric generators (TEGs) with a gill-inspired form were proposed by Zhu *et al.* (Fig. 21(i)–(iv)).<sup>277</sup> FDM printing with TPU was used to arrange PANI/MWCNT thermoelectric pellets for enhanced voltage generation on low-temperature surfaces like skin. This self-powered sensor detected signals such as breathing and joint movement using body heat, enabling long-term health monitoring. The innovative design highlights FDM printing's role in harnessing thermoelectricity for wearable applications.

Furthermore, the adaptability of 3D printing enables the creation of devices personalized to match specific physiological

and anatomical needs, enhancing their functionality in biomedical wearable and implanted applications.<sup>279</sup> The inclusion of various materials is also made easier by this creative manufacturing technique, which enhances the devices' functional qualities and biocompatibility. Using  $\mu$ CLIP 3D printing, Chen's team rapidly fabricated piezoelectric sensors from a PEGDA matrix with barium titanate (BTO) fillers functionalized by TMSPMA to improve particle dispersion and bonding. The lattice-structured sensors effectively detected signals such as finger taps, stomping, and coughing, demonstrating piezoelectricity's ability to capture both large and subtle mechanical movements.<sup>280</sup> Li *et al.* increased the dispersibility of Potassium sodium niobate (KNN) piezoceramic particles embedded within a PVDF polymer matrix by covalently grafting them using the same 3-(trimethoxysilyl)propylmethacrylate.<sup>281</sup>

Another intriguing energy conversion method for converting motion, such as sliding,<sup>282</sup> friction,<sup>283</sup> and contact separation,<sup>284</sup> into electric impulses is the triboelectric effect.

For example, Park's group created a toroidal triboelectric generator designed to sense hand movements and translating them into commands for human–machine interfaces, enabling control of robotic hands, interactive tabletop games, and household appliances.<sup>285</sup> A 3D-printed TPU mold was utilized to produce pyramid-patterned MXene/Ecoflex composites, serving as the negative layer in a triboelectric sensor. The pyramidal design enhanced sensitivity by changing contact areas during muscle movement, generating voltage through triboelectrification and electrostatic induction. When integrated into a 3D-printed glove, the sensor detected finger and thumb motions, offering promising applications for advanced human–machine interfaces and gaming.

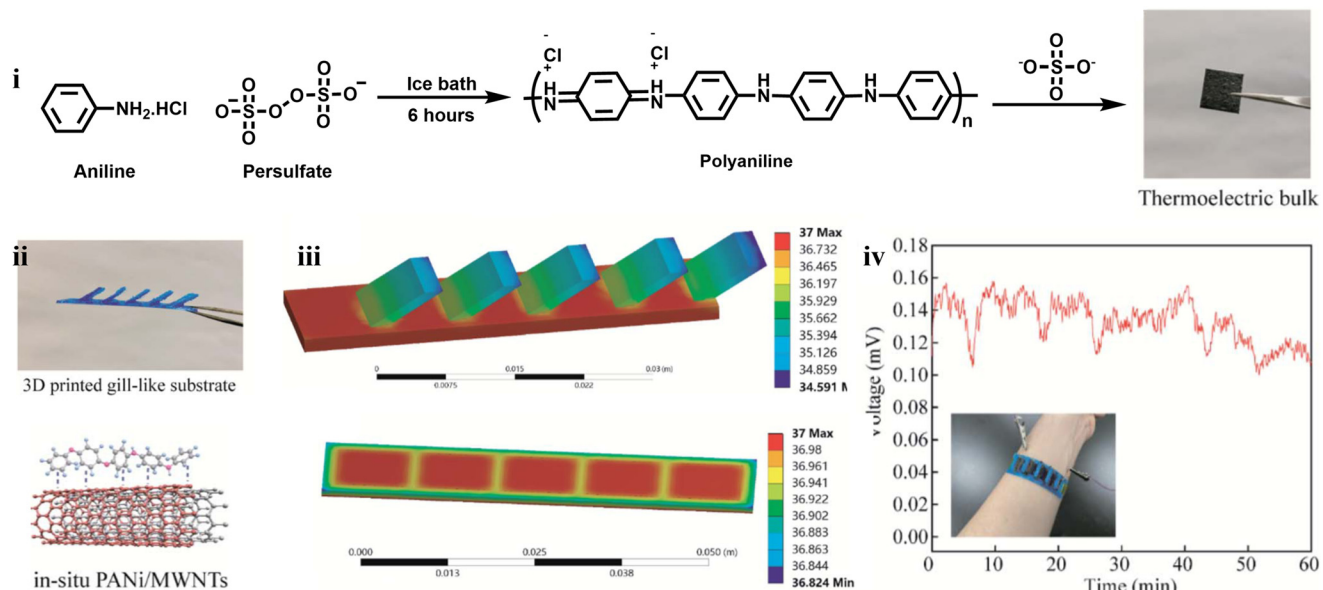


Fig. 21 (i) Synthesis route of the thermoelectric generator. (ii and iii) Image and simulated thermal profile of thermoelectric generators, with (iv) showing the voltage output when the device was applied to the forearm. Reproduced with permission from ref. 278. Copyright 2021, Royal Society of Chemistry.

Examples of how mechanical energy can be transformed into electrical energy include thermoelectricity, piezoelectricity, triboelectricity, and pyroelectricity. Theoretically, these systems can therefore generate signals for sensing or internet-of-things (IoT) connections on their own. However, because of the low power these effects can provide, these signals are somewhat preliminary. Batteries are still required for more sophisticated features like data display and bluetooth signal transfer.<sup>286</sup> However, given that some consumers complain about the need for regular charging of certain commercial smart wearables, there may be advantages, such as prolonging the battery life. Beyond improving energy efficiency, self-powered systems have the potential to minimize the dimensions of *in vitro* and *in vivo* medical devices can be minimized by lowering battery requirements, leading to improved user comfort. Notably, the use of biocompatible polymer matrices such as TPU, PEGDA, and Ecoflex supports their safe application in biological environments, including *in vivo* use. It illustrates how the 3D-printed, self-powered devices might be implanted in the future. More thorough views on 3D-printed energy devices have been offered by Son *et al.*<sup>287</sup>

### 5.8. Printed hydrogels as soft actuators and robots

A 3D network of polymers with a lot of water in it is called hydrogel. Hydrogels have a lot of promise in the biomedical and undersea engineering domains because of their resemblance to soft biological tissues, high biocompatibility, and ability to function in damp or moist conditions.<sup>288,289</sup> Hydrogels provide a flexible design environment that enables the addition of different functional elements to satisfy a range of needs. Importantly, hydrogels are considered ideal materials for developing soft actuators and robots because of their strong responsiveness to external stimuli. The development of various tough hydrogels with remarkable strength and elasticity has significantly expanded their use in soft robotics and actuators.<sup>290</sup> Extrusion-based and photocuring printing methods can be used to create hydrogels.<sup>291</sup> Shear-thinning behavior or sol-gel transition essential for extrusion-based printing inks can be achieved through techniques such as solvent exchange, charge shielding, temperature control, and post-curing. Despite being widely employed in many hydrogel systems, extrusion-based printing has low printing efficiency, relatively poor accuracy, and difficulties manufacturing small, highly precise objects. On the other hand, photocuring printing, particularly voxel printing made possible by careful control of the light source, provides excellent accuracy and efficiency and encourages the printing of more intricate structures.<sup>292-295</sup> PAAc gels,<sup>295</sup> polyacrylamide,<sup>293</sup> PNIPAm gels,<sup>185,296</sup> hyaluronic acid gels,<sup>296</sup> chitosan gels,<sup>297</sup> and alginate gels,<sup>298</sup> are the most popular hydrogel systems for printed soft actuators and robots.

Hydrogel actuators or robots can be classified into three categories based on their mechanical properties and responsiveness: matrix stimulus-responsive actuation, solvent-induced swelling actuation, and external pressure-driven actuation. Among these, pneumatic or hydraulic actuation is the

most straightforward and rapid method, utilizing the inherent softness and flexibility of passive materials instead of relying on the hydrogel's responsiveness to stimuli.

For these pressure-driven hydrogel actuators to produce various actions, sensitive internal and external structural designs are needed. High production requirements can be satisfied *via* 3D printing. Heiden *et al.*, for example, developed gelatin gel-based pneumatic actuators using fused deposition modelling.<sup>299</sup> These actuators were implanted with flexible optical waveguides for proprioception. Accurately detecting their bending state and collisions with nearby objects, these hydrogel actuators demonstrated omnidirectional deformations in less than a second (Fig. 22(i)). The materials' stimuli-response can also be used by hydraulic actuators to accomplish particular tasks. Mishra *et al.* fabricated fluidic actuators using multimaterial stereolithography, combining a PNIPAm body with a microporous PAAm dorsal layer. Upon gripping a heated object, the PNIPAm body contracted while the micropores expanded, releasing liquid to cool the object. These sweat-inspired actuators demonstrated a cooling rate 600% higher than conventional actuators.<sup>294,300</sup> For instance, Wang *et al.* used DLP processing to print pneumatic hydrogel suckers that resembled octopus tentacles.<sup>293</sup> These suckers were then included into a biomimetic gripper to enable efficient gripping in both underwater and airborne settings. However, the application scenarios of this type of hydrogel actuator are limited by the need for non-detachable pipelines and driving equipment for pressure-driven actuators.<sup>301</sup>

One general property of hydrogels is their responsiveness, which enables them to alter their volumes in various conditions.<sup>291,302</sup> Hydrogels must experience asymmetric swelling in order to accomplish 3D deformations including bending, folding, and twisting.<sup>303</sup>

By selecting two or more gels with varying compositions and solvent-absorbing capabilities, it is possible to encode alternative swelling ratios in the structure.<sup>304,305</sup> It is possible to build in-plane and through-thickness gradients in the structures using 3D printing techniques, particularly multimaterial printing. The multilayer structure of the hydrogel-based soft actuator created through multimaterial printing serves as an illustration.<sup>304</sup> When exposed to water, the top layer of this hydrogel actuator expands, while the bottom layer does not. Underwater, this gripper was able to grasp live goldfish. Shape morphing can also be achieved within a single hydrogel by incorporating regions with different swelling behaviors, which result from variations in cross-linking density or the orientation of nanofillers.

For example, Sydney Gladman and colleagues utilized extrusion-based printing with an ink composed of nanocellulose fibers, which became aligned during extrusion, to fabricate a hydrogel capable of shape transformation.<sup>306</sup> Because of the anisotropic rigidity and swelling of the resulting gel fibers, the printed structures were able to change and take on intricate shapes. A hydrogel jumper with a microgroove and a double-curved structure serving as the "leg" was created by Fang *et al.* (Fig. 22(iii)).<sup>307</sup>

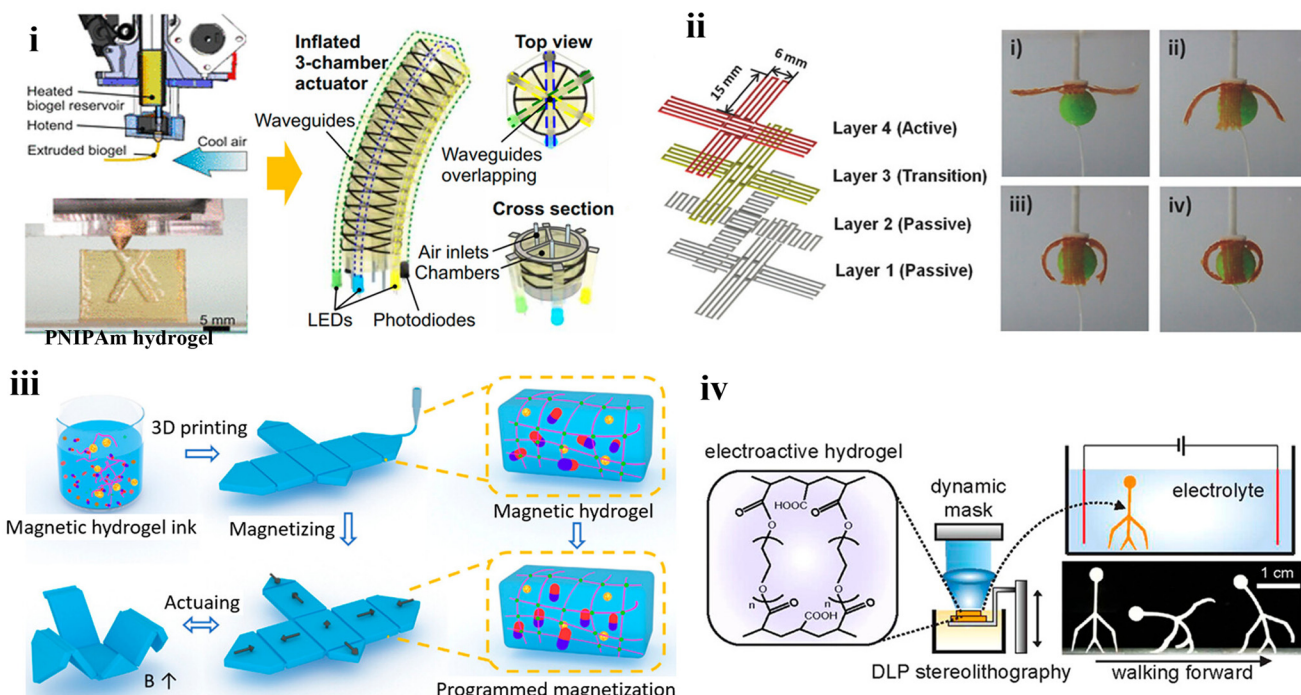


**Fig. 22** (i) 3D printed gelatin hydrogel actuator with all-directional shape change and built-in sensing via optical waveguides. Reproduced with permission from ref. 299. Copyright 2022, AAAS. (ii) Extrusion-printed tough gel gripper with fast response and strong output in saline solution. Reproduced with permission from ref. 311. Copyright 2018, Wiley-VCH. (iii) A magnetically responsive arthropod-inspired millirobot fabricated via DIW. Reproduced with permission from ref. 310. Copyright 2022, Wiley-VCH. (iv) SLA-printed polyelectrolyte hydrogel walker actuated by electric field. Reproduced with permission from ref. 312. Copyright 2018, American Chemical Society.

Beyond swelling-induced shape transformation, 3D printing is also employed to fabricate hydrogel-based soft actuators and robots that respond to stimuli such as temperature, pH, ionic strength, and light. Among these, PNIPAm-based gels are widely used due to their thermoresponsive behavior. Below its lower critical solution temperature (LCST) of approximately 32 °C, PNIPAm chains remain hydrated; however, when the temperature exceeds the LCST, the chains lose water, leading to significant gel shrinkage. After adding photothermal agents to the PNIPAm matrix, this reversible volume shift can also be initiated by light, allowing for both local and remote stimulation for particular functionalities. Bakarich *et al.*<sup>308</sup> for instance, used an active PNIPAm gel to print a multimaterial valve. The hydrogel contracts and shuts the valve at high temperatures. The PNIPAm gel responds to the ionic strength in addition to temperature. Zheng *et al.* used multimaterial printing to build a durable gel-based soft gripper.<sup>309</sup> The printed gel construct bent along the active fibers as a result of the active gel's volume contracting when submerged in a concentrated saline solution (Fig. 22(ii)).

To enable continuous motion in hydrogel-based soft robots, their interactions with the environment must be actively controlled. This is typically achieved through cyclic actuation, which drives the dynamic deformation of the printed gels. For example, incorporating soft or hard magnetic particles into hydrogels allows their shape to be altered in response to external magnetic or electromagnetic fields.<sup>310</sup> A

magnetically responsive gel robot can be fabricated using direct ink writing of a viscous ink containing nanoclay and neodymium iron boron (NdFeB) microparticles. The template-assisted magnetization approach was used to program the printed gel robot's magnetic domains. The gel robot was operated to exhibit preprogrammed deformations in magnetic fields. Cheng *et al.* have used DIW 3D printing to create soft robotic devices using a variety of hydrogels with various driving systems.<sup>185</sup>

Electroactive hydrogels combined with 3D printing are also used to develop soft robots. When exposed to an electric field, polyelectrolyte hydrogels exhibit ion migration and osmotic pressure differences within the gel, leading to movement. Polycation gels bend toward the anode, while polyanion gels bend toward the cathode. By using electric fields for actuation and 3D printing to control the robot's structure, smooth and programmable movements can be achieved. For example, Han *et al.*<sup>313</sup> used stereolithography printing of PAAc gel to create a soft robot that could move in both directions in an electrolyte solution when activated by an electric field (Fig. 22(iv)). As discussed earlier, the responsiveness of hydrogels to various stimuli and their similarity to soft biological tissues have made them attractive materials for creating soft actuators and robots. Advanced 3D printing techniques, especially multimaterial printing, enable the fabrication of hydrogel devices with intricate geometries. These printed gel-based actuators and robots hold significant potential for biomedical applications.

However, their relatively low actuation speed and limited output force highlight the need for further improvements in material properties and performance. Additionally, maintaining the stability of hydrogel-based machines in real-world environments remains a challenge due to their sensitivity to external stimuli.

### 5.9. SMP based smart materials

Another type of smart material is SMPs, which, when stimulated, may recall and restore the original shapes.<sup>182,314</sup> Two steps are typically involved in shape programming of shape memory polymers (SMPs): temporary shape fixation and permanent shape recovery. The “writing” of temporary structures involves heating the polymer over its thermal transition temperature, which for semi-crystalline materials is the melting temperature ( $T_m$ ) or glass transition temperature ( $T_g$ ). This heating enhances chain mobility, resulting in a soft and rubber-like material<sup>315</sup> At this elevated temperature, the material is deformed by applying external tension, causing polymer chains to align in specific regions. This external force is converted into stored entropic energy within the polymer chains. Upon cooling below the glass transition temperature ( $T_g$ ) or melting temperature ( $T_m$ ), the mobility of the chain segments is restricted by the vitrified or crystalline phase, locking the oriented chains in place and thus fixing the temporary shape.<sup>316</sup> Heating over  $T_g$  or  $T_m$  can cause recovery to the original shape by allowing chain segments to move and the material’s entropy elasticity to increase.<sup>317,318</sup> At this stage, a new temporary shape can be created by reprogramming the material.<sup>318,319</sup> Beyond traditional one-way SMPs, two-way shape memory polymers that can reversibly switch between two distinct shapes have gained significant interest and are now ideal materials for designing soft actuators and robotics.

By using 3D printing processes, the SMPs may be designed to create intricate structures that change when heated or exposed to light. 4D printing is another name for the process of combining form morphing with 3D printing materials. SMPs have been thoroughly investigated and applied in the development of soft actuators and robots.<sup>318</sup> For example, Zarek *et al.*<sup>320</sup> utilized SLA printing to fabricate thermally activated shape memory devices suitable for flexible circuits, using methacrylate-modified polycaprolactone as the base material. Ren *et al.*’s<sup>321</sup> fabrication serves as another illustration.

SMP-based soft robots which are 3D printed can react to inputs by changing their shape and color simultaneously. In order to make biomimetic masking octopuses and color-shifting flowers, thermochromic dyes were 3D printed into the SMP. Furthermore, Chen *et al.*<sup>69</sup> used FDM printing methods in conjunction with photoresponsive hybrids made of SMP and carbon black particles acting as photothermal materials to fabricate shape memory devices. The printed SMP-based device exhibited remarkable shape memory performance when exposed to natural sunlight (Fig. 23(i)).

While most one-way SMPs can only remember one temporary shape, many multiSMPs retain multiple shapes, depending

on a large number of phase transition temperatures,<sup>319,323</sup> or having a wide range of phase transition temperatures.<sup>315</sup> The perfluorosulfonic acid ionomer is a well-known example, exhibiting dual, triple, and even quadruple shape memory effects in addition to a single broad phase change.<sup>315</sup> Multimaterial printing of SMPs can also provide a multiple shape memory effect. Wu *et al.*<sup>176</sup> for instance, 3D printed several SMPs with a multilayer structure; these SMPs had varying  $T_g$ , allowing them to sequentially transform the printed construct into various shapes. After thermomechanical programming, the strip bends when the temperature rises between the two transition temperatures ( $T$  values) and returns to its original shape when the temperature exceeds both  $T$  values. This behavior allows the 3D-printed hook to grip and release objects on demand. Ma *et al.*<sup>324</sup> added polycaprolactone to PLA in varying amounts to create a shape memory composite with highly adjustable  $T_g$ . By FDM printing the hybrid materials with varying  $T_g$ , a bilayer flower was created. The heating method caused the petals to open sequentially. Oriented fibers can also be embedded to control the SMP’s morphing direction. For example, Ren *et al.*<sup>325</sup> used magnetically assisted 3D printing to align short steel fibers in targeted directions within different regions of the printed structure. As a result, the fabricated flower and robotic hand exhibited stepwise deformations when exposed to specific stimuli.

Since the thickness of the material affects the recovery or thermal reaction time, designing the geometry of the local locations of the printed constructions is another method to achieve different shape memory characteristics.<sup>326</sup> Liu *et al.*<sup>327</sup> used jet printing to create SMP structures of varying thicknesses and investigated how thickness affected the printed constructs’ response time. They discovered that it is possible to precisely control the response sequence by adjusting the thickness of each structural element. In addition to temperature, prestress or prestrain also affects how quickly SMPs recover. Cold programming is the method of creating plastic deformation at room temperature under severe stress, Qi and associates.<sup>328</sup> During the DLP printing process, the light intensity of each pixel was adjusted, resulting in printed structures with varying  $T_g$  values at various locations. The printed structure exhibited diverse overall shapes during the shape-morphing process by cold-programming individual segments at ambient temperature. Additionally, the development of 3D architectures can improve robotic functions. Qian *et al.*<sup>329</sup> recently demonstrated this by using DLP printing to fabricate interconnected torsional compression elements with embedded chirality from multiple SMPs (Fig. 23(ii)). Each chiral unit could be individually programmed *via* mechanical compression at a specific temperature. These programmable elements were assembled into lattice-like structures, both in planar and multilayer formats, that exhibited distinct deformation behaviors.

One-way SMPs’ inability to switch between temporal and permanent shapes reversibly restricts the printed structures’ ability to perform continuous robotic functions.<sup>330</sup> To address this challenge, two-way SMPs have been developed, allowing

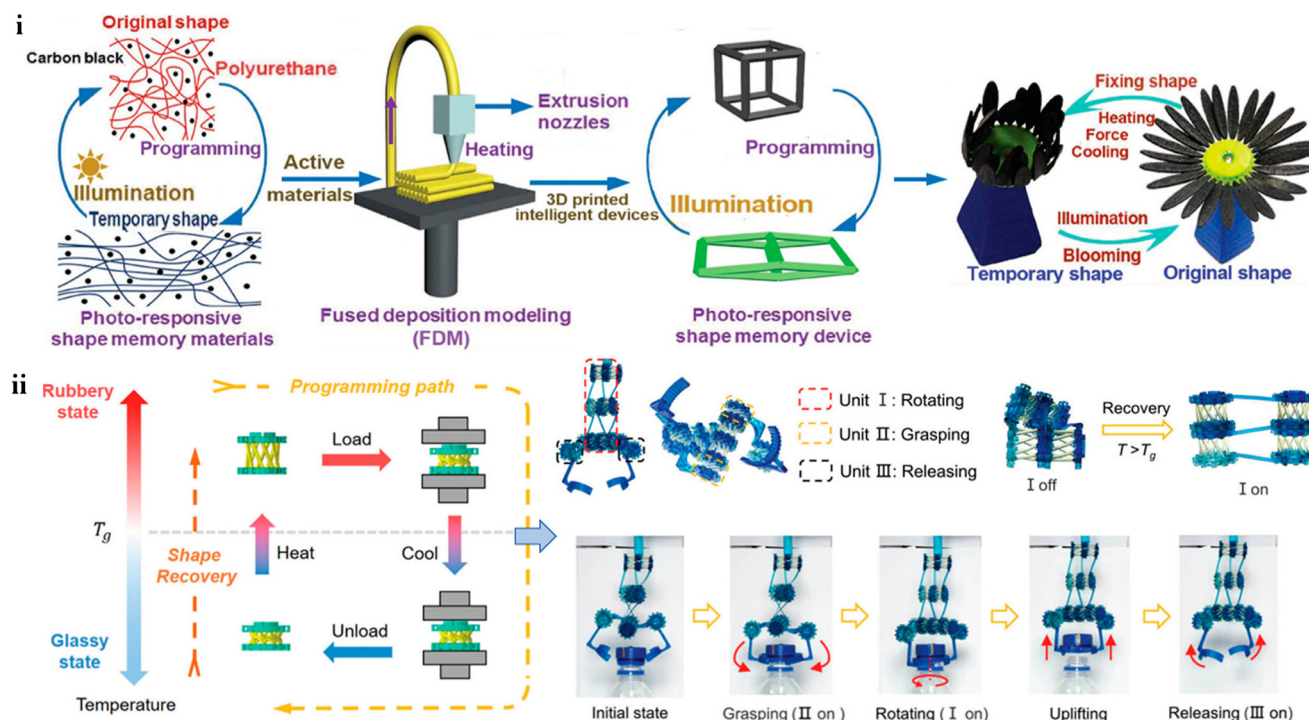


Fig. 23 (i) FDM-printed SMP flower with carbon black, activated by visible light. Reproduced with permission from ref. 69. Copyright 2017, Wiley-VCH. (ii) 3D-printed SMP pressure-twist units assembled into a versatile soft gripper. Reproduced with permission from ref. 322. Copyright 2023, Wiley-VCH.

reversible transformation between two distinct shapes. Here, the specific characteristics and workings of two-way SMPs have been left out. The ability to reprogramme the shape transformation in the same material is another crucial characteristic of two-way SPMs. Using two-way shape memory polymers, a twisted actuator was developed that can reversibly rotate an arrow indicator to three different positions within a manikin's hand.<sup>331</sup> Advanced soft actuators and robots can be created by combining this material's function with manufacturing techniques. For example, Xie *et al.*<sup>332</sup> employed thiol-acrylate chemistry and DLP printing to create a two-way SMP actuator containing dual crystalline phases. By digitally controlling exposure time and location, various geometric shapes were programmed, allowing for reversible 3D kirigami or origami-like movements. Demonstrations, such as a printed gripper and a cartoon figure, showcased diverse, reversible shape transformations. Compared to hydrogels, SMP-based actuators and robots offer stronger output forces, greater stability, and enhanced commercial potential for both biomedical and engineering applications.

### 5.10. Bio-medical applications

Careful selection of materials, fabrication methods, and design approaches allows for the customization of 3D-printed components, offering significant advantages for biomedical applications.<sup>333–338</sup>

**5.10.1 Tissue scaffolds.** Smart polymer 3D printing has recently attracted attention for tissue engineering applications, where scaffold structure customization depends on materials, processes, and design approaches.<sup>339</sup> The main aim of polymeric scaffolds, which are utilized in tissue engineering for organ synthesis, is tissue regeneration or function restoration.<sup>340,341</sup> Skeletal muscle, bone, cartilage, ligaments, skin, vasculature, and neurons are among the tissues that are targeted. 3D printing is useful for producing structures that are optimized for clinical applications through effective modular designs and for giving patients personalization.<sup>342</sup> It is difficult to optimize scaffolds and tune their designs, and in the case of bone tissue engineering, this also necessitates adjusting mechanical and biological properties.<sup>343</sup> In addition, scaffold features that are applicable to different scales, like hierarchical networks of pores for tissue growth and nutrient transport, must be taken into account. One popular configuration method is topology optimization.<sup>344</sup> A 3D-printed scaffold for spinal fusion applications was made using PolyJet printing and was set up after several topology layouts, beam diameter sizes, unit cell sizes, and localized reinforcements were investigated.<sup>333</sup> In order to find scaffold structures that would promote bone growth, the research used a computational method for assessing the corresponding agreements between designs. Asymmetric unit cell structures produced by computational design and tissue growth simulations have been used in subsequent studies to examine trade-offs.<sup>345,346</sup>

Using digital light processing, 4D-printable aliphatic polycarbonate scaffolds exhibiting shape memory and surface erosion were fabricated as self-fitting implants that enabled adipocyte infiltration, neovascularization, and low fibrotic response in murine subcutaneous models, demonstrating their efficacy for soft tissue repair.<sup>347</sup> In general, 3D printing applications in medicine benefit from computational design and automated methods because designs frequently benefit from customized configurations for individual patients.

**5.10.2. Dental implants.** Smart polymers are transforming the landscape of dental implantology by enabling the fabrication of intelligent, patient-specific implants through 3D printing techniques such as DLP, SLA FDM, and SLS.<sup>348</sup> For instance, poly(lactic acid) reinforced with chitosan was 3D printed into scaffolds exhibiting a shape memory recovery of 18.8%, good wettability, and enhanced cell proliferation, indicating potential for self-healing dental implants in bone defect applications.<sup>349</sup> Similarly, hydroxyapatite-reinforced PLA scaffolds demonstrated a high shape memory effect of 95.77% with favorable mechanical strength and hydrophilicity, further supporting their use in dental implant constructs with tunable recovery behavior.<sup>350</sup> The integration of electroactive polymers like PVDF/graphene/BaTiO<sub>3</sub> composites led to mechanically robust dental prototypes with peak strength of 42.98 MPa and excellent surface properties, making them suitable for stress-bearing dental prostheses.<sup>351</sup> Moreover, polyurethane scaffolds coated with boric acid *via* vacuum arc deposition showed enhanced osteogenic differentiation of dental pulp stem cells, as evidenced by elevated calcium accumulation and upregulation of osteogenic markers *i.e.* Runx2, OCN, DSPP, offering a promising route for bioinductive implants.<sup>352</sup> Polymethyl methacrylate composites containing 1% TiO<sub>2</sub> and 1% PEEK fillers exhibited improved mechanical and antibacterial properties, suitable for long-lasting, light-curable dental restorations.<sup>353</sup> Additionally, studies comparing PPSU and PEEK revealed that while PPSU exhibited higher wear, PEEK maintained superior hardness and modulus, positioning it as a strong candidate for 3D printed prosthetics and load-bearing dental components.<sup>361</sup> Table 1 of the review further highlights

the use of pH-responsive polymers *i.e.* PAA, PMAA, light-sensitive polymers *i.e.* azobenzene, spiropyran, and temperature-responsive PNIPAM for targeted drug delivery, light-triggered adhesives, and scaffold fabrication, respectively, all printed *via* vat polymerization or jetting methods. These examples collectively demonstrate how material customization, combined with advanced printing techniques, is enhancing the functionality, bioactivity, and patient compatibility of modern dental implants.

**5.10.3. Wearable prosthetics.** With a wide range of materials available and the ability to be customized to meet an individual's needs, 3D printing provides a multitude of options for new prosthetics. Children with upper limb problems can use a 3D printed prosthetic hand made of PLA and ABS materials.<sup>335</sup> The inexpensive wearable hand offers users a wide range of motion. Individually designed stretchable prosthetics have also been developed with sensors, signal processors, and actuators integrated.<sup>362,363</sup> A programmable heater and embedded temperature sensor, for example, were incorporated into a smart wearable therapeutic device that could self-activate based on a patient's body temperature.<sup>364</sup> A wearable device made of 3D-printed elastomer with a built-in pressure sensor was recently created.<sup>365</sup> Potential as an electronic skin is implied by the device's ability to detect and track external pressure, movement of the human body, and the direction of external forces. Worldwide, hundreds of thousands of people who have spinal cord injuries each year could use prosthetics.<sup>366</sup> A spinal cord injury may impact movement and hand function. For the benefit of patients, a wearable, 3D-printed hand orthosis made of polylactic acid has been created.<sup>367</sup> The gadget responds to the electromyography signal and helps the patient grasp objects. Another common medical issue is bone fractures, for which customized wearable casts made of high-density polyethylene or polypropylene have been developed and put into use for effective bone healing.<sup>368</sup>

**5.10.4. Surgical planning.** Rigid plastics like PLA and ABS have been used to 3D print surgical planning models so that patients can see organ models of themselves before surgery. In a number of medical specialities, including cardiology,<sup>369,370</sup>

**Table 1** Application of 3D-printed dental implants incorporating stimuli-responsive polymers

Polymer type	Example polymers	Application in dental implants	Numeric details	3D printing technique	Ref.
pH-responsive	PAA, PMAA, acidic group-containing copolymers.	Implant-based drug delivery systems	Drug release rate adjustable by pH	Vat photopolymerization, material jetting	354 and 355
Light-sensitive (photo responsive)	Azobenzene, spiropyran	Light-activated dental adhesives	Activation time ranges from seconds to minutes	DLP, SLM, SLA, and SLS	354 and 356
Electroactive	PANI, PPy, polythiophene	Conductive structures to enhance osseointegration	Conductivity: up to 100 S cm <sup>-1</sup>	VAT photo polymerization, material jetting	356 and 357
Shape memory	TPU, crosslinked PE, polyurethane-based block copolymers	Custom dental retainers and braces	Recovery stress: up to 5 MPa	Stereolithography (SLA), material jetting	357 and 358
Temperature-responsive	PNIPAM	Tissue engineering scaffolds	Transition temperature around 32 °C	SLA, DLP material jetting, material extrusion (ME)	359 and 360

Published on 17 Ndzhati 2025. Downloaded on 2026-02-14 00:00:57.

neurology,<sup>371,372</sup> urology,<sup>373,374</sup> and osteology,<sup>375</sup> 3D-printed organ models are inexpensive and can be made for each patient. In order to improve inflow during a device implantation procedure, cardiologists have utilized ABS filaments to create the anatomical form of hearts tailored to individual patients.<sup>370,376</sup> Using thermoplastic polyester resins, studies have also created anatomically precise 3D-printed models of the ventricular outflow tract and pulmonary trunk.<sup>377</sup> 3D-printed aneurysm models with rigid walls and hollow craniums have been created utilizing PLA filaments and photo-sensitive liquid resins.<sup>371,372</sup> These aneurysm models are designed to replicate patient-specific anatomies for investigating the system's hydrodynamic behavior. To create 3D-printed prostates and kidney models, rigid photopolymers have been used.<sup>373,378</sup> Additionally, patient-specific modelling was carried out for a kidney with a detachable tumour.<sup>379</sup> Collectively, these printing applications provide surgeons with a minimally invasive approach to rehearse and strategize procedures prior to performing them.<sup>380</sup> In a recent study, biodegradable poly(glycerol-dodecanoate) acrylate (PGD-A) blended with acrylic acid was 4D printed *via* DLP to create personalized vascular grafts and occluders that undergo shape recovery near body temperature and exhibit *in vivo* bioresorption after implantation in mouse aorta models.<sup>381</sup> Yeazel and Becker demonstrated the potential of 3D-printed bioresorbable shape-memory polymer stents as next-generation cardiovascular and ureteral implants that self-expand at physiological temperatures and eliminate the need for surgical removal, addressing limitations of both metal and balloon-deployed stents.<sup>382</sup> Paunović *et al.* developed DLP 3D printed biodegradable stents composed of poly(DLLA-*co*-CL) and PEGylated gold nanorods that exhibited NIR-triggered photothermal and shape-memory responses, enabling rapid *in situ* expansion and localized cell ablation within a porcine intestinal model.<sup>383</sup> Le Fer and Becker reported the 4D printing of fully resorbable star-shaped poly(propylene fumarate) gyroid scaffolds *via* DLP, demonstrating tunable shape-memory behavior, high porosity, and temperature-responsive recovery suitable for minimally invasive bone defect repair.<sup>384</sup>

**5.10.5. Drug delivery.** Drug delivery using 3D printing makes it possible to produce solvent-free drug-containing materials, distribute drugs uniformly, and fabricate medications for patient-specific needs.<sup>385</sup> Drug delivery effectiveness is influenced by micro-architecture, as shown by 3D-printed polycaprolactone and tricalcium phosphate meshes.<sup>386,387</sup> Both *in vitro* and *in vivo* research show that these drug delivery systems are capable of delivering a greater proportion of the integrated medication to the body while simultaneously exhibiting resistance to both Gram-positive and Gram-negative bacteria. Additionally, 3D prints can be applied outside of the body to deliver drugs. Drugs are driven directly through the skin for microcirculation in the body using a 3D-printed array of microneedles.<sup>336</sup> In general, these delivery methods are painless while facilitating effective transportation, which calls for intricate geometric fabrication at the micro-scale made possible by 3D printing. The microneedles

measure between 422–481 µm in height, have a pitch of 700 µm, and feature tip widths ranging from 65–84 µm. Additional developments include time-controlled release tablets,<sup>388</sup> multilayer caplets,<sup>389</sup> and drug delivery platforms containing multiple active ingredients.<sup>390</sup> are also made using polymeric 3D printing. It has been demonstrated that the technology can regulate the drug combination, release rate, and dosing intervals for personalized drug delivery.<sup>391</sup> Patients have different needs for dosage depending on how their bodies function, which encourages customization to enhance patient reactions. The robustness of 3D-printed polymeric microcapsules and nanocapsules in biological fluids and liquid suspensions contributes to improved drug effectiveness<sup>392</sup> which encourages their application in controlled drug release.

## 6. Conclusion and future perspectives

The creation of intricate and useful structures for a variety of uses, such as soft robotics, biomedical devices, smart actuators, sensors, and aerospace systems, has been made possible by recent developments in 3D printing methods.<sup>393–397</sup> By combining stimuli-responsive polymers with methods like extrusion-based printing, vat photopolymerization, *etc.*, 3D printing makes it easier to create intelligent designs. As the deployment of 3D-printed smart materials expands into demanding industrial domains,<sup>398</sup> it becomes essential to address the technical limitations associated with this transformative manufacturing strategy. Presently, 3D printing methods capable of processing stimuli-responsive properties remain largely confined to academic and research settings. Technologies like FDM, DIW, SLA, and inkjet printing are employed for fabricating intricate geometries.<sup>399</sup> Nevertheless, each technique has material constraints: FDM requires thermoplastic filaments which are not widely available; SLA demands photocurable resins; and DIW necessitates printable inks with specific rheological properties and swelling behavior. Consequently, the range of stimuli-responsive materials compatible with current 3D printing platforms remains restricted.

The 3D printing of stimuli-responsive polymers remains at an early developmental stage, with printable materials currently limited to laboratory-scale research. At present, there are no commercially available printers tailored specifically for the fabrication of stimuli-responsive polymers. Moreover, existing printing technologies lack the resolution and performance needed to fully exploit the potential of stimuli-responsive polymers. As a result, further advancements are necessary to produce highly responsive and structurally precise components. Key challenges also include limited actuation force and delayed response times. These limitations often stem from the strong dependence of material stiffness on temperature, which reduces mechanical output, and from the relatively slow responsiveness of stimuli-responsive polymers, which may take several minutes to activate. Addressing these issues

in the future will require strategic material design and optimization to enhance performance.

Numerous polymers that respond to stimuli and their composites have demonstrated the capability to undergo functional, structural, or visual changes when exposed to external stimuli.<sup>400</sup> For biomedical applications, these materials must satisfy stringent criteria such as biocompatibility, non-toxicity, suitable mechanical performance, and dynamic responsiveness that does not adversely affect surrounding tissues. However, only a limited number of responsive materials currently meet all these requirements. Additionally, most stimuli-responsive polymers are designed to react to a single type of stimulus,<sup>401</sup> underscoring the need for advanced research focused on developing multi-responsive systems capable of delivering controlled and multidirectional responses. Given the complexity and variability of biological environments from person to person, 3D-printed structures should be engineered to adapt dynamically to specific physiological microenvironments. Progress in the synthesis of new stimuli-responsive polymer composites or the functional modification of existing polymers holds promise for producing multifunctional scaffolds for biomedical applications and dynamic devices for broader engineering uses. While current 3D printing efforts predominantly explore shape-transforming capabilities, expanding the functional scope of smart printed materials could unlock new possibilities in the creation of intelligent, multifunctional systems.

Currently, most stimuli-responsive polymers exhibit only basic mechanical transformations, such as bending or folding, primarily at the macroscale level.<sup>402–404</sup> To enhance their utility, especially in precise small-scale applications, there is a pressing need to advance design strategies that enable control at the microscale. Achieving high precision in stimulus application, printing resolution, and response behavior is critical for enabling accurate deformation in patient-specific medical devices. In parallel, bilayer shape memory polymer composites have been explored for actuator and gripper development, leveraging asymmetric deformation between layers.<sup>405</sup> However, these systems are still confined to simple actuation patterns, such as bending or stretching. Future research should focus on creating advanced bilayer SMP composites that allow more intricate and programmable deformation behaviors, which could significantly broaden their functional scope.

When predicting how stimuli-responsive polymers may change shape, computational modeling is essential.<sup>406</sup> Such predictive tools have shown considerable accuracy for materials with linear and rigid mechanical properties. However, applying these models to soft stimuli-responsive polymers remains a significant challenge due to their inherently nonlinear and complex motion dynamics. Moving forward, integrating comprehensive experimental datasets with computational simulation outcomes could establish a robust foundation for artificial intelligence AI-driven frameworks, thereby accelerating the discovery and design of new stimuli-responsive polymer-based composites.

Although the present drawbacks, the integration of stimuli-responsive polymers with 3D printing technologies has enormous potential and could revolutionize a number of technical fields. Because of this synergy, highly customized, complex, and dynamic structures that were previously impossible to create with traditional methods of fabrication can now be created. However, current advancements merely scratch the surface of what is possible. As the technology continues to evolve and mature, it is unlocking new avenues for innovation, encouraging researchers and engineers to explore its vast potential for industrial applications. Looking ahead, the convergence of smart materials, 3D printing, and personalized design algorithms could lead to the realization of multifunctional, tailored structures with real-world utility in diverse sectors.

## Conflicts of interest

There are no conflicts to declare.

## Data availability

No primary research results, software or code have been included and no new data were generated or analysed as part of this review.

## Acknowledgements

All the contributions of the co-workers cited in the review are acknowledged. The authors acknowledge financial support received from Anusandhan National Research Foundation (ANRF), India through Core Research Grant (CRG/2022/002359). N.S. and D.K.S. acknowledges ANRF, Govt. of India and CSIR, Govt. of India, respectively for their fellowships.

## References

- 1 M. R. Aguilar, C. Elvira, A. Gallardo, B. Vazquez and J. Román, Smart polymers and their applications as biomaterials, *Top. Tissue Eng.*, 2007, **3**(6), 1–27.
- 2 M. K. Nguyen and D. S. Lee, Injectable Biodegradable Hydrogels, *Macromol. Biosci.*, 2010, **10**(6), 563–579.
- 3 P. H. L. Tran, T. T. D. Tran, V. T. Vo and B. J. Lee, in pH-Sensitive Polymeric Systems for Controlling Drug Release in Nocturnal Asthma Treatment, *4th International Conference on Biomedical Engineering in Vietnam*, Springer, 2013, pp. 304–308.
- 4 A. R. C. Duarte, J. F. Mano and R. L. Reis, Thermosensitive polymeric matrices for three-dimensional cell culture strategies, *Acta Biomater.*, 2011, **7**(2), 526–529.
- 5 B. Guillerm, S. Monge, V. Lapinte and J.-J. Robin, How to Modulate the Chemical Structure of Polyoxazolines by Appropriate Functionalization, *Macromol. Rapid Commun.*, 2012, **33**(19), 1600–1612.

6 R. M. Arnold, N. E. Huddleston and J. Locklin, Utilizing click chemistry to design functional interfaces through post-polymerization modification, *J. Mater. Chem.*, 2012, **22**(37), 19357–19365.

7 A. K. Shakya, H. Sami, A. Srivastava and A. Kumar, Stability of responsive polymer–protein bioconjugates, *Prog. Polym. Sci.*, 2010, **35**(4), 459–486.

8 M. A. C. Stuart, W. T. S. Huck, J. Genzer, M. Müller, C. Ober, M. Stamm, G. B. Sukhorukov, I. Szleifer, V. V. Tsukruk, M. Urban, F. Winnik, S. Zauscher, I. Luzinov and S. Minko, Emerging applications of stimuli-responsive polymer materials, *Nat. Mater.*, 2010, **9**(2), 101–113.

9 T. Wohlers, T. Gornet, N. Mostow, I. Campbell, O. Diegel, J. Kowen, R. Huff, B. Stucker, I. Fidan and A. Doukas, in *History of additive manufacturing*, 2016.

10 C. W. Hull, Apparatus for production of three-dimensional objects by stereolithography, *US Pat.*, US4575330A, 1986.

11 S. S. Crump, Apparatus and method for creating three-dimensional objects, *US Pat.*, US5121329A, 1992.

12 K. V. Wong and A. Hernandez, A Review of Additive Manufacturing, *Int. Scholarly Res. Not.*, 2012, **2012**(1), 208760.

13 M. Monzón, Z. Ortega, A. Martínez and F. Ortega, Standardization in additive manufacturing: activities carried out by international organizations and projects, *J. Adv. Manuf. Technol.*, 2015, **76**, 1111–1121.

14 J. Edgar and S. Tint, Additive Manufacturing Technologies: 3D Printing, Rapid Prototyping, and Direct Digital Manufacturing, 2nd Edition, *Johnson Matthey Technol. Rev.*, 2015, **59**(3), 193–198.

15 E. T. Brett, *The New Orleans Sisters of the Holy Family African American Missionaries to the Garifuna of Belize*, University of Notre Dame Press, 2012.

16 A. Uriondo, M. Esperon-Miguez and S. Perinpanayagam, The present and future of additive manufacturing in the aerospace sector: A review of important aspects, *Proc. Inst. Mech. Eng., Part G*, 2015, **229**(11), 2132–2147.

17 M. Vaezi and S. Yang, Extrusion-based additive manufacturing of PEEK for biomedical applications, *Phys. Prototyping*, 2015, **10**(3), 123–135.

18 S. Singh and S. Ramakrishna, Biomedical applications of additive manufacturing: Present and future, *Curr. Opin. Biomed. Eng.*, 2017, **2**, 105–115.

19 Y. Wang, M. M. A. Zeinhom, M. Yang, R. Sun, S. Wang, J. N. Smith, C. Timechalk, L. Li, Y. Lin and D. Du, A 3D-Printed, Portable, Optical-Sensing Platform for Smartphones Capable of Detecting the Herbicide 2,4-Dichlorophenoxyacetic Acid, *Anal. Chem.*, 2017, **89**(17), 9339–9346.

20 H. Yang, M. T. Rahman, D. Du, R. Panat and Y. Lin, 3-D printed adjustable microelectrode arrays for electrochemical sensing and biosensing, *Sens. Actuators, B*, 2016, **230**, 600–606.

21 G. D. Goh, S. Agarwala, G. L. Goh, V. Dikshit, S. L. Sing and W. Y. Yeong, Additive manufacturing in unmanned aerial vehicles (UAVs): Challenges and potential, *Aerospace Sci. Technol.*, 2017, **63**, 140–151.

22 M. Saari, B. Cox, E. Richer, P. S. Krueger and A. L. Cohen, Fiber Encapsulation Additive Manufacturing: An Enabling Technology for 3D Printing of Electromechanical Devices and Robotic Components, *3D Print. Addit. Manuf.*, 2015, **2**(1), 32–39.

23 M. Bogers, R. Hadar and A. Bilberg, Additive manufacturing for consumer-centric business models: Implications for supply chains in consumer goods manufacturing, *Technol. Forecast. Soc. Change*, 2016, **102**, 225–239.

24 C. Weller, R. Kleer and F. T. Piller, Economic implications of 3D printing: Market structure models in light of additive manufacturing revisited, *Int. J. Prod. Econ.*, 2015, **164**, 43–56.

25 A. Pongwisuthiruchte and P. Potiyaraj, Challenges and innovations in sustainable 3D printing, *Mater. Today Sustain.*, 2025, **31**, 101134.

26 T. D. Ngo, A. Kashani, G. Imbalzano, K. T. Q. Nguyen and D. Hui, Additive manufacturing (3D printing): A review of materials, methods, applications and challenges, *Composites, Part B*, 2018, **143**, 172–196.

27 C. M. Thakar, S. S. Parkhe, A. Jain, K. Phasianam, G. Murugesan and R. J. M. Ventayen, 3d Printing: Basic principles and applications, *Mater. Today*, 2022, **51**, 842–849.

28 P. K. Mishra and T. Jagadish, Applications and Challenges of 3D Printed Polymer Composites in the Emerging Domain of Automotive and Aerospace: A Converged Review, *J. Inst. Eng. (India): Ser. D*, 2023, **104**(2), 849–866.

29 B. G. Pavan Kalyan and L. Kumar, 3D Printing: Applications in Tissue Engineering, Medical Devices, and Drug Delivery, *AAPS PharmSciTech*, 2022, **23**(4), 92.

30 Z. U. Arif, M. Y. Khalid, A. Tariq, M. Hossain and R. Umer, 3D printing of stimuli-responsive hydrogel materials: Literature review and emerging applications, *Giant*, 2024, **17**, 100209.

31 T. D. Ngo, A. Kashani, G. Imbalzano, K. T. Q. Nguyen and D. Hui, Additive manufacturing (3D printing): A review of materials, methods, applications and challenges, *Composites, Part B*, 2018, **143**, 172–196.

32 D. Han, Z. Lu, S. A. Chester and H. Lee, Micro 3D Printing of a Temperature-Responsive Hydrogel Using Projection Micro-Stereolithography, *Sci. Rep.*, 2018, **8**(1), 1963.

33 S. Banerjee, J. Emert, P. Wright, T. Skourlis, R. Severt and R. Faust, Polymerization of isobutylene catalyzed by EtAlCl 2/bis (2-chloroethyl) ether complex in steel vessels, *Polym. Chem.*, 2015, **6**(27), 4902–4910.

34 I. Roppolo, A. Chiappone, A. Angelini, S. Stassi, F. Frascella, C. F. Pirri, C. Ricciardi and E. Descrovi, 3D printable light-responsive polymers, *Mater. Horiz.*, 2017, **4**(3), 396–401.

35 A. Martorana, C. Fiorica, F. S. Palumbo, S. Federico, G. Giammona and G. Pitarresi, Redox responsive 3D-printed nanocomposite polyurethane-urea scaffold for

Doxorubicin local delivery, *J. Drug Delivery Sci. Technol.*, 2023, **88**, 104890.

36 S. Ganguly and S. Margel, 3D printed magnetic polymer composite hydrogels for hyperthermia and magnetic field driven structural manipulation, *Prog. Polym. Sci.*, 2022, **131**, 101574.

37 A. Tariq, Z. U. Arif, M. Y. Khalid, M. Hossain, P. I. Rasool, R. Umer and S. Ramakrishna, Recent Advances in the Additive Manufacturing of Stimuli-Responsive Soft Polymers, *Adv. Eng. Mater.*, 2023, **25**(21), 2301074.

38 M. Falahati, P. Ahmadvand, S. Safaee, Y.-C. Chang, Z. Lyu, R. Chen, L. Li and Y. Lin, Smart polymers and nanocomposites for 3D and 4D printing, *Mater. Today*, 2020, **40**, 215–245.

39 J. Z. Manapat, Q. Chen, P. Ye and R. C. Advincula, 3D Printing of Polymer Nanocomposites via Stereolithography, *Macromol. Mater. Eng.*, 2017, **302**(9), 1600553.

40 A. Awad, F. Fina, A. Goyanes, S. Gaisford and A. W. Basit, 3D printing: Principles and pharmaceutical applications of selective laser sintering, *Int. J. Pharm.*, 2020, **586**, 119594.

41 K. Zub, S. Hoeppener and U. S. Schubert, Inkjet Printing and 3D Printing Strategies for Biosensing, Analytical, and Diagnostic Applications, *Adv. Mater.*, 2022, **34**(31), 2105015.

42 J. K. Placone and A. J. Engler, Recent Advances in Extrusion-Based 3D Printing for Biomedical Applications, *Adv. Healthcare Mater.*, 2018, **7**(8), 1701161.

43 N. Mohd Nurazzi, M. M. Asyraf, A. Khalina, N. Abdullah, F. A. Sabaruddin, S. H. Kamarudin, S. b. Ahmad, A. M. Mahat, C. L. Lee and H. J. P. Aisyah, Fabrication, functionalization, and application of carbon nanotube-reinforced polymer composite: An overview, *Polymer*, 2021, **13**(7), 1047.

44 J. J. V. Gardan, Smart materials in additive manufacturing: state of the art and trends, *Virtual Phys. Prototyping*, 2019, **14**(1), 1–18.

45 P. Theato, B. S. Sumerlin, R. K. O'Reilly and T. H. Epps III, Stimuli responsive materials, *Chem. Soc. Rev.*, 2013, **42**(17), 7055–7056.

46 P. Schattling, F. D. Jochum and P. J. P. C. Theato, Multi-stimuli responsive polymers—the all-in-one talents, *Polym. Chem.*, 2014, **5**(1), 25–36.

47 D. Kumar, B. Sahu and S. Banerjee, Amino Acid-Derived Smart and Functional Polymers for Biomedical Applications: Current Status and Future Perspectives, *Macromol. Chem. Phys.*, 2023, **224**(24), 2300207.

48 F. Doberenz, K. Zeng, C. Willems, K. Zhang and T. Groth, Thermoresponsive polymers and their biomedical application in tissue engineering – a review, *J. Mater. Chem. B*, 2020, **8**(4), 607–628.

49 H. Koide, K. Yamaguchi, K. Sato, M. Aoshima, S. Kanata, S. Yonezawa and T. Asai, Engineering Temperature-Responsive Polymer Nanoparticles that Load and Release Paclitaxel, a Low-Molecular-Weight Anticancer Drug, *ACS Omega*, 2024, **9**(1), 1011–1019.

50 N. R. B. Boase, E. R. Gillies, R. Goh, R. E. Kieltyka, J. B. Matson, F. Meng, A. Sanyal and O. Sedláček, Stimuli-Responsive Polymers at the Interface with Biology, *Biomacromolecules*, 2024, **25**(9), 5417–5436.

51 S. Xian and M. J. Webber, Temperature-responsive supramolecular hydrogels, *J. Mater. Chem. B*, 2020, **8**(40), 9197–9211.

52 X. Han, X. Zhang, H. Zhu, Q. Yin, H. Liu and Y. Hu, Effect of Composition of PDMAEMA-b-PAA Block Copolymers on Their pH- and Temperature-Responsive Behaviors, *Langmuir*, 2013, **29**(4), 1024–1034.

53 N. Jin, J. W. Woodcock, C. Xue, T. G. O'Lenick, X. Jiang, S. Jin, M. D. Dadmun and B. Zhao, Tuning of Thermo-Triggered Gel-to-Sol Transition of Aqueous Solution of Multi-Responsive Diblock Copolymer Poly(methoxytri(ethylene glycol) acrylate-co-acrylic acid)-b-poly(ethoxydi(ethylene glycol) acrylate), *Macromolecules*, 2011, **44**(9), 3556–3566.

54 J. Zhao, R. Hoogenboom, G. Van Assche and B. Van Mele, Demixing and Remixing Kinetics of Poly(2-isopropyl-2-oxazoline) (PIPOZ) Aqueous Solutions Studied by Modulated Temperature Differential Scanning Calorimetry, *Macromolecules*, 2010, **43**(16), 6853–6860.

55 M. Oh, Y. Yoon and T. S. Lee, Synthesis of poly(N-isopropylacrylamide) polymer crosslinked with an AIE-active azonaphthol for thermoreversible fluorescence, *RSC Adv.*, 2020, **10**(64), 39277–39283.

56 D. S. Lima, E. T. Tenório-Neto, M. K. Lima-Tenório, M. R. Guilherme, D. B. Scariot, C. V. Nakamura, E. C. Muniz and A. F. Rubira, pH-responsive alginate-based hydrogels for protein delivery, *J. Mol. Liq.*, 2018, **262**, 29–36.

57 K. Lavanya, S. V. Chandran, K. Balagangadharan and N. Selvamurugan, Temperature- and pH-responsive chitosan-based injectable hydrogels for bone tissue engineering, *Mater. Sci. Eng., C*, 2020, **111**, 110862.

58 B. Wang, X.-D. Xu, Z.-C. Wang, S.-X. Cheng, X.-Z. Zhang and R.-X. Zhuo, Synthesis and properties of pH and temperature sensitive P(NIPAAm-co-DMAEMA) hydrogels, *Colloids Surf., B*, 2008, **64**(1), 34–41.

59 C. R. Fellin and A. Nelson, Direct-Ink Write 3D Printing Multistimuli-Responsive Hydrogels and Post-Functionalization Via Disulfide Exchange, *ACS Appl. Polym. Mater.*, 2022, **4**(5), 3054–3061.

60 G. Falcone, P. Mazzei, A. Piccolo, T. Esposito, T. Mencherini, R. P. Aquino, P. Del Gaudio and P. Russo, Advanced printable hydrogels from pre-cross-linked alginate as a new tool in semi solid extrusion 3D printing process, *Carbohydr. Polym.*, 2022, **276**, 118746.

61 B. Liu, B. Dong, C. Xin, C. Chen, L. Zhang, D. Wang, Y. Hu, J. Li, L. Zhang, D. Wu and J. Chu, 4D Direct Laser Writing of Submerged Structural Colors at the Microscale, *Small*, 2023, **19**(2), 2204630.

62 P. Zhang, G. Wang and H. Yu, Ultraviolet-visible-near-infrared light-responsive soft materials: Fabrication,

photomechanical deformation and applications, *Responsive Mater.*, 2024, **2**(3), e20240016.

63 D. Klinger and K. Landfester, Dual Stimuli-Responsive Poly(2-hydroxyethyl methacrylate-co-methacrylic acid) Microgels Based on Photo-Cleavable Cross-Linkers: pH-Dependent Swelling and Light-Induced Degradation, *Macromolecules*, 2011, **44**(24), 9758–9772.

64 R. Yang, W. Jin, C. Huang and Y. Liu, Azobenzene Based Photo-Responsive Hydrogel: Synthesis, Self-Assembly, and Antimicrobial Activity, *Gels*, 2022, **8**(7), 414.

65 J. Keyvan Rad, Z. Balzade and A. R. Mahdavian, Spiropyran-based advanced photoswitchable materials: A fascinating pathway to the future stimuli-responsive devices, *J. Photochem. Photobiol. C*, 2022, **51**, 100487.

66 Y. Zou, H. Gao, C. Su, M. Wang and J. Gao, Photo- and pH-dually responsive hydrogel containing spirooxazine groups, *J. Polym. Res.*, 2024, **31**(2), 34.

67 B. Du, Y. He, M. Shen, Z. Hu, W. Fu, J. Zou, R. Huang and T. Yu, Recent development of photoresponsive materials toward 3D printing: From materials to application, *Polym. Sci.*, 2024, **62**(21), 4809–4834.

68 D. Han, Z. Lu, S. A. Chester and H. Lee, Micro 3D Printing of a Temperature-Responsive Hydrogel Using Projection Micro-Stereolithography, *Sci. Rep.*, 2018, **8**(1), 1963.

69 H. Yang, W. R. Leow, T. Wang, J. Wang, J. Yu, K. He, D. Qi, C. Wan and X. Chen, 3D printed photoresponsive devices based on shape memory composites, *Adv. Mater.*, 2017, **29**(33), 1701627.

70 M. Y. Khalid, Z. U. Arif, A. Tariq, M. Hossain, K. Ahmed Khan and R. Umer, 3D printing of magneto-active smart materials for advanced actuators and soft robotics applications, *Eur. Polym. J.*, 2024, **205**, 112718.

71 E. Yarali, M. Baniasadi, A. Zolfagharian, M. Chavoshi, F. Arefi, M. Hossain, A. Bastola, M. Ansari, A. Foyouzat, A. Dabbagh, M. Ebrahimi, M. J. Mirzaali and M. Bodaghi, Magneto-/electro-responsive polymers toward manufacturing, characterization, and biomedical/soft robotic applications, *Appl. Mater. Today*, 2022, **26**, 101306.

72 D. Podstawczyk, M. Nizioł, P. Szymczyk, P. Wiśniewski and A. Guiseppi-Elie, 3D printed stimuli-responsive magnetic nanoparticle embedded alginate-methylcellulose hydrogel actuators, *Addit. Manuf.*, 2020, **34**, 101275.

73 T. N. Edirisuriya, T. M. S. U. Gunathilake, Y. C. Ching and H. Noothalapati, Curcumin Targeted Drug Delivery Using Iron Oxide Nanoparticle Incorporated Magnetic Responsive Carboxymethyl Cellulose Hydrogel, *Polym. Sci. Ser. B*, 2024, **66**(2), 213–226.

74 M. S. Amini-Fazl, R. Mohammadi and K. Kheiri, 5-Fluorouracil loaded chitosan/polyacrylic acid/Fe<sub>3</sub>O<sub>4</sub> magnetic nanocomposite hydrogel as a potential anticancer drug delivery system, *Int. J. Biol. Macromol.*, 2019, **132**, 506–513.

75 J. Tang, Q. Yin, M. Shi, M. Yang, H. Yang, B. Sun, B. Guo and T. Wang, Programmable shape transformation of 3D printed magnetic hydrogel composite for hyperthermia cancer therapy, *Extreme Mech. Lett.*, 2021, **46**, 101305.

76 J. Hu, G. Zhang and S. Liu, Enzyme-responsive polymeric assemblies, nanoparticles and hydrogels, *Chem. Soc. Rev.*, 2012, **41**(18), 5933–5949.

77 R. Chandrawati, Enzyme-responsive polymer hydrogels for therapeutic delivery, *Exp. Biol. Med.*, 2016, **241**(9), 972–979.

78 Y. Xiong, L. Qi, Y. Niu, Y. Lin, Q. Xue and Y. Zhao, Autonomous Drug Release Systems with Disease Symptom-Associated Triggers, *Int. Mat.*, 2020, **2**(3), 1900124.

79 C. Alexander and K. M. Shakesheff, Responsive Polymers at the Biology/Materials Science Interface, *Adv. Mater.*, 2006, **18**(24), 3321–3328.

80 S. F. Peteu, F. Oancea, O. A. Sicuia, F. Constantinescu and S. Dinu, Responsive Polymers for Crop Protection, *Polymers*, 2010, **2**(3), 229–251.

81 M. Sobczak, Enzyme-Responsive Hydrogels as Potential Drug Delivery Systems—State of Knowledge and Future Prospects, *Int. J. Mol. Sci.*, 2022, **23**(8), 4421.

82 B. Narupai, P. T. Smith and A. Nelson, 4D Printing of Multi-Stimuli Responsive Protein-Based Hydrogels for Autonomous Shape Transformations, *Adv. Funct. Mater.*, 2021, **31**(23), 2011012.

83 S. Wang, H. Liu, D. Wu and X. Wang, Temperature and pH dual-stimuli-responsive phase-change microcapsules for multipurpose applications in smart drug delivery, *J. Colloid Interface Sci.*, 2021, **583**, 470–486.

84 J. Odent, S. Vanderstappen, A. Toncheva, E. Pichon, T. J. Wallin, K. Wang, R. F. Shepherd, P. Dubois and J.-M. Raquez, Hierarchical chemomechanical encoding of multi-responsive hydrogel actuators via 3D printing, *J. Mater. Chem. A*, 2019, **7**(25), 15395–15403.

85 F. D. Jochum and P. Theato, Temperature- and light-responsive smart polymer materials, *Chem. Soc. Rev.*, 2013, **42**(17), 7468–7483.

86 A. Abdollahi, H. Roghani-Mamaqani, B. Razavi and M. Salami-Kalajahi, The light-controlling of temperature-responsivity in stimuli-responsive polymers, *Polym. Chem.*, 2019, **10**(42), 5686–5720.

87 D. G. Karis, R. J. Ono, M. Zhang, A. Vora, D. Storti, M. A. Ganter and A. Nelson, Cross-linkable multi-stimuli responsive hydrogel inks for direct-write 3D printing, *Polym. Chem.*, 2017, **8**(29), 4199–4206.

88 D. Park, J. W. Kim and C. O. Osuji, Programmable Thermo- and Light-Responsive Hydrogel Actuator Reinforced with Bacterial Cellulose, *ACS Appl. Eng. Mater.*, 2024, **2**(3), 772–780.

89 A. Pourjavadi, R. Heydarpour and Z. M. Tehrani, Multi-stimuli-responsive hydrogels and their medical applications, *New J. Chem.*, 2021, **45**(35), 15705–15717.

90 A. S. Gladman, E. A. Matsumoto, R. G. Nuzzo, L. Mahadevan and J. A. Lewis, Biomimetic 4D printing, *Nat. Mater.*, 2016, **15**, 413–418.

91 Y.-W. Lee, H. Ceylan, I. C. Yasa, U. Kilic and M. Sitti, 3D-Printed Multi-Stimuli-Responsive Mobile Micromachines, *ACS Appl. Mater. Interfaces*, 2021, **13**(11), 12759–12766.

92 M. Shahbazi and H. Jäger, Current status in the utilization of biobased polymers for 3D printing process: a systematic review of the materials, processes, and challenges, *ACS Appl. Bio Mater.*, 2020, **4**(1), 325–369.

93 N. Shahrubudin, T. C. Lee and R. Ramlan, An overview on 3D printing technology: Technological, materials, and applications, *Procedia Manuf.*, 2019, **35**, 1286–1296.

94 J. Gopinathan and I. Noh, Recent trends in bioinks for 3D printing, *Biomater. Res.*, 2018, **22**(1), 11.

95 H. Nulwala, A. Mirjafari and X. Zhou, Ionic liquids and poly (ionic liquid)s for 3D printing—A focused mini-review, *Eur. Polym. J.*, 2018, **108**, 390–398.

96 M. Shahbazi, G. Rajabzadeh, A. Rafe, R. Ettelaie and S. J. Ahmadi, Physico-mechanical and structural characteristics of blend film of poly (vinyl alcohol) with biodegradable polymers as affected by disorder-to-order conformational transition, *Food Hydrocolloids*, 2017, **71**, 259–269.

97 L. Y. Zhou, J. Fu and Y. He, A review of 3D printing technologies for soft polymer materials, *Adv. Funct. Mater.*, 2020, **30**(28), 2000187.

98 K. McLellan, Y.-C. Sun, T. Li, T. Chen and H. Naguib, 4D precipitation printing technologies toward sensing devices using microporous structures, *Prog. Addit. Manuf.*, 2024, **9**(1), 15–26.

99 G. Gonzalez, I. Roppolo, C. F. Pirri and A. Chiappone, Current and emerging trends in polymeric 3D printed microfluidic devices, *Addit. Manuf.*, 2022, **55**, 102867.

100 C. Zhang, Y. Li, W. Kang, X. Liu and Q. Wang, Current advances and future perspectives of additive manufacturing for functional polymeric materials and devices, *SusMat*, 2021, **1**(1), 127–147.

101 M. Mabrouk, H. H. Beherei and D. B. Das, Recent progress in the fabrication techniques of 3D scaffolds for tissue engineering, *Mater. Sci. Eng., C*, 2020, **110**, 110716.

102 D. Bahati, M. Bricha and K. El Mabrouk, Vat photopolymerization additive manufacturing technology for bone tissue engineering applications, *Adv. Eng. Mater.*, 2023, **25**(1), 2200859.

103 M. Touri, F. Kabirian, M. Saadati, S. Ramakrishna and M. Mozafari, Additive manufacturing of biomaterials—the evolution of rapid prototyping, *Adv. Eng. Mater.*, 2019, **21**(2), 1800511.

104 Y. Y. C. Choong, S. Maleksaeedi, H. Eng, S. Yu, J. Wei and P.-C. Su, High speed 4D printing of shape memory polymers with nanosilica, *Appl. Mater. Today*, 2020, **18**, 100515.

105 Q. Zhang, X. Kuang, S. Weng, L. Yue, D. J. Roach, D. Fang and H. J. Qi, Shape-memory balloon structures by pneumatic multi-material 4D printing, *Adv. Funct. Mater.*, 2021, **31**(21), 2010872.

106 X. Xu, A. Awad, P. Robles-Martinez, S. Gaisford, A. Goyanes and A. W. Basit, Vat photopolymerization 3D printing for advanced drug delivery and medical device applications, *J. Controlled Release*, 2021, **329**, 743–757.

107 C. Mendes-Felipe, J. Oliveira, I. Etxebarria, J. L. Vilas-Vilela and S. Lanceros-Mendez, State-of-the-art and future challenges of UV curable polymer-based smart materials for printing technologies, *Adv. Mater. Technol.*, 2019, **4**(3), 1800618.

108 S. Park, W. Shou, L. Makatura, W. Matusik and K. K. Fu, 3D printing of polymer composites: Materials, processes, and applications, *Matter*, 2022, **5**(1), 43–76.

109 X. Wang, M. Jiang, Z. Zhou, J. Gou and D. Hui, 3D printing of polymer matrix composites: A review and prospective, *Composites, Part B*, 2017, **110**, 442–458.

110 S. Corbel, O. Dufaud and T. Roques-Carmes, Materials for stereolithography, in *Stereolithography: Materials, processes and applications*, Springer, 2011, pp. 141–159.

111 O. Abdulhameed, A. Al-Ahmari, W. Ameen and S. H. Mian, Additive manufacturing: Challenges, trends, and applications, *Adv. Mech. Eng.*, 2019, **11**(2), 1687814018822880.

112 Q. Mu, L. Wang, C. K. Dunn, X. Kuang, F. Duan, Z. Zhang, H. J. Qi and T. Wang, Digital light processing 3D printing of conductive complex structures, *Addit. Manuf.*, 2017, **18**, 74–83.

113 L. Ge, L. Dong, D. Wang, Q. Ge and G. Gu, A digital light processing 3D printer for fast and high-precision fabrication of soft pneumatic actuators, *Sens. Actuators, A*, 2018, **273**, 285–292.

114 H. Chu, W. Yang, L. Sun, S. Cai, R. Yang, W. Liang, H. Yu and L. Liu, 4D printing: a review on recent progresses, *Micromachines*, 2020, **11**(9), 796.

115 D. Dendukuri, D. C. Pregibon, J. Collins, T. A. Hatton and P. S. Doyle, Continuous-flow lithography for high-throughput microparticle synthesis, *Nat. Mater.*, 2006, **5**(5), 365–369.

116 S. C. Ligon, R. Liska, J. Stampfl, M. Gurr and R. Mülhaupt, Polymers for 3D printing and customized additive manufacturing, *Chem. Rev.*, 2017, **117**(15), 10212–10290.

117 S. K. Melly, L. Liu, Y. Liu and J. Leng, On 4D printing as a revolutionary fabrication technique for smart structures, *Smart Mater. Struct.*, 2020, **29**(8), 083001.

118 S. A. Tofail, E. P. Koumoulos, A. Bandyopadhyay, S. Bose, L. O'Donoghue and C. Charitidis, Additive manufacturing: scientific and technological challenges, market uptake and opportunities, *Mater. Today*, 2018, **21**(1), 22–37.

119 M. Hofmann, 3D printing gets a boost and opportunities with polymer materials, *ACS Macro Lett.*, 2014, **3**(4), 382–386.

120 C. A. Chatham, T. E. Long and C. B. Williams, A review of the process physics and material screening methods for polymer powder bed fusion additive manufacturing, *Prog. Polym. Sci.*, 2019, **93**, 68–95.

121 B. Scherer, I. L. Kottenstedde and F.-M. Matysik, Material characterization of polyamide 12 and related agents used in the multi-jet fusion process: complementary application of high-resolution mass spectrometry and other

advanced instrumental techniques, *Monatsh. Chem.*, 2020, **151**, 1203–1215.

122 Z. Xu, Y. Wang, D. Wu, K. P. Ananth and J. Bai, The process and performance comparison of polyamide 12 manufactured by multi jet fusion and selective laser sintering, *J. Manuf. Process.*, 2019, **47**, 419–426.

123 F. Sillani, R. G. Kleijnen, M. Vetterli, M. Schmid and K. J. A. M. Wegener, Selective laser sintering and multi jet fusion: Process-induced modification of the raw materials and analyses of parts performance, *Addit. Manuf.*, 2019, **27**, 32–41.

124 S. Yuan, F. Shen, C. K. Chua and K. Zhou, Polymeric composites for powder-based additive manufacturing: Materials and applications, *Prog. Polym. Sci.*, 2019, **91**, 141–168.

125 R. Goodridge and S. Ziegelmeyer, 7 – Powder bed fusion of polymers, in *Laser Additive Manufacturing Materials, Design, Technologies, and Applications*, ed. M. Brandt, Woodhead Publishing, 2017, pp. 181–204.

126 F. Sillani, R. G. Kleijnen, M. Vetterli, M. Schmid and K. Wegener, Selective laser sintering and multi jet fusion: Process-induced modification of the raw materials and analyses of parts performance, *Addit. Manuf.*, 2019, **27**, 32–41.

127 S. Rosso, R. Meneghelli, L. Biasetto, L. Grigolato, G. Concheri and G. Savio, In-depth comparison of polyamide 12 parts manufactured by Multi Jet Fusion and Selective Laser Sintering, *Addit. Manuf.*, 2020, **36**, 101713.

128 C. Cai, W. S. Tey, J. Chen, W. Zhu, X. Liu, T. Liu, L. Zhao and K. Zhou, Comparative study on 3D printing of polyamide 12 by selective laser sintering and multi jet fusion, *Mater. Processes Technol.*, 2021, **288**, 116882.

129 F. Calignano, F. Giuffrida and M. Galati, Effect of the build orientation on the mechanical performance of polymeric parts produced by multi jet fusion and selective laser sintering, *J. Manuf. Process.*, 2021, **65**, 271–282.

130 F. Wang, F. Luo, Y. Huang, X. Cao and C. Yuan, 4D printing via multispeed fused deposition modeling, *Adv. Mater. Technol.*, 2023, **8**(2), 2201383.

131 B. I. Oladapo, J. F. Kayode, J. O. Akinyoola and O. M. Ikumapayi, Shape memory polymer review for flexible artificial intelligence materials of biomedical, *Mater. Chem. Phys.*, 2023, **293**, 126930.

132 Y. Wang, J. Zhang, M. Li, M. Lei, Y. Wang and Q. Wei, 3D printing thermo-responsive shape memory polymer composite based on PCL/TPU blends, *J. Polym. Res.*, 2022, **29**(6), 243.

133 O. A. Mohamed, S. H. Masood and J. L. Bhowmik, Optimization of fused deposition modeling process parameters: a review of current research and future prospects, *Adv. Manuf.*, 2015, **3**, 42–53.

134 O. S. Carneiro, A. Silva and R. Gomes, Fused deposition modeling with polypropylene, *Mater. Des.*, 2015, **83**, 768–776.

135 H. R. Dana, F. Barbe, L. Delbreilh, M. B. Azzouna, A. Guillet and T. Breteau, Polymer additive manufacturing of ABS structure: Influence of printing direction on mechanical properties, *J. Manuf. Process.*, 2019, **44**, 288–298.

136 Y. Wang and X. Li, An accurate finite element approach for programming 4D-printed self-morphing structures produced by fused deposition modeling, *Mech. Mater.*, 2020, **151**, 103628.

137 S. C. Daminabo, S. Goel, S. A. Grammatikos, H. Y. Nezhad and V. K. Thakur, Fused deposition modeling-based additive manufacturing (3D printing): techniques for polymer material systems, *Mater. Today Chem.*, 2020, **16**, 100248.

138 A. Rayate and P. K. Jain, A review on 4D printing material composites and their applications, *Mater. Today: Proc.*, 2018, **5**(9), 20474–20484.

139 A. Shen, D. Caldwell, A. W. Ma and S. Dardona, Direct write fabrication of high-density parallel silver interconnects, *Addit. Manuf.*, 2018, **22**, 343–350.

140 J. Cesarano, R. Segalman and P. Calvert, Robocasting provides MOULDLESS fabrication from slurry deposition, *Ceram. Ind.*, 1998, **148**(4), 94–96.

141 R. D. Farahani, M. Dubé and D. Therriault, Three-dimensional printing of multifunctional nanocomposites: manufacturing techniques and applications, *Adv. Mater.*, 2016, **28**(28), 5794–5821.

142 Y.-W. Moon, I.-J. Choi, Y.-H. Koh and H.-E. Kim, Porous alumina ceramic scaffolds with biomimetic macro/micro-porous structure using three-dimensional (3-D) ceramic/camphene-based extrusion, *Ceram. Int.*, 2015, **41**(9), 12371–12377.

143 V. C. Li, A. Mulyadi, C. K. Dunn, Y. Deng and H. J. Qi, Direct ink write 3D printed cellulose nanofiber aerogel structures with highly deformable, shape recoverable, and functionalizable properties, *ACS Sustainable Chem. Eng.*, 2018, **6**(2), 2011–2022.

144 A. Haake, R. Tutika, G. M. Schloer, M. D. Bartlett and E. J. Markvicka, On-demand programming of liquid metal–composite microstructures through direct ink write 3D printing, *Adv. Mater.*, 2022, **34**(20), 2200182.

145 Y. Jian, B. Wu, X. Yang, Y. Peng, D. Zhang, Y. Yang, H. Qiu, H. Lu, J. Zhang and T. Chen, Stimuli-responsive hydrogel sponge for ultrafast responsive actuator, *Supramol. Mater.*, 2022, **1**, 100002.

146 L. Li, Q. Lin, M. Tang, A. J. Duncan and C. Ke, Advanced polymer designs for direct-ink-write 3D printing, *Chem. – Eur. J.*, 2019, **25**(46), 10768–10781.

147 V. Domsta and A. Seidlitz, 3D-printing of drug-eluting implants: an overview of the current developments described in the literature, *Molecules*, 2021, **26**(13), 4066.

148 C. Liu, N. Huang, F. Xu, J. Tong, Z. Chen, X. Gui, Y. Fu and C. Lao, 3D printing technologies for flexible tactile sensors toward wearable electronics and electronic skin, *Polymers*, 2018, **10**(6), 629.

149 P. T. Smith, A. Basu, A. Saha and A. Nelson, Chemical modification and printability of shear-thinning hydrogel inks for direct-write 3D printing, *Polymer*, 2018, **152**, 42–50.

150 P. Zarrintaj, M. Jouyandeh, M. R. Ganjali, B. S. Hadavand, M. Mozafari, S. S. Sheiko, M. Vatankhah-Varnoosfaderani, T. J. Gutiérrez and M. R. Saeb, Thermo-sensitive polymers in medicine: A review, *Eur. Polym. J.*, 2019, **117**, 402–423.

151 A. Ghilan, A. P. Chiriac, L. E. Nita, A. G. Rusu, I. Neamtu and V. M. Chiriac, Trends in 3D printing processes for biomedical field: opportunities and challenges, *J. Polym. Environ.*, 2020, **28**, 1345–1367.

152 M. R. Matanović, J. Kristl and P. A. Grabnar, Thermoresponsive polymers: Insights into decisive hydrogel characteristics, mechanisms of gelation, and promising biomedical applications, *Int. J. Pharm.*, 2014, **472**(1–2), 262–275.

153 H. Sekine, T. Shimizu, K. Sakaguchi, I. Dobashi, M. Wada, M. Yamato, E. Kobayashi, M. Umezawa and T. Okano, In vitro fabrication of functional three-dimensional tissues with perfusable blood vessels, *Nat. Commun.*, 2013, **4**(1), 1399.

154 L. Klouda, Thermoresponsive hydrogels in biomedical applications: A seven-year update, *Eur. J. Pharm. Biopharm.*, 2015, **97**, 338–349.

155 Q. Xing, K. Yates, C. Vogt, Z. Qian, M. C. Frost and F. Zhao, Increasing mechanical strength of gelatin hydrogels by divalent metal ion removal, *Sci. Rep.*, 2014, **4**(1), 4706.

156 H. Rastin, B. Zhang, J. Bi, K. Hassan, T. T. Tung and D. Lasic, 3D printing of cell-laden electroconductive bioinks for tissue engineering applications, *J. Mater. Chem. B*, 2020, **8**(27), 5862–5876.

157 S. A. Mohammad, S. Dolui, D. Kumar, S. R. Mane and S. Banerjee, Facile access to functional polyacrylates with dual stimuli response and tunable surface hydrophobicity, *Polym. Chem.*, 2021, **12**(20), 3042–3051.

158 W. Xu, X. Wang, N. Sandler, S. Willfor and C. Xu, Three-dimensional printing of wood-derived biopolymers: a review focused on biomedical applications, *ACS Sustainable Chem. Eng.*, 2018, **6**(5), 5663–5680.

159 Y. Guo, H. S. Patanwala, B. Bognet and A. W. Ma, Inkjet and inkjet-based 3D printing: connecting fluid properties and printing performance, *Rapid Prototyping*, 2017, **23**(3), 562–576.

160 B. Derby, Inkjet printing of functional and structural materials: fluid property requirements, feature stability, and resolution, *Annu. Rev. Mater. Res.*, 2010, **40**(1), 395–414.

161 P. Vinogradov, 3D printing in medicine: Current challenges and potential applications, in *3D Printing Technology in Nanomedicine*, Missouri, Elsevier Inc, 2019.

162 S. Waheed, J. M. Cabot, N. P. Macdonald, T. Lewis, R. M. Guijt, B. Paull and M. C. Breadmore, 3D printed microfluidic devices: enablers and barriers, *Lab Chip*, 2016, **16**(11), 1993–2013.

163 S. F. S. Shirazi, S. Gharehkhani, M. Mehrali, H. Yarmand, H. S. C. Metselaar, N. A. Kadri and N. A. A. Osman, A review on powder-based additive manufacturing for tissue engineering: selective laser sintering and inkjet 3D printing, *Sci. Technol. Adv. Mater.*, 2015, **16**(3), 033502.

164 Y. Tsukamoto, T. Akagi, F. Shima and M. Akashi, Fabrication of orientation-controlled 3D tissues using a layer-by-layer technique and 3D printed a thermo-responsive gel frame, *Tissue Eng., Part C*, 2017, **23**(6), 357–366.

165 L. R. Hart, S. Li, C. Sturgess, R. Wildman, J. R. Jones and W. Hayes, 3D printing of biocompatible supramolecular polymers and their composites, *ACS Appl. Mater. Interfaces*, 2016, **8**(5), 3115–3122.

166 Y. Li, X. Sun, G. Chang and R. Li, Novel inkjet direct printing technology based on thermosensitive sol-gel transition inks, *Text. Res. J.*, 2022, **92**(23–24), 4606–4617.

167 J. Pardeike, D. M. Strohmeier, N. Schrödl, C. Voura, M. Gruber, J. G. Khinast and A. Zimmer, Nanosuspensions as advanced printing ink for accurate dosing of poorly soluble drugs in personalized medicines, *Int. J. Pharm.*, 2011, **420**(1), 93–100.

168 A. Cazón, P. Morer and L. Matey, PolyJet technology for product prototyping: Tensile strength and surface roughness properties, *Proc. Inst. Mech. Eng., Part B*, 2014, **228**(12), 1664–1675.

169 M. Fahad, P. Dickens and M. Gilbert, Novel polymeric support materials for jetting based additive manufacturing processes, *Rapid Prototyping J.*, 2013, **19**(4), 230–239.

170 O. Ivanova, A. Elliott, T. Campbell and C. Williams, Unclonable security features for additive manufacturing, *Addit. Manuf.*, 2014, **1**, 24–31.

171 J. W. Stansbury and M. J. Idacavage, 3D printing with polymers: Challenges among expanding options and opportunities, *Dent. Mater.*, 2016, **32**(1), 54–64.

172 R. Singh, Process capability study of polyjet printing for plastic components, *J. Mech. Sci. Technol.*, 2011, **25**(4), 1011–1015.

173 R. Singh, Process capability study of polyjet printing for plastic components, *J. Mech. Sci. Technol.*, 2011, **25**(4), 1011–1015.

174 D. Raviv, W. Zhao, C. McKnelly, A. Papadopoulou, A. Kadambi, B. Shi, S. Hirsch, D. Dikovsky, M. Zyracki, C. Olgun, R. Raskar and S. Tibbits, Active Printed Materials for Complex Self-Evolving Deformations, *Sci. Rep.*, 2014, **4**(1), 7422.

175 Z. Ding, C. Yuan, X. Peng, T. Wang, H. J. Qi and M. L. Dunn, Direct 4D printing via active composite materials, *Sci. Adv.*, 2017, **3**(4), e1602890.

176 J. Wu, C. Yuan, Z. Ding, M. Isakov, Y. Mao, T. Wang, M. L. Dunn and H. J. Qi, Multi-shape active composites by 3D printing of digital shape memory polymers, *Sci. Rep.*, 2016, **6**(1), 24224.

177 Y. L. Yap and W. Y. Yeong, Shape recovery effect of 3D printed polymeric honeycomb, *Virtual Phys. Prototyp.*, 2015, **10**(2), 91–99.

178 M. Wagner, T. Chen and K. Shea, Large Shape Transforming 4D Auxetic Structures, *3D Print. Addit. Manuf.*, 2017, **4**(3), 133–142.

179 Q. Ge, C. K. Dunn, H. J. Qi and M. L. Dunn, Active origami by 4D printing, *Smart Mater. Struct.*, 2014, **23**(9), 094007.

180 X. Kong, M. Dong, M. Du, J. Qian, J. Yin, Q. Zheng and Z. L. Wu, Recent Progress in 3D Printing of Polymer Materials as Soft Actuators and Robots, *Chem Bio Eng.*, 2024, **1**(4), 312–329.

181 M. K. Porwal, M. M. Hausladen, C. J. Ellison and T. M. Reineke, Biobased and degradable thiol-ene networks from levoglucosan for sustainable 3D printing, *Green Chem.*, 2023, **25**(4), 1488–1502.

182 J.-J. Wu, L.-M. Huang, Q. Zhao and T. Xie, 4D printing: history and recent progress, *Chin. J. Polym. Sci.*, 2018, **36**, 563–575.

183 H. Wei, Q. Zhang, Y. Yao, L. Liu, Y. Liu and J. Leng, Direct-Write Fabrication of 4D Active Shape-Changing Structures Based on a Shape Memory Polymer and Its Nanocomposite, *ACS Appl. Mater. Interfaces*, 2017, **9**(1), 876–883.

184 J. Li, C. Wu, P. K. Chu and M. Gelinsky, 3D printing of hydrogels: Rational design strategies and emerging biomedical applications, *Mater. Sci. Eng., R*, 2020, **140**, 100543.

185 Y. Cheng, K. H. Chan, X.-Q. Wang, T. Ding, T. Li, X. Lu and G. W. Ho, Direct-ink-write 3D printing of hydrogels into biomimetic soft robots, *ACS Nano*, 2019, **13**(11), 13176–13184.

186 M. Bahram, N. Mohseni and M. Moghtader, An introduction to hydrogels and some recent applications, in *Emerging concepts in analysis and applications of hydrogels*, IntechOpen, 2016.

187 N. Singh, P. Sinha, B. Sahu, S. Mandal, S. Bhattacharyya and S. Banerjee, Ultrasmall Sulfur-Dots-Mediated Facile Photopolymerization for the Production of Smart Injectable Ink for 3D Printing Applications, *Adv. Funct. Mater.*, 2025, **35**(6), 2415125.

188 Z. Xiang, N. Li, Y. Rong, L. Zhu and X. Huang, 3D-printed high-toughness double network hydrogels via digital light processing, *Colloids Surf., A*, 2022, **639**, 128329.

189 M. Guvendiren, H. D. Lu and J. A. Burdick, Shear-thinning hydrogels for biomedical applications, *Soft Matter*, 2012, **8**(2), 260–272.

190 J. Jin, L. Cai, Y.-G. Jia, S. Liu, Y. Chen and L. Ren, Progress in self-healing hydrogels assembled by host–guest interactions: preparation and biomedical applications, *J. Mater. Chem. B*, 2019, **7**(10), 1637–1651.

191 C. Yuan, D. J. Roach, C. K. Dunn, Q. Mu, X. Kuang, C. M. Yakacki, T. J. Wang, K. Yu and H. J. Qi, 3D printed reversible shape changing soft actuators assisted by liquid crystal elastomers, *Soft Matter*, 2017, **13**(33), 5558–5568.

192 A. Kotikian, R. L. Truby, J. W. Boley, T. J. White and J. A. Lewis, 3D printing of liquid crystal elastomeric actuators with spatially programed nematic order, *Adv. Mater.*, 2018, **30**(10), 1706164.

193 L. R. Jaidev and K. Chatterjee, Surface functionalization of 3D printed polymer scaffolds to augment stem cell response, *Mater. Des.*, 2019, **161**, 44–54.

194 K. Lee, N. Corrigan and C. Boyer, Rapid High-Resolution 3D Printing and Surface Functionalization via Type I Photoinitiated RAFT Polymerization, *Angew. Chem., Int. Ed.*, 2021, **60**(16), 8839–8850.

195 A. Mautner, X. Qin, H. Wutz, S. C. Ligon, B. Kapeller, D. Moser, G. Russmueller, J. Stampfl and R. Liska, Thiol-ene photopolymerization for efficient curing of vinyl esters, *J. Polym. Sci., Part A: Polym. Chem.*, 2013, **51**(1), 203–212.

196 L. Ren, Z. Wang, L. Ren, Z. Han, X. L. Zhou, Z. Song and Q. Liu, 4D printing of shape-adaptive tactile sensor with tunable sensing characteristics, *Composites, Part B*, 2023, **265**, 110959.

197 Y. Wang and X. Li, 4D printing reversible actuator with strain self-sensing function via structural design, *Composites, Part B*, 2021, **211**, 108644.

198 T. Ma, Y. Zhang, K. Ruan, H. Guo, M. He, X. Shi, Y. Guo, J. Kong and J. Gu, Advances in 3D printing for polymer composites: A review, *InfoMat*, 2024, **6**(6), e12568.

199 C. B. Sweeney, B. A. Lackey, M. J. Pospisil, T. C. Achee, V. K. Hicks, A. G. Moran, B. R. Teipel, M. A. Saed and M. J. Green, Welding of 3D-printed carbon nanotube-polymer composites by locally induced microwave heating, *Sci. Adv.*, 2017, **3**(6), e1700262.

200 G. S. Wilson and R. Gifford, Biosensors for real-time in vivo measurements, *Biosens. Bioelectron.*, 2005, **20**(12), 2388–2403.

201 S. Zhang, G. Wright and Y. Yang, Materials and techniques for electrochemical biosensor design and construction, *Biosens. Bioelectron.*, 2000, **15**(5–6), 273–282.

202 G. Remaggi, A. Zaccarelli and L. Elviri, 3D printing technologies in biosensors production: Recent developments, *Chemosensors*, 2022, **10**(2), 65.

203 T. Distler and A. R. Boccaccini, 3D printing of electrically conductive hydrogels for tissue engineering and biosensors—A review, *Acta Biomater.*, 2020, **101**, 1–13.

204 R. Baughman, Conducting polymer artificial muscles, *Synth. Met.*, 1996, **78**(3), 339–353.

205 S. Adelaju and G. Wallace, Conducting polymers and the bioanalytical sciences: new tools for biomolecular communications. A review, *Analyst*, 1996, **121**(6), 699–703.

206 Y. Song, H. Dong, W. Liu, X. Fu, Z. Fu, P. Li, L. Chen, Z. Ahmad, J. Liu and X. Chen, Electrostatic jet engineering of flexible composite pressure sensors for physical applications, *ACS Appl. Polym. Mater.*, 2022, **4**(2), 868–878.

207 J. Odent, N. Baleine, V. Biard, Y. Dobashi, C. Vancaeyzeele, G. T. Nguyen, J. D. Madden, C. Plesse and J. M. Raquez, 3D-printed stacked ionic assemblies for iontronic touch sensors, *Adv. Funct. Mater.*, 2023, **33**(3), 2210485.

208 Y. Song, H. Dong, W. Liu, X. Fu, Z. Fu, P. Li, L. Chen, Z. Ahmad, J. Liu and X. Chen, Electrostatic jet engineering of flexible composite pressure sensors for physical applications, *ACS Appl. Polym. Mater.*, 2022, **4**(2), 868–878.

209 J. Odent, N. Baleine, V. Biard, Y. Dobashi, C. Vancaeyzeele, G. T. Nguyen, J. D. Madden, C. Plesse and J. M. Raquez, 3D-printed stacked ionic assemblies

for iontronic touch sensors, *Adv. Funct. Mater.*, 2023, **33**(3), 2210485.

210 Z. Zhu, H. Park and M. McAlpine, 3D printed deformable sensors, *Sci. Adv.*, 2020, **6**(25), eaba5575.

211 C. Berggren, B. Bjarnason and G. Johansson, Capacitive biosensors, *Int. J. Devoted Fundam. Pract. Asp. Electroanal.*, 2001, **13**(3), 173–180.

212 Q. Yi, S. Najafikhoshnou, P. Das, S. Noh, E. Hoang, T. Kim and R. Esfandyarpour, All-3D-printed, flexible, and hybrid wearable bioelectronic tactile sensors using biocompatible nanocomposites for health monitoring, *Adv. Mater. Technol.*, 2022, **7**(5), 2101034.

213 U. Witt, T. Einig, M. Yamamoto, I. Kleeberg, W.-D. Deckwer and R.-J. Müller, Biodegradation of aliphatic–aromatic copolymers: evaluation of the final biodegradability and ecotoxicological impact of degradation intermediates, *Chemosphere*, 2001, **44**(2), 289–299.

214 S. Smart, A. Cassady, G. Lu and D. Martin, The biocompatibility of carbon nanotubes, *Carbon*, 2006, **44**(6), 1034–1047.

215 R. Herbert, S. Mishra, H. R. Lim, H. Yoo and W. H. Yeo, Fully printed, wireless, stretchable implantable biosystem toward batteryless, real-time monitoring of cerebral aneurysm hemodynamics, *Adv. Sci.*, 2019, **6**(18), 1901034.

216 T. Kim, A. H. Kalhori, T.-H. Kim, C. Bao and W. S. Kim, 3D designed battery-free wireless origami pressure sensor, *Microsyst. Nanoeng.*, 2022, **8**(1), 120.

217 C. C. Collins, Miniature passive pressure transensor for implanting in the eye, *IEEE Trans. Biomed. Eng.*, 2008, 74–83.

218 Q.-A. Huang, L. Dong and L.-F. Wang, LC passive wireless sensors toward a wireless sensing platform: status, prospects, and challenges, *J. Microelectromech. Syst.*, 2016, **25**(5), 822–841.

219 C. M. Bouthy, L. Beker, Y. Kaizawa, C. Vassos, H. Tran, A. C. Hinckley, R. Pfattner, S. Niu, J. Li and J. Claverie, Biodegradable and flexible arterial-pulse sensor for the wireless monitoring of blood flow, *Nat. Biomed. Eng.*, 2019, **3**(1), 47–57.

220 C. P. Constantin, M. Aflori, R. F. Damian and R. D. Rusu, Biocompatibility of polyimides: A mini-review, *Materials*, 2019, **12**(19), 3166.

221 T. Kim, A. H. Kalhori, T.-H. Kim, C. Bao and W. S. Kim, 3D designed battery-free wireless origami pressure sensor, *Microsyst. Nanoeng.*, 2022, **8**(1), 120.

222 Y. Yang and W. Gao, Wearable and flexible electronics for continuous molecular monitoring, *Chem. Soc. Rev.*, 2019, **48**(6), 1465–1491.

223 W. Shi, S. Jang, M. A. Kuss, O. A. Alimi, B. Liu, J. Palik, L. Tan, M. A. Krishnan, Y. Jin and C. Yu, Digital Light Processing 4D Printing of Poloxamer Micelles for Facile fabrication of multifunctional biocompatible hydrogels as tailored wearable sensors, *ACS Nano*, 2024, **18**(10), 7580–7595.

224 T. Kim, Q. Yi, E. Hoang and R. Esfandyarpour, A 3D printed wearable bioelectronic patch for multi-sensing and in situ sweat electrolyte monitoring, *Adv. Mater. Technol.*, 2021, **6**(4), 2001021.

225 N. J. Kinar and M. Brinkmann, Development of a sensor and measurement platform for water quality observations: Design, sensor integration, 3D printing, and open-source hardware, *Environ. Monit. Assess.*, 2022, **194**(3), 207.

226 Z. Sonner, E. Wilder, J. Heikenfeld, G. Kasting, F. Beyette, D. Swaile, F. Sherman, J. Joyce, J. Hagen and N. Kelley-Loughnane, The microfluidics of the eccrine sweat gland, including biomarker partitioning, transport, and biosensing implications, *Biomicrofluidics*, 2015, **9**(3), 031301.

227 T. Kim, Q. Yi, E. Hoang and R. Esfandyarpour, A 3D Printed Wearable Bioelectronic Patch for Multi-Sensing and In Situ Sweat Electrolyte Monitoring, *Adv. Mater. Technol.*, 2021, **6**(4), 2001021.

228 C.-H. Wu, H. J. H. Ma, P. Baessler, R. K. Balanay and T. R. Ray, Skin-interfaced microfluidic systems with spatially engineered 3D fluidics for sweat capture and analysis, *Sci. Adv.*, 2023, **9**(18), eadg4272.

229 D. S. Yang, Y. Wu, E. E. Kanatzidis, R. Avila, M. Zhou, Y. Bai, S. Chen, Y. Sekine, J. Kim, Y. Deng, H. Guo, Y. Zhang, R. Ghaffari, Y. Huang and J. A. Rogers, 3D-printed epidermal sweat microfluidic systems with integrated microcuvettes for precise spectroscopic and fluorometric biochemical assays, *Mater. Horiz.*, 2023, **10**(11), 4992–5003.

230 C. Schmidlein, S. Malferrari, R. Palgrave, D. Bomze, M. Schwentenwein and D. M. Kalaskar, Application of high resolution DLP stereolithography for fabrication of tricalcium phosphate scaffolds for bone regeneration, *Biomed. Mater.*, 2019, **14**(4), 045018.

231 E. George, P. Liacouras, F. J. Rybicki and D. Mitsouras, Measuring and establishing the accuracy and reproducibility of 3D printed medical models, *Radiographics*, 2017, **37**(5), 1424–1450.

232 G. L. Goh, H. Zhang, T. H. Chong and W. Y. Yeong, 3D printing of multilayered and multimaterial electronics: A review, *Adv. Electron. Mater.*, 2021, **7**(10), 2100445.

233 Q. Shi, H. Liu, D. Tang, Y. Li, X. Li and F. Xu, Bioactuators based on stimulus-responsive hydrogels and their emerging biomedical applications, *NPG Asia Mater.*, 2019, **11**(1), 64.

234 L. Sun, Z. Li, Y. Zhang, Y. Lu and S. Zhang, Stimuli-responsive shape-morphing soft actuators: metrics, materials, mechanism, design and applications, *Prog. Polym. Sci.*, 2026, **155**, 101531.

235 B. E.-F. de Ávila, P. Angsantikul, J. Li, M. Angel Lopez-Ramirez, D. E. Ramirez-Herrera, S. Thamphiwatana, C. Chen, J. Delezuk, R. Samakapiruk, V. Ramez, M. Obonyo, L. Zhang and J. Wang, Micromotor-enabled active drug delivery for in vivo treatment of stomach infection, *Nat. Commun.*, 2017, **8**(1), 272.

236 S. Roy, J. Kim, M. Kotal, K. J. Kim and I.-K. Oh, Electroionic Antagonistic Muscles Based on Nitrogen-Doped Carbons Derived from Poly(Triazine-Triptycene), *Adv. Sci.*, 2017, **4**(12), 1700410.

237 L. Zhang and P. Naumov, Light- and Humidity-Induced Motion of an Acidochromic Film, *Angew. Chem., Int. Ed.*, 2015, **54**(30), 8642–8647.

238 R. Mestre, T. Patiño, X. Barceló, S. Anand, A. Pérez-Jiménez and S. Sánchez, Force Modulation and Adaptability of 3D-Bioprinted Biological Actuators Based on Skeletal Muscle Tissue, *Adv. Mater. Technol.*, 2019, **4**(2), 1800631.

239 H. Xu, C. Wang, C. Wang, J. Zoval and M. Madou, Polymer actuator valves toward controlled drug delivery application, *Biosens. Bioelectron.*, 2006, **21**(11), 2094–2099.

240 M. Pan, C. Yuan, X. Liang, T. Dong, T. Liu, J. Zhang, J. Zou, H. Yang and C. Bowen, Soft Actuators and Robotic Devices for Rehabilitation and Assistance, *Adv. Intell. Syst.*, 2022, **4**(4), 2100140.

241 Q. Song, Y. Chen, P. Hou, P. Zhu, D. Helmer, F. Kotz-Helmer and B. E. Rapp, Fabrication of multi-material pneumatic actuators and microactuators using stereolithography, *Micromachines*, 2023, **14**(2), 244.

242 M. Schaffner, J. A. Faber, L. Pianegonda, P. A. Rühs, F. Coulter and A. R. Stuwart, 3D printing of robotic soft actuators with programmable bioinspired architectures, *Nat. Commun.*, 2018, **9**(1), 878.

243 D. Ravichandran, M. Kakarla, W. Xu, S. Jambhulkar, Y. Zhu, M. Bawareth, N. Fonseca, D. Patil and K. Song, 3D-printed in-line and out-of-plane layers with stimuli-responsive intelligence, *Composites, Part B*, 2022, **247**, 110352.

244 M. Schaffner, J. A. Faber, L. Pianegonda, P. A. Rühs, F. Coulter and A. R. Stuwart, 3D printing of robotic soft actuators with programmable bioinspired architectures, *Nat. Commun.*, 2018, **9**(1), 878.

245 D. Ravichandran, M. Kakarla, W. Xu, S. Jambhulkar, Y. Zhu, M. Bawareth, N. Fonseca, D. Patil and K. Song, 3D-printed in-line and out-of-plane layers with stimuli-responsive intelligence, *Composites, Part B*, 2022, **247**, 110352.

246 D. Ravichandran, W. Xu, M. Kakarla, S. Jambhulkar, Y. Zhu and K. Song, Multiphase direct ink writing (MDIW) for multilayered polymer/nanoparticle composites, *Addit. Manuf.*, 2021, **47**, 102322.

247 R. L. Truby, M. Wehner, A. K. Grosskopf, D. M. Vogt, S. G. M. Uzel, R. J. Wood and J. A. Lewis, Soft Somatosensitive Actuators via Embedded 3D Printing, *Adv. Mater.*, 2018, **30**(15), 1706383.

248 M. Zhu, S. Biswas, S. I. Dinulescu, N. Kastor, E. W. Hawkes and Y. Visell, Soft, Wearable Robotics and Haptics: Technologies, Trends, and Emerging Applications, *Proc. IEEE*, 2022, **110**(2), 246–272.

249 J. Z. Gul, S. Memoon, R. M. Muqeet, S. G. Uddin, S. Imran, K. Kyung-Hwan, L. Jae-Wook and K. H. Choi, 3D printing for soft robotics – a review, *Sci. Technol. Adv. Mater.*, 2018, **19**(1), 243–262.

250 A. Mohammadi, J. Lavranos, H. Zhou, R. Mutlu, G. Alici, Y. Tan, P. Choong and D. Oetomo, A practical 3D-printed soft robotic prosthetic hand with multi-articulating capabilities, *PLoS One*, 2020, **15**(5), e0232766.

251 B. A. W. Keong and R. Y. C. Hua, A novel fold-based design approach toward printable soft robotics using flexible 3D printing materials, *Adv. Mater. Technol.*, 2018, **3**(2), 1700172.

252 J. D. Hubbard, R. Acevedo, K. M. Edwards, A. T. Alsharhan, Z. Wen, J. Landry, K. Wang, S. Schaffer and R. D. Sochol, Fully 3D-printed soft robots with integrated fluidic circuitry, *Sci. Adv.*, 2021, **7**(29), eabe5257.

253 A. Mohammadi, J. Lavranos, H. Zhou, R. Mutlu, G. Alici, Y. Tan, P. Choong and D. Oetomo, A practical 3D-printed soft robotic prosthetic hand with multi-articulating capabilities, *PLoS One*, 2020, **15**(5), e0232766.

254 D. Qi, K. Zhang, G. Tian, B. Jiang and Y. Huang, Stretchable Electronics Based on PDMS Substrates, *Adv. Mater.*, 2021, **33**(6), 2003155.

255 A. Larmagnac, S. Eggenberger, H. Janossy and J. Vörös, Stretchable electronics based on Ag-PDMS composites, *Sci. Rep.*, 2014, **4**(1), 7254.

256 M. Cianchetti, C. Laschi, A. Menciassi and P. Dario, Biomedical applications of soft robotics, *Nat. Rev. Mater.*, 2018, **3**(6), 143–153.

257 G. Gu, N. Zhang, C. Chen, H. Xu and X. Zhu, Soft robotics enables neuroprosthetic hand design, *ACS Nano*, 2023, **17**(11), 9661–9672.

258 Y. L. Yap, S. L. Sing and W. Y. Yeong, A review of 3D printing processes and materials for soft robotics, *Rapid Prototyp.*, 2020, **26**(8), 1345–1361.

259 M. Yu, Y. Peng, X. Wang and F. Ran, Emerging design strategies toward developing next-generation implantable batteries and supercapacitors, *Adv. Funct. Mater.*, 2023, **33**(37), 2301877.

260 M. Y. Khalid, Z. U. Arif, A. Tariq, M. Hossain, R. Umer and M. Bodaghi, 3D printing of active mechanical metamaterials: A critical review, *Mater. Des.*, 2024, **246**, 113305.

261 Z. Yi, F. Xie, Y. Tian, N. Li, X. Dong, Y. Ma, Y. Huang, Y. Hu, X. Xu and D. Qu, A battery-and leadless heart-worn pacemaker strategy, *Adv. Funct. Mater.*, 2020, **30**(25), 2000477.

262 S. A. Han, M. Naqi, S. Kim and J. H. Kim, All-day wearable health monitoring system, *EcoMat*, 2022, **4**(4), e12198.

263 J. Zhang, J. Xu, J. Lim, J. K. Nolan, H. Lee and C. H. Lee, Wearable glucose monitoring and implantable drug delivery systems for diabetes management, *Adv. Healthcare Mater.*, 2021, **10**(17), 2100194.

264 O. Frazier, Prologue: ventricular assist devices and total artificial hearts: a historical perspective, *Cardiol. Clin.*, 2003, **21**(1), 1–13.

265 J. B. Goodenough and K.-S. Park, The Li-ion rechargeable battery: a perspective, *J. Am. Chem. Soc.*, 2013, **135**(4), 1167–1176.

266 A. Maurel, M. Courty, B. Fleutot, H. Tortajada, K. Prashantha, M. Armand, S. Grugéon, S. Panier and L. Dupont, Highly loaded graphite–polylactic acid composite-based filaments for lithium-ion battery three-dimensional printing, *Chem. Mater.*, 2018, **30**(21), 7484–7493.

267 W. Gao, C. Iffelsberger and M. Pumera, Dual polymer engineering enables high-performance 3D printed Zn-organic battery cathodes, *Appl. Mater. Today*, 2022, **28**, 101515.

268 M. H. Lee, J. Lee, S. K. Jung, D. Kang, M. S. Park, G. D. Cha, K. W. Cho, J. H. Song, S. Moon and Y. S. Yun, A biodegradable secondary battery and its biodegradation mechanism for eco-friendly energy-storage systems, *Adv. Mater.*, 2021, **33**(10), 2004902.

269 Z. Lyu, G. J. Lim, J. J. Koh, Y. Li, Y. Ma, J. Ding, J. Wang, Z. Hu, J. Wang and W. Chen, Design and manufacture of 3D-printed batteries, *Joule*, 2021, **5**(1), 89–114.

270 X. Huang, D. Wang, Z. Yuan, W. Xie, Y. Wu, R. Li, Y. Zhao, D. Luo, L. Cen and B. Chen, A fully biodegradable battery for self-powered transient implants, *Small*, 2018, **14**(28), 1800994.

271 M. Parvez Mahmud, N. Huda, S. H. Farjana, M. Asadnia and C. Lang, Recent advances in nanogenerator-driven self-powered implantable biomedical devices, *Adv. Energy Mater.*, 2018, **8**(2), 1701210.

272 Y. Jia, Q. Jiang, H. Sun, P. Liu, D. Hu, Y. Pei, W. Liu, X. Crispin, S. Fabiano and Y. Ma, Wearable thermoelectric materials and devices for self-powered electronic systems, *Adv. Mater.*, 2021, **33**(42), 2102990.

273 Y. Wu, Y. Ma, H. Zheng and S. Ramakrishna, Piezoelectric materials for flexible and wearable electronics: A review, *Mater. Des.*, 2021, **211**, 110164.

274 Z. Liu, H. Li, B. Shi, Y. Fan, Z. L. Wang and Z. Li, Wearable and implantable triboelectric nanogenerators, *Adv. Funct. Mater.*, 2019, **29**(20), 1808820.

275 H. Xue, Q. Yang, D. Wang, W. Luo, W. Wang, M. Lin, D. Liang and Q. Luo, A wearable pyroelectric nanogenerator and self-powered breathing sensor, *Nano Energy*, 2017, **38**, 147–154.

276 W. Xu, S. Jambhulkar, D. Ravichandran, Y. Zhu, M. Kakarla, Q. Nian, B. Azeredo, X. Chen, K. Jin and B. Vernon, 3D printing-enabled nanoparticle alignment: a review of mechanisms and applications, *Small*, 2021, **17**(45), 2100817.

277 Y. Zhu, W. Xu, D. Ravichandran, S. Jambhulkar and K. Song, A gill-mimicking thermoelectric generator (TEG) for waste heat recovery and self-powering wearable devices, *J. Mater. Chem. A*, 2021, **9**(13), 8514–8526.

278 Y. Zhu, W. Xu, D. Ravichandran, S. Jambhulkar and K. Song, A gill-mimicking thermoelectric generator (TEG) for waste heat recovery and self-powering wearable devices, *J. Mater. Chem. A*, 2021, **9**(13), 8514–8526.

279 Z. Wang and Y. Yang, Application of 3D printing in implantable medical devices, *BioMed Res. Int.*, 2021, **2021**(1), 6653967.

280 S. Liu, W. Wang, W. Xu, L. Liu, W. Zhang, K. Song and X. Chen, Continuous three-dimensional printing of architected piezoelectric sensors in minutes, *Research*, 2022, 9790307.

281 J. Li, Y. Long, F. Yang, H. Wei, Z. Zhang, Y. Wang, J. Wang, C. Li, C. Carlos and Y. Dong, Multifunctional artificial artery from direct 3D printing with built-in ferroelectricity and tissue-matching modulus for real-time sensing and occlusion monitoring, *Adv. Funct. Mater.*, 2020, **30**(39), 2002868.

282 T. Bhatta, P. Maharjan, M. Salauddin, M. T. Rahman, S. S. Rana and J. Y. Park, A battery-less arbitrary motion sensing system using magnetic repulsion-based self-powered motion sensors and hybrid nanogenerator, *Adv. Funct. Mater.*, 2020, **30**(36), 2003276.

283 W. Li, L. Wan, Y. Lin, G. Liu, H. Qu, H. Wen, J. Ding, H. Ning and H. Yao, Synchronous nanogenerator with intermittent sliding friction self-excitation for water wave energy harvesting, *Nano Energy*, 2022, **95**, 106994.

284 V. Vivekananthan, A. Chandrasekhar, N. R. Alluri, Y. Purusothaman and S.-J. Kim, A highly reliable, impermeable and sustainable triboelectric nanogenerator as a zero-power consuming active pressure sensor, *Nanoscale Adv.*, 2020, **2**(2), 746–754.

285 S. Zhang, S. S. Rana, T. Bhatta, G. B. Pradhan, S. Sharma, H. Song, S. Jeong and J. Y. Park, 3D printed smart glove with pyramidal MXene/Ecoflex composite-based toroidal triboelectric nanogenerators for wearable human-machine interaction applications, *Nano Energy*, 2023, **106**, 108110.

286 N. Van Toan, T. T. K. Tuoi and T. Ono, High-performance flexible thermoelectric generator for self-powered wireless BLE sensing systems, *J. Power Sources*, 2022, **536**, 231504.

287 J.-h. Son, H. Kim, Y. Choi and H. Lee, 3D printed energy devices: generation, conversion, and storage, *Microsyst. Nanoeng.*, 2024, **10**(1), 93.

288 Y. S. Zhang and A. Khademhosseini, Advances in engineering hydrogels, *Science*, 2017, **356**(6337), eaaf3627.

289 C. Ni, D. Chen, Y. Yin, X. Wen, X. Chen, C. Yang, G. Chen, Z. Sun, J. Wen and Y. Jiao, Shape memory polymer with programmable recovery onset, *Nature*, 2023, **622**(7984), 748–753.

290 H. C. Yu, S. Y. Zheng, L. Fang, Z. Ying, M. Du, J. Wang, K. F. Ren, Z. L. Wu and Q. Zheng, Reversibly transforming a highly swollen polyelectrolyte hydrogel to an extremely tough one and its application as a tubular grasper, *Adv. Mater.*, 2020, **32**(49), 2005171.

291 M. Champeau, D. A. Heinze, T. N. Viana, E. R. de Souza, A. C. Chinellato and S. Titotto, 4D printing of hydrogels: a review, *Adv. Funct. Mater.*, 2020, **30**(31), 1910606.

292 T. Wallin, J. Pikul and R. F. Shepherd, 3D printing of soft robotic systems, *Nat. Rev. Mater.*, 2018, **3**(6), 84–100.

293 Y. Wang, D. Liu, C. Wang, J. Wu, X. Xu, X. Yang, C. Sun, P. Jiang and X. Wang, 3D printing of octopi-inspired hydrogel suckers with underwater adaptation for reversible adhesion, *Chem. Eng. J.*, 2023, **457**, 141268.

294 A. K. Mishra, T. J. Wallin, W. Pan, A. Xu, K. Wang, E. P. Giannelis, B. Mazzolai and R. F. Shepherd, Autonomic perspiration in 3D-printed hydrogel actuators, *Sci. Robot.*, 2020, **5**(38), eaaz3918.

295 D. Han, C. Farino, C. Yang, T. Scott, D. Browne, W. Choi, J. W. Freeman and H. Lee, Soft robotic manipulation and

locomotion with a 3D printed electroactive hydrogel, *ACS Appl. Mater. Interfaces*, 2018, **10**(21), 17512–17518.

296 S. Tavakoli, N. Krishnan, H. Mokhtari, O. P. Oommen and O. P. Varghese, Fine-tuning dynamic cross-linking for enhanced 3D bioprinting of hyaluronic acid hydrogels, *Adv. Funct. Mater.*, 2024, **34**(4), 2307040.

297 P. Jiang, P. Lin, C. Yang, H. Qin, X. Wang and F. Zhou, 3D printing of dual-physical cross-linking hydrogel with ultra-high strength and toughness, *Chem. Mater.*, 2020, **32**(23), 9983–9995.

298 W. Sun, A. S. Williamson, R. Sukhnandan, C. Majidi, L. Yao, A. W. Feinberg and V. A. Webster-Wood, Biodegradable, sustainable hydrogel actuators with shape and stiffness morphing capabilities via embedded 3D printing, *Adv. Funct. Mater.*, 2023, **33**(36), 2303659.

299 A. Heiden, D. Preninger, L. Lehner, M. Baumgartner, M. Drack, E. Woritzka, D. Schiller, R. Gerstmayr, F. Hartmann and M. Kaltenbrunner, 3D printing of resilient biogels for omnidirectional and exteroceptive soft actuators, *Sci. Rob.*, 2022, **7**(63), eabk2119.

300 A. K. Mishra, W. Pan, E. P. Giannelis, R. F. Shepherd and T. J. Wallin, Making bioinspired 3D-printed autonomic perspiring hydrogel actuators, *Nat. Protoc.*, 2021, **16**(4), 2068–2087.

301 M. Kaynak, P. Dirix and M. S. Sakar, Addressable acoustic actuation of 3D printed soft robotic microsystems, *Adv. Sci.*, 2020, **7**(20), 2001120.

302 H. Na, Y.-W. Kang, C. S. Park, S. Jung, H.-Y. Kim and J.-Y. Sun, Hydrogel-based strong and fast actuators by electroosmotic turgor pressure, *Science*, 2022, **376**(6590), 301–307.

303 X.-Q. Wang and G. W. Ho, Design of untethered soft material micromachine for life-like locomotion, *Mater. Today*, 2022, **53**, 197–216.

304 Y. Yao, C. Yin, S. Hong, H. Chen, Q. Shi, J. Wang, X. Lu and N. Zhou, Lanthanide-ion-coordinated supramolecular hydrogel inks for 3D printed full-color luminescence and opacity-tuning soft actuators, *Chem. Mater.*, 2020, **32**(20), 8868–8876.

305 D. Jiao, Q. L. Zhu, C. Y. Li, Q. Zheng and Z. L. Wu, Programmable morphing hydrogels for soft actuators and robots: from structure designs to active functions, *Acc. Chem. Res.*, 2022, **55**(11), 1533–1545.

306 A. Sydney Gladman, E. A. Matsumoto, R. G. Nuzzo, L. Mahadevan and J. A. Lewis, Biomimetic 4D printing, *Nat. Mater.*, 2016, **15**(4), 413–418.

307 H. Lee, C. Xia and N. X. Fang, First jump of microgel; actuation speed enhancement by elastic instability, *Soft Matter*, 2010, **6**(18), 4342–4345.

308 S. E. Bakarich, R. Gorkin and G. M. Spinks, 4D Printing with Mechanically Robust, Thermally Actuating Hydrogels, *Macromol. Rapid Commun.*, 2015, **36**(12), 1211.

309 S. Y. Zheng, Y. Shen, F. Zhu, J. Yin, J. Qian, J. Fu, Z. L. Wu and Q. Zheng, Programmed deformations of 3D-printed tough physical hydrogels with high response speed and large output force, *Adv. Funct. Mater.*, 2018, **28**(37), 1803366.

310 B. Sun, R. Jia, H. Yang, X. Chen, K. Tan, Q. Deng and J. Tang, Magnetic arthropod millirobots fabricated by 3D-printed hydrogels, *Adv. Intell. Syst.*, 2022, **4**(1), 2100139.

311 S. Y. Zheng, Y. Shen, F. Zhu, J. Yin, J. Qian, J. Fu, Z. L. Wu and Q. Zheng, Programmed deformations of 3D-printed tough physical hydrogels with high response speed and large output force, *Adv. Funct. Mater.*, 2018, **28**(37), 1803366.

312 D. Han, C. Farino, C. Yang, T. Scott, D. Browe, W. Choi, J. W. Freeman and H. Lee, Soft robotic manipulation and locomotion with a 3D printed electroactive hydrogel, *ACS Appl. Mater. Interfaces*, 2018, **10**(21), 17512–17518.

313 D. Han, C. Farino, C. Yang, T. Scott, D. Browe, W. Choi, J. W. Freeman and H. Lee, Soft robotic manipulation and locomotion with a 3D printed electroactive hydrogel, *ACS Appl. Mater. Interfaces*, 2018, **10**(21), 17512–17518.

314 E. Sachyani Keneth, A. Kamyshny, M. Totaro, L. Beccai and S. Magdassi, 3D printing materials for soft robotics, *Adv. Mater.*, 2021, **33**(19), 2003387.

315 T. Xie, Tunable polymer multi-shape memory effect, *Nature*, 2010, **464**(7286), 267–270.

316 A. Lendlein and O. E. Gould, Reprogrammable recovery and actuation behaviour of shape-memory polymers, *Nat. Rev. Mater.*, 2019, **4**(2), 116–133.

317 J.-J. Wu, L.-M. Huang, Q. Zhao and T. Xie, 4D printing: history and recent progress, *Chin. J. Polym. Sci.*, 2018, **36**, 563–575.

318 J. Zhang, Z. Yin, L. Ren, Q. Liu, L. Ren, X. Yang and X. Zhou, Advances in 4D printed shape memory polymers: from 3D printing, smart excitation, and response to applications, *Adv. Mater. Technol.*, 2022, **7**(9), 2101568.

319 H. Li, X. Gao and Y. Luo, Multi-shape memory polymers achieved by the spatio-assembly of 3D printable thermoplastic building blocks, *Soft Matter*, 2016, **12**(13), 3226–3233.

320 M. Zarek, M. Layani, I. Cooperstein, E. Sachyani, D. Cohn and S. Magdassi, 3D printing of shape memory polymers for flexible electronic devices, *Adv. Mater.*, 2015, **28**(22), 4449–4454.

321 J. Wang, Z. Wang, Z. Song, L. Ren, Q. Liu and L. Ren, Biomimetic shape-color double-responsive 4D printing, *Adv. Mater. Technol.*, 2019, **4**(9), 1900293.

322 Y. Wu, Y. Han, Z. Wei, Y. Xie, J. Yin and J. Qian, 4D printing of chiral mechanical metamaterials with modular programmability using shape memory polymer, *Adv. Funct. Mater.*, 2023, **33**(52), 2306442.

323 Q. Ge, A. H. Sakhaei, H. Lee, C. K. Dunn, N. X. Fang and M. L. Dunn, Multimaterial 4D printing with tailororable shape memory polymers, *Sci. Rep.*, 2016, **6**(1), 31110.

324 S. Ma, Z. Jiang, M. Wang, L. Zhang, Y. Liang, Z. Zhang, L. Ren and L. Ren, 4D printing of PLA/PCL shape memory composites with controllable sequential deformation, *Bio-Des. Manuf.*, 2021, **4**, 867–878.

325 L. Ren, B. Li, Z. Song, Q. Liu, L. Ren and X. Zhou, Bioinspired fiber-regulated composite with tunable permanent shape and shape memory properties via 3d magnetic printing, *Composites, Part B*, 2019, **164**, 458–466.

326 D. Goswami, S. Liu, A. Pal, L. G. Silva and R. V. Martinez, 3D–architected soft machines with topologically encoded motion, *Adv. Funct. Mater.*, 2019, **29**(24), 1808713.

327 J. E. M. Teoh, Y. Zhao, J. An, C. K. Chua and Y. Liu, Multi-stage responsive 4D printed smart structure through varying geometric thickness of shape memory polymer, *Smart Mater. Struct.*, 2017, **26**(12), 125001.

328 L. Yue, X. Sun, L. Yu, M. Li, S. M. Montgomery, Y. Song, T. Nomura, M. Tanaka and H. J. Qi, Cold-programmed shape-morphing structures based on grayscale digital light processing 4D printing, *Nat. Commun.*, 2023, **14**(1), 5519.

329 Y. Wu, Y. Han, Z. Wei, Y. Xie, J. Yin and J. Qian, 4D printing of chiral mechanical metamaterials with modular programmability using shape memory polymer, *Adv. Funct. Mater.*, 2023, **33**(52), 2306442.

330 T. Chung, A. Romo-Uribe and P. T. Mather, Two-way reversible shape memory in a semicrystalline network, *Macromolecules*, 2008, **41**(1), 184–192.

331 M. Farhan, T. Rudolph, U. Nöchel, W. Yan, K. Kratz and A. Lendlein, Noncontinuously responding polymeric actuators, *ACS Appl. Mater. Interfaces*, 2017, **9**(39), 33559–33564.

332 Y. Shi, G. Fang, Z. Cao, F. Shi, Q. Zhao, Z. Fang and T. Xie, Digital light fabrication of reversible shape memory polymers, *Chem. Eng. J.*, 2021, **426**, 131306.

333 P. F. Egan, V. C. Gonella, M. Engensperger, S. J. Ferguson and K. Shea, Computationally designed lattices with tuned properties for tissue engineering using 3D printing, *PLoS One*, 2017, **12**(8), e0182902.

334 M. Revilla-León, Ó. González-Martín, J. Pérez López, J. L. Sánchez-Rubio and M. Özcan, Position accuracy of implant analogs on 3D printed polymer versus conventional dental stone casts measured using a coordinate measuring machine, *J. Prosthodontics*, 2018, **27**(6), 560–567.

335 J. Zuniga, D. Katsavelis, J. Peck, J. Stollberg, M. Petrykowski, A. Carson and C. Fernandez, Cyborg beast: a low-cost 3d-printed prosthetic hand for children with upper-limb differences, *BMC Res. Notes*, 2015, **8**(1), 10.

336 S. N. Economidou, D. A. Lamprou and D. Douroumis, 3D printing applications for transdermal drug delivery, *Int. J. Pharm.*, 2018, **544**(2), 415–424.

337 I. Rubio-Pérez and A. Diaz Lantada, Surgical planning of sacral nerve stimulation procedure in presence of sacral anomalies by using personalized polymeric prototypes obtained with additive manufacturing techniques, *Polymers*, 2020, **12**(3), 581.

338 M. M. Erickson, E. S. Richardson, N. M. Hernandez, D. W. Bobbert II, K. Gall and P. Fearis, Helmet modification to PPE with 3D printing during the COVID-19 pandemic at Duke University Medical Center: a novel technique, *J. Arthroplasty*, 2020, **35**(7), S23–S27.

339 P. F. Egan, Integrated design approaches for 3D printed tissue scaffolds, Review and outlook, *Materials*, 2019, **12**(15), 2355.

340 B. Dhandayuthapani, Y. Yoshida, T. Maekawa and D. S. Kumar, Polymeric scaffolds in tissue engineering application: a review, *Int. J. Polym. Sci.*, 2011, **1**, 290602.

341 E. P. Childers, M. O. Wang, M. L. Becker, J. P. Fisher and D. Dean, 3D printing of resorbable poly (propylene fumarate) tissue engineering scaffolds, *MRS Bull.*, 2015, **40**(2), 119–126.

342 S. J. Hollister, C. L. Flanagan, D. A. Zopf, R. J. Morrison, H. Nasser, J. J. Patel, E. Ebramzadeh, S. N. Sangiorgio, M. B. Wheeler and G. E. Green, Design control for clinical translation of 3D printed modular scaffolds, *Ann. Biomed. Eng.*, 2015, **43**(3), 774–786.

343 A. Boccaccio, A. E. Uva, M. Fiorentino, G. Mori and G. Monno, Geometry design optimization of functionally graded scaffolds for bone tissue engineering: A mechano-biological approach, *PLoS One*, 2016, **11**(1), e0146935.

344 H. Kang, S. J. Hollister, F. La Marca, P. Park and C.-Y. Lin, Porous biodegradable lumbar interbody fusion cage design and fabrication using integrated global-local topology optimization with laser sintering, *J. Biomech. Eng.*, 2013, **135**(10), 101013.

345 A. M. E. Arefin and P. F. Egan. In Computational Design Generation and Evaluation of Beam-Based Tetragonal Bravais Lattice Structures for Tissue Engineering, ASME 2020 International Design Engineering Technical Conferences and Computers and Information in Engineering Conference, 2020.

346 P. F. Egan, K. A. Shea and S. J. Ferguson, Simulated tissue growth for 3D printed scaffolds, *Biomech. Model. Mechanobiol.*, 2018, **17**(5), 1481–1495.

347 A. C. Weems, M. C. Arno, W. Yu, R. T. R. Huckstepp and A. P. Dove, 4D polycarbonates via stereolithography as scaffolds for soft tissue repair, *Nat. Commun.*, 2021, **12**(1), 3771.

348 A. Abouchenari, N. Tajbakhsh, A. Shahbaz and G. Alamdari-Mahd, Advancements in dental implant technology: the impact of smart polymers utilized through 3D printing, *Synth. Sintering*, 2024, **4**(2), 108–123.

349 A. Pandey, G. Singh, S. Singh, K. Jha and C. Prakash, 3D printed biodegradable functional temperature-stimuli shape memory polymer for customized scaffoldings, *J. Mech. Behav. Biomed. Mater.*, 2020, **108**, 103781.

350 G. Singh, S. Singh, C. Prakash, R. Kumar, R. Kumar and S. Ramakrishna, Characterization of three-dimensional printed thermal-stimulus polylactic acid-hydroxyapatite-based shape memory scaffolds, *Polym. Compos.*, 2020, **41**(9), 3871–3891.

351 R. Sharma, R. Singh and A. Batish, On mechanical and surface properties of electro-active polymer matrix-based 3D printed functionally graded prototypes, *J. Thermoplast. Compos. Mater.*, 2022, **35**(5), 615–630.

352 B. Çelebi-Saltik, S. Babadag, E. Ballikaya, S. Pat and M. Ö. Öteyaka, Osteogenic Differentiation Capacity of Dental Pulp Stem Cells on 3D Printed Polyurethane/Boric Acid Scaffold, *Biol. Trace Elem. Res.*, 2024, **202**(4), 1446–1456.

353 S.-G. Chen, J. Yang, Y.-G. Jia, B. Lu and L. Ren, TiO<sub>2</sub> and PEEK Reinforced 3D Printing PMMA Composite Resin for Dental Denture Base Applications, *Nanomaterials*, 2019, **9**(7), 1049.

354 C. Cristache and E. Totu, *Reactive and Functional Polymers Volume Three*, J Springer International Publishing, Cham, Switzerland, 2021.

355 L. K. Hakim, A. Yari, N. Nikparto, S. H. Mehraban, S. Cheperli, A. Asadi, A. A. Darchdor, S. Nezaminia, D. Dortaj, Y. Nazari, M. Dehghan, P. Hojjat, M. Mohajeri and M. S. Hasani Jebelli, The current applications of nano and biomaterials in drug delivery of dental implant, *BMC Oral Health*, 2024, **24**(1), 126.

356 P. Balamurugan and N. Selvakumar, Development of patient specific dental implant using 3D printing, *J. Ambient Intell. Humaniz. Comput.*, 2021, **12**(3), 3549–3558.

357 S. Vasiliu, S. Racovita, I. A. Gugoasa, M.-A. Lungan, M. Popa and J. Desbrieres, The Benefits of Smart Nanoparticles in Dental Applications, *Int. J. Mol. Sci.*, 2021, **22**(5), 2585.

358 S. M. Desai, R. Y. Sonawane and A. P. More, Thermoplastic polyurethane for three-dimensional printing applications: A review, *Polym. Adv. Technol.*, 2023, **34**(7), 2061–2082.

359 M. Dimitrova, A. Vlahova, Y. Kalachev, S. Zlatev, R. Kazakova and S. Capodiferro, Recent Advances in 3D Printing of Polymers for Application in Prosthodontics, *Polymers*, 2023, **15**(23), 4525.

360 K. Jain, R. Shukla, A. Yadav, R. R. Ujjwal and S. J. S. Flora, 3D Printing in Development of Nanomedicines, *Nanomaterials*, 2021, **11**(2), 420.

361 L. M. Schönhoff, F. Mayinger, M. Eichberger, E. Reznikova and B. Stawarczyk, 3D printing of dental restorations: Mechanical properties of thermoplastic polymer materials, *J. Mech. Behav. Biomed. Mater.*, 2021, **119**, 104544.

362 H. Yang, W. R. Leow and X. Chen, 3D Printing of Flexible Electronic Devices, *Small Methods*, 2018, **2**(1), 1700259.

363 S. K. Powell, R. L. J. Cruz, M. T. Ross and M. A. Woodruff, Past, Present, and Future of Soft-Tissue Prosthetics: Advanced Polymers and Advanced Manufacturing, *Adv. Mater.*, 2020, **32**(42), 2001122.

364 H. Ota, M. Chao, Y. Gao, E. Wu, L.-C. Tai, K. Chen, Y. Matsuoka, K. Iwai, H. M. Fahad, W. Gao, H. Y. Y. Nyein, L. Lin and A. Javey, 3D Printed “Earable” Smart Devices for Real-Time Detection of Core Body Temperature, *ACS Sens.*, 2017, **2**(7), 990–997.

365 Y. Gao, G. Yu, T. Shu, Y. Chen, W. Yang, Y. Liu, J. Long, W. Xiong and F. Xuan, 3D-Printed Coaxial Fibers for Integrated Wearable Sensor Skin, *Adv. Mater. Technol.*, 2019, **4**(10), 1900504.

366 B. B. Lee, R. A. Cripps, M. Fitzharris and P. C. Wing, The global map for traumatic spinal cord injury epidemiology: update 2011, global incidence rate, *Spinal Cord*, 2014, **52**(2), 110–116.

367 H.-J. Yoo, S. Lee, J. Kim, C. Park and B. Lee, Development of 3D-printed myoelectric hand orthosis for patients with spinal cord injury, *J. Neuroeng. Rehabilitat.*, 2019, **16**(1), 162.

368 H. Lin, L. Shi and D. Wang, A rapid and intelligent designing technique for patient-specific and 3D-printed orthopedic cast, *3D Print. Med.*, 2016, **2**(1), 4.

369 M. Vukicevic, B. Mosadegh, J. K. Min and S. H. Little, Cardiac 3D Printing and its Future Directions, *JACC Cardiovasc. Imaging*, 2017, **10**(2), 171–184.

370 K. M. Farooqi, C. G. Lengua, A. D. Weinberg, J. C. Nielsen and J. Sanz, Blood Pool Segmentation Results in Superior Virtual Cardiac Models than Myocardial Segmentation for 3D Printing, *Pediatr. Cardiol.*, 2016, **37**(6), 1028–1036.

371 A. Scerrati, F. Trovalusci, A. Albanese, G. S. Ponticelli, V. Tagliaferri, C. L. Sturiale, M. A. Cavallo and E. Marchese, A workflow to generate physical 3D models of cerebral aneurysms applying open source freeware for CAD modeling and 3D printing, *Interdiscip. Neurosurg.*, 2019, **17**, 1–6.

372 J. R. Anderson, W. L. Thompson, A. K. Alkattan, O. Diaz, R. Klucznik, Y. J. Zhang, G. W. Britz, R. G. Grossman and C. Karmonik, Three-dimensional printing of anatomically accurate, patient specific intracranial aneurysm models, *J. Neurointerv. Surg.*, 2016, **8**(5), 517.

373 N. Wake, H. Chandarana, W. C. Huang, S. S. Taneja and A. B. Rosenkrantz, Application of anatomically accurate, patient-specific 3D printed models from MRI data in urological oncology, *Clin. Radiol.*, 2016, **71**(6), 610–614.

374 J.-C. Bernhard, S. Isotani, T. Matsugasaki, V. Duddalwar, A. J. Hung, E. Suer, E. Baco, R. Satkunasivam, H. Djaladat, C. Metcalfe, B. Hu, K. Wong, D. Park, M. Nguyen, D. Hwang, S. T. Bazargani, A. L. de Castro Abreu, M. Aron, O. Ukimura and I. S. Gill, Personalized 3D printed model of kidney and tumor anatomy: a useful tool for patient education, *World J. Urol.*, 2016, **34**(3), 337–345.

375 J. B. Hochman, J. Kraut, K. Kazmerik and B. J. Unger, Generation of a 3D Printed Temporal Bone Model with Internal Fidelity and Validation of the Mechanical Construct, *Otolaryngol., Head Neck Surg.*, 2014, **150**(3), 448–454.

376 K. M. Farooqi, O. Saeed, A. Zaidi, J. Sanz, J. C. Nielsen, D. T. Hsu and U. P. Jorde, 3D Printing to Guide Ventricular Assist Device Placement in Adults With Congenital Heart Disease and Heart Failure, *JACC: Heart Failure*, 2016, **4**(4), 301–311.

377 S. Schievano, F. Migliavacca, L. Coats, S. Khambadkone, M. Carminati, N. Wilson, J. E. Deanfield, P. Bonhoeffer and A. M. Taylor, Percutaneous Pulmonary Valve Implantation Based on Rapid Prototyping of Right Ventricular Outflow Tract and Pulmonary Trunk from MR Data, *Radiology*, 2007, **242**(2), 490–497.

378 M. Kusaka, M. Sugimoto, N. Fukami, H. Sasaki, M. Takenaka, T. Anraku, T. Ito, T. Kenmochi, R. Shiroki and K. Hoshinaga, Initial Experience With a Tailor-made Simulation and Navigation Program Using a 3-D Printer Model of Kidney Transplantation Surgery, *Transplant. Proc.*, 2015, **47**(3), 596–599.

379 Y. Komai, M. Sugimoto, N. Gotohda, N. Matsubara, T. Kobayashi, Y. Sakai, Y. Shiga and N. Saito, Patient-specific 3-dimensional Printed Kidney Designed for “4D” Surgical Navigation: A Novel Aid to Facilitate Minimally Invasive Off-clamp Partial Nephrectomy in Complex Tumor Cases, *Urology*, 2016, **91**, 226–233.

380 N. Paunović, D. Meyer, A. Krivitsky, A. R. Studart, Y. Bao and J. C. Leroux, 4D printing of biodegradable elastomers with tailorable thermal response at physiological temperature, *J. Controlled Release*, 2023, **361**, 417–426.

381 Y. Ma, C.-J. Shih and Y. Bao, Advances in 4D printing of biodegradable photopolymers, *Responsive Mater.*, 2024, **2**(3), e20240008.

382 T. R. Yeazel and M. L. Becker, Advancing Toward 3D Printing of Bioresorbable Shape Memory Polymer Stents, *Biomacromolecules*, 2020, **21**(10), 3957–3965.

383 N. Paunović, J. Marbach, Y. Bao, V. Berger, K. Klein, S. Schleich, F. B. Coulter, N. Kleger, A. R. Studart and D. J. A. S. Franzen, Digital Light 3D Printed Bioresorbable and NIR-Responsive Devices with Photothermal and Shape-Memory Functions, *Adv. Sci.*, 2022, **9**(27), 2200907.

384 G. Le Fer and M. L. Becker, 4D Printing of Resorbable Complex Shape-Memory Poly(propylene fumarate) Star Scaffolds, *ACS Appl. Mater. Interfaces*, 2020, **12**(20), 22444–22452.

385 S. E. Moulton and G. G. Wallace, 3-dimensional (3D) fabricated polymer based drug delivery systems, *J. Controlled Release*, 2014, **193**, 27–34.

386 E. Y. Teo, S.-Y. Ong, M. S. Khoon Chong, Z. Zhang, J. Lu, S. Moothala, B. Ho and S.-H. Teoh, Polycaprolactone-based fused deposition modeled mesh for delivery of antibacterial agents to infected wounds, *Biomaterials*, 2011, **32**(1), 279–287.

387 H.-G. Yi, Y.-J. Choi, K. S. Kang, J. M. Hong, R. G. Pati, M. N. Park, I. K. Shim, C. M. Lee, S. C. Kim and D.-W. Cho, A 3D-printed local drug delivery patch for pancreatic cancer growth suppression, *J. Controlled Release*, 2016, **238**, 231–241.

388 J. Wang, A. Goyanes, S. Gaisford and A. W. Basit, Stereolithographic (SLA) 3D printing of oral modified-release dosage forms, *Int. J. Pharm.*, 2016, **503**(1), 207–212.

389 A. Goyanes, J. Wang, A. Buanz, R. Martínez-Pacheco, R. Telford, S. Gaisford and A. W. Basit, 3D Printing of Medicines: Engineering Novel Oral Devices with Unique Design and Drug Release Characteristics, *Mol. Pharm.*, 2015, **12**(11), 4077–4084.

390 S. A. Khaled, J. C. Burley, M. R. Alexander, J. Yang and C. J. Roberts, 3D printing of tablets containing multiple drugs with defined release profiles, *Int. J. Pharm.*, 2015, **494**(2), 643–650.

391 M. Alomari, F. H. Mohamed, A. W. Basit and S. Gaisford, Personalised dosing: Printing a dose of one's own medicine, *Int. J. Pharm.*, 2015, **494**(2), 568–577.

392 A. R. Pohlmann, F. N. Fonseca, K. Paese, C. B. Detoni, K. Coradini, R. C. R. Beck and S. S. Guterres, Poly( $\epsilon$ -caprolactone) microcapsules and nanocapsules in drug delivery, *Expert Opin. Drug Delivery*, 2013, **10**(5), 623–638.

393 L. Wu, J. Huang, M. Zhai, B. Sun, H. Chang, S. Huang and H. Liu, Deformable bowtie antenna realized by 4D printing, *Electronics*, 2021, **10**(15), 1792.

394 T. Langford, A. Mohammed, K. Essa, A. Elshaer and H. Hassanin, 4D printing of origami structures for minimally invasive surgeries using functional scaffold, *Appl. Sci.*, 2020, **11**(1), 332.

395 R. Cui, S. Li, T. Li, X. Gou, T. Jing, G. Zhang, G. Wei, Z. Jin, X. Xiong and S. Qu, Natural polymer derived hydrogel bioink with enhanced thixotropy improves printability and cellular preservation in 3D bioprinting, *J. Mater. Chem. B*, 2023, **11**(17), 3907–3918.

396 L. Wang, F. Zhang, S. Du and J. Leng, Advances in 4D printed shape memory composites and structures: Actuation and application, *Sci. China: Technol. Sci.*, 2023, **66**(5), 1271–1288.

397 K. McLellan, Y.-C. Sun and H. E. Naguib, A review of 4D printing: Materials, structures, and designs towards the printing of biomedical wearable devices, *Bioprinting*, 2022, **27**, e00217.

398 E. Pei and G. H. Loh, Technological considerations for 4D printing: an overview, *Prog. Addit. Manuf.*, 2018, **3**(1), 95–107.

399 X. Kang, X.-B. Zhang, X.-D. Gao, D.-J. Hao, T. Li and Z.-W. Xu, Bioprinting for bone tissue engineering, *Front. Bioeng. Biotechnol.*, 2022, **10**, 1036375.

400 A. P. Piedade, 4D printing: the shape-morphing in additive manufacturing, *J. Funct. Biomater.*, 2019, **10**(1), 9.

401 N. Sabahi, W. Chen, C.-H. Wang, J. J. Kruzic and X. Li, A review on additive manufacturing of shape-memory materials for biomedical applications, *JOM*, 2020, **72**(3), 1229–1253.

402 I. T. Garces and C. Ayrancı, Advances in additive manufacturing of shape memory polymer composites, *Rapid Prototyping*, 2021, **27**(2), 379–398.

403 C. A. Spiegel, M. Hippler, A. Münchinger, M. Bastmeyer, C. Barner-Kowollik, M. Wegener and E. Blasco, 4D printing at the microscale, *Adv. Funct. Mater.*, 2020, **30**(26), 1907615.

404 M. S. Khan, S. A. Khan, S. Shabbir, M. Umar, S. Mohapatra, T. Khuroo, P. P. Naseef, M. S. Kurunian, Z. Iqbal and M. A. Mirza, Raw materials, technology, healthcare applications, patent repository and clinical trials on 4D printing technology: An updated review, *Pharmaceutics*, 2022, **15**(1), 116.

405 J. Choi, O.-C. Kwon, W. Jo, H. J. Lee and M.-W. Moon, 4D printing technology: a review, *3D Print. Addit. Manuf.*, 2015, **2**(4), 159–167.

406 H. Qu, Additive manufacturing for bone tissue engineering scaffolds, *Mater. Today Commun.*, 2020, **24**, 101024.